Impacts of Partial Cambial Dieback on Tree-Ring Records from Ancient Conifers

Caroline Leland

Submitted in partial fulfillment of the
requirements for the degree of
Doctor of Philosophy
in the Graduate School of Arts and Sciences

COLUMBIA UNIVERSITY

2019

ABSTRACT

Impacts of Partial Cambial Dieback on

Tree-Ring Records from Ancient Conifers

Caroline Leland

Tree-ring records from long-lived trees are instrumental for understanding climate variability during the Common Era. Some of the oldest and most valuable conifers used to reconstruct past climate exhibit strip-bark morphology, in which vertical segments of the tree have died in response to environmental stress. This form of localized stem mortality, also referred to as partial cambial dieback, is particularly common on conifers growing in xeric, cold, or exposed environments. Some studies note that strip-bark trees have increasing ring-width trends relative to trees with a fully living stem circumference, but there is substantial uncertainty as to what extent partial cambial dieback can influence tree-ring records and subsequent climate reconstructions. This dissertation explores the environmental drivers of partial cambial dieback on Siberian pine (*Pinus sibirica* Du Tour) from Mongolia, the effect of cambial dieback on the radial growth and physiology of affected trees, and methods for reducing strip-bark biases in tree-ring records.

Chapter 1 assesses the causes and radial growth impacts of partial cambial dieback on Siberian pine trees growing on an ancient lava flow in central Mongolia. Using a combination of field observations and dendrochronological methods, this chapter demonstrates that strip-bark trees from this site exhibit dieback primarily on the southern side of stems, and that dieback was most common during a cold and dry period in the mid-19th century. Given the directionality and timing of dieback on these strip-bark trees, it is hypothesized that localized mortality events are linked to physiological injuries spurred from solar heating combined with unfavorable climatic

conditions. This chapter also reveals that strip-bark trees from this site have increasing radial growth trends relative to trees with a full circular morphology ("whole-bark" trees). Strip-bark trees showed an especially rapid increase in ring widths following the cambial dieback period in the mid-19th century, providing initial evidence that dieback events can lead to increasing ring widths in strip-bark Siberian pine.

Chapter 2 seeks to discern the physiological mechanisms of increasing radial growth trends in the Siberian pine strip-bark trees using stable carbon and oxygen isotopes from tree rings. One simple hypothesis is that strip-bark trees show increasing ring-width trends because radial growth is restricted to a smaller stem area after cambial dieback events. Conversely, some studies have hypothesized that increasing ring widths in strip-bark trees reflect a CO_2 fertilization effect on growth that is not readily apparent in whole-bark trees. This chapter finds that strip-bark and whole-bark trees responded similarly to increasing atmospheric CO_2 and climate variability in their radial growth and leaf-level gas exchange inferred from tree-ring stable isotopes. However, strip-bark and whole-bark trees showed notably different behavior following documented cambial dieback events. After dieback events, strip-bark trees exhibited an increase in ring widths and an enrichment in stable carbon and oxygen isotopes that was not apparent in whole-bark trees. These results further support the notion that partial cambial dieback leads directly to increasing ring widths in strip-bark trees, and that this response could reflect an increase in the ratio of leaf to live stem area after dieback occurs.

Chapters 1 and 2 demonstrate that partial cambial dieback events and morphological changes impact the radial growth and physiology of strip-bark trees. Therefore, prior to developing climate reconstructions, it is necessary to remove variance associated with these non-climatic, morphological changes in tree-ring series. Chapter 3 outlines two chronology

development methods for reducing strip-bark biases in tree-ring records. These methods, applied to Siberian pine and Great Basin bristlecone pine (*Pinus longaeva* Bailey), successfully reduce a strip-bark bias without removing low-to-medium frequency climate variance inferred from whole-bark trees, which were not impacted by dieback activity. While one approach directly corrects the bias in strip-bark series using a whole-bark chronology as a target, another method is based on the development of a low-percentile chronology, which can be applied to a site collection where the stem morphology of individual trees is unknown. Some limitations and caveats of these methods are discussed in context of the analyzed tree species.

The findings from this dissertation have significantly contributed to our understanding of the radial growth and physiological responses of Siberian pine to partial cambial dieback and environmental changes. This dissertation also provides new methods for removing strip-bark biases in tree-ring chronologies. The conclusions presented here have important implications regarding the potential effects of partial cambial dieback on tree-ring records from other tree species and climate reconstructions derived from them. Continued and detailed study of the causes and impacts of partial cambial dieback on other tree species will be critical for understanding the interactions between ancient trees and their environment, and for improving the reliability of climate reconstructions based fully or partly on strip-bark trees.

Table of Contents

List of Figures

List of Tables

Acknowledgements

I would like to thank the members of my advisory committee, Dr. Ed Cook, Dr. Laia Andreu Hayles, and Dr. Kevin Griffin. I am extremely fortunate to have had Ed as an academic advisor. Ed was always supportive of my research goals, even when my research interests (occasionally) meandered, and his extensive knowledge, expertise and creativity truly helped elevate my research. During times of great confusion or uncertainty, Ed would reassure me with Albert Einstein's quote, "If we knew what we were doing, it wouldn't be called research". Thank you, Ed, for the perpetual encouragement, guidance, and inspiration. I am also deeply grateful for my co-advisor, Laia Andreu Hayles, who has been a supreme teacher and mentor during the last six years. Through example, Laia has taught me how to be a creative, thoughtful, and persistent researcher. Her wide knowledgebase helped me tie many of the ideas in this dissertation together. I would also like to thank my third committee member, Kevin, for providing continual support and plant physiological perspectives. Kevin's enthusiasm for plant ecophysiology is infectious and I have learned so much from him over the years.

In addition to my current advisory committee, I am indebted to two of my former advisors, Dr. Neil Pederson and Dr. Amy Hessl, who continue to play important roles in my academic life. In fact, this dissertation would not have existed without them. Both Neil and Amy have been influential in my development as a tree-ring scientist, and they gave me the opportunity to study some of the most venerable trees in one of the most awe-inspiring regions in the world (Mongolia). Their generosity and support brought me to Columbia University to work on many of the topics covered here.

My deepest gratitude goes out to my colleagues from the National University of Mongolia, including Baatarbileg Nachin, Oyunsanaa Byambasuren, and Byambagerel Suran,

who introduced me to their beautiful country and taught me so much over the last decade. Their warmth and generosity is deeply appreciated, and I am thankful for all the memories I have acquired in Mongolia. I would also like to especially thank Jennie Zhu and Khashaa Eldovechir for their immense help and friendship during the field season of 2015. Our field excursion to Khorgo that summer was pivotal to the development of this dissertation.

I would also like to thank my friends and colleagues at the Lamont-Doherty Earth Observatory, especially those in the Tree-ring Lab. The Tree-ring Lab has felt like my home away from home for almost a decade. All of the PIs, technicians, post-docs, and graduate students in this lab have always been happy to provide feedback, share their knowledge, and offer encouragement. I am fortunate to have been surrounded by such a friendly and bright community of people. Thanks especially to fellow tree-ring PhD students, Mukund Palat Rao, Dan Bishop, and Rose Oelkers, for your friendship. In addition to colleagues at the Tree-ring Lab, I am extremely grateful to Dr. Wei Huang, the Lab Manager of the Stable Isotope Lab, who provided significant support (even during off-hours) for my stable isotope measurements.

Last but not least, I would like to express my heartfelt appreciation for my family and friends who have provided endless encouragement and love through the years. To my parents, Richard and Elizabeth Leland, my sister, Catherine Leland, and my grandmother, Nancy Wogan, thank you for everything you have done for me. An incredible amount of my gratitude also goes to my best friend and spouse, Chris Aloezos, who was a continual pillar of strength, source of reason, and provider of laughs.

This dissertation was made possible by support from the Department of Earth and Environmental Sciences at Columbia University, and the following funding sources: the National Science Foundation (award BCS-1210360) and the Lamont Climate Center.

Introduction

Annual growth rings in trees provide a valuable record of past climatic and ecological variability. Various properties of tree rings, such as ring width, wood density, and stable isotopic composition, are used to evaluate environmental changes across local, regional, and continental scales (Fritts 1976, Cook and Kairiukstis 1990, Gagen et al. 2011, D'Arrigo et al. 2014). These records can span several centuries, or in some cases, millennia, and are especially important for placing recent climatic changes into a long-term historical context. In several regions of the world, tree-ring reconstructions reveal extreme or unprecedented conditions in both temperature and hydroclimate during recent decades compared to past centuries (e.g., Wilson et al. 2016, Cook et al. 2016, Hessl et al. 2018). Tree-ring records, therefore, are instrumental for understanding the range of natural and anthropogenic climatic variability during the Common Era.

Measurements of the widths of annual tree rings are traditionally and most commonly used for tree-ring climate reconstructions. The radial growth of trees, inferred from tree-ring width records, is governed by the Principle of Liebig's Law of the Minimum, indicating that the most limiting environmental factor at a site will determine how much a tree is able to grow each year (Fritts 1976, Speer 2010). Thus, in water-limited sites, radial tree growth is dictated primarily by changes in moisture availability, whereas at high-elevation and extremely cold sites, trees might respond to temperature variability. A statistical relationship between radial tree growth and a limiting climate variable is determined over the instrumental period, and a transfer function is applied to tree-ring series to reconstruct climate variability in the past, preceding instrumental records (Fritts et al. 1971, Fritts 1976). However, in addition to climate-related variance, tree-ring series also consist of non-climatic variance that must be significantly reduced

or removed in order to isolate a climatic signal for reconstruction. In this dissertation, I describe non-climatic, morphology-related signals imprinted in tree-ring records of some of the oldest and most important trees for climate reconstruction. These morphological signals result from partial cambial dieback, also known as 'strip bark', which affects many conifers growing under adverse environmental conditions. The causes of partial cambial dieback and its impact on tree-ring records have not been described or studied widely. Understanding this phenomenon will be essential for improving assessments of climate variability over the Common Era.

Tree-ring signals

The linear aggregate model for tree rings (Cook 1985, Cook and Kairiukstis 1990) states that ring width in any given year (R_t) can be decomposed into the following sources of variance:

$$R_t = A_t + C_t + \delta D1_t + \delta D2_t + E_t$$

Where:

A_t = age/size-related trend

C_t = climate-related variance

$D1_t$ = endogenous (local or individual tree-level) disturbance

$D2_t$ = exogenous (stand-level) disturbance

E_t = unexplained variance

In this formulation, the δ refers to the presence (δ=1) or absence (δ=0) of a particular signal. In other words, while A_t, C_t, and E_t are always present, the disturbance signals affecting R_t are transient and can be present or absent in any given year (Cook and Kairiukstis 1990).

The aforementioned factors of tree-ring variance have been studied extensively, and for climate reconstruction purposes, numerous statistical methods have been proposed to isolate climate signals in tree-ring series through reducing variance associated with non-climatic signals (e.g., Fritts 1976, Cook and Peters 1981, Briffa et al. 1992, Cook and Peters 1997, Druckenbrod et al. 2013). Unwanted non-climatic signals are diminished in tree-ring widths through the process of standardization, which results in a series of dimensionless indices that ideally capture the climate signal of interest. In a traditional sense, curves representing unwanted signals (i.e., age and/or disturbance-related variance) are fitted to tree-ring widths, and the ratio between the actual and expected (i.e., curve fit) values yield variance theoretically only related to climate. As the traditional 'ratios method' of index calculation has a proclivity to introduce inflationary biases, especially in very slow growing trees, calculating residuals from curve fits of power-transformed series is sometimes more appropriate (Cook and Peters 1997).

Regardless of the method used for index calculation, choosing the most suitable type of standardization (or detrending) curve to apply to tree-ring series is an age-old challenge, and should ideally be informed by characteristics of the sampled site and trees, as well as the objectives of the study. Curve fits range from 'conservative' and rather rigid, such as modified negative exponential curves for removing age-related signals (Fritts et al. 1969), to more flexible varieties, such as cubic smoothing splines (Cook and Peters 1981). While conservative methods might not effectively remove signals associated with forest dynamics and disturbances, more flexible methods can remove these signals with the potential loss of some low to medium-frequency variability. The amount of recoverable low-frequency information retained in a tree-ring chronology is dependent on the length of individual tree-ring series, as well as the flexibility of the curves applied to them (Briffa et al. 1992, Cook et al. 1995, Briffa et al. 1996). Therefore,

there is an inherent balance between the amount of long-term, low-frequency climate variance that can be retained versus the amount of non-climatic variance that can be removed. When the objective is to reconstruct past climate variability, an understanding of potential climatic and non-climatic signals in tree-ring series is imperative for reducing non-climatic 'noise' while retaining as much low-frequency climatic information as possible.

Partial cambial dieback as a non-climatic signal

Non-climatic sources of variance in ring-width series are most commonly attributed to the changing age/size of trees and various forms of disturbance that can impact radial tree growth. However, this dissertation focuses on ring-width signals associated with partial cambial dieback, another potential source of ring-width variance that largely remains an enigma. Trees with partial cambial dieback, also known as trees with strip-bark morphology, have strips of dead wood extending along the full axis of the tree, quite often from the root to the upper canopy (Schulman 1954, Schulman and Ferguson 1956, Wright and Mooney 1965, LaMarche 1969). As a result, annual growth layers are restricted to only living portions of the stem where the cambium is active. Strip-bark morphology is particularly common in tree species that attain extremely old ages and are growing in very hostile environments (e.g., cold, xeric, and/or exposed; Schulman 1954). Thus, trees that exhibit stripping behavior are typically very important for tree-ring based climate reconstructions due to their longevity, and in many cases, strong sensitivity to climate. Several studies have found that strip-bark trees tend to have increasing ring-width trends relative to whole-bark trees (i.e., trees with a living cambium fully around the stem) from the same site (Graybill and Idso 1993, Ababneh 2006, Bunn et al. 2003, Pederson et al. 2014, Yang et al. 2014), but the physiological reason as to why strip-bark trees have increasing ring-width trends is currently not well understood.

Partial cambial dieback is particularly common among conifers in the Pinaceae and the Cupressaceae family, such as the Great Basin bristlecone pine (*Pinus longaeva* Bailey), northern white cedar (*Thuja occidentalis* L.), eastern red cedar (*Juniperus virginiana* L.), and Qilian juniper (*Juniperus przewalskii* Kom.), in addition to many others (see Schaurer et al. 2001, Matthes et al. 2002). Many of these tree species are known for their great longevity, especially when growing on adverse environmental sites (Schulman 1954, Larson 2001). In many cases, the oldest individuals exhibit extensive cambial dieback where only a small strip of living stem tissue remains (Wright and Mooney 1965, Kelly et al. 1992, Matthes et al. 2008).

Partial cambial dieback is likely associated with a localized disruption in water and/or carbohydrate transport and may be associated with a sectored vascular architecture, where vertical sections of the shoot are spatially connected only to particular roots (Larson et al. 1993, 1994). Thus, xylem pathways are independent and isolated, where injury incurred on one section of the tree will only impact spatially connected sectors, and will not negatively affect other axes of the stem. The extent of sectoriality in terms of hydraulic pathways (i.e., sectored versus integrated) can vary between species, but high sectoriality appears to be common in plants growing in xeric environments, perhaps as a mechanism to reduce embolism spread (Zanne et al. 2006). While the factors initiating cambial dieback are dependent on the environmental hazards unique to a particular site, such as wind abrasion (Beasley and Klemmedson 1973, Schauer et al. 2001), soil erosion (LaMarche 1969), rockfall (Larson et al. 1993), or drought (Matthes et al. 2002), cambial dieback is a response to physiological stress in resource-limited and patchy environments (Larson et al. 1993, 1994, Matthes et al. 2002).

The question of whether, to what extent, and why partial cambial dieback influences not only measures of tree radial growth, but also the carbon balance in trees, has eluded

dendrochronologists over the last several decades (Graumlich 1991, Bunn et al. 2003). Some studies indicate a tendency for strip-bark trees to have gradual or step-change increases in ring-width records (Graybill and Idso 1993, Bunn et al. 2003, Ababneh 2006, Pederson et al. 2014, Hessl et al. 2018). However, there are still many uncertainties regarding the relationship between cambial dieback and radial ring width. First, comparisons of strip-bark and whole-bark growth forms have not been performed across many different species or sites, so there is no consensus on whether partial cambial dieback on tree stems consistently influences ring-width trends in strip-bark trees. Secondly, when tree-ring records are statistically treated (i.e., standardized) to produce dimensionless indices of growth, as is commonly done for climate reconstructions, biases or artifacts in tree-ring series can be introduced making it difficult to discern whether strip-bark and whole-bark radial growth trends are truly different, especially in recent centuries (Salzer et al. 2009). For example, a 20th century divergence between strip-bark and whole-bark bristlecone pine growth trends reported by Graybill and Idso (1993) was largely caused by their standardization methods (Salzer et al. 2009). Lastly, an explanation of why or how partial cambial dieback causes increasing radial growth trends in strip-bark trees remains unknown.

Several hypotheses have been proposed to explain increasing radial growth trends in strip-bark trees, but very few studies have directly tested these hypotheses. Graybill and Idso (1993) first proposed that strip-bark bristlecone pine trees uniquely exhibit a carbon fertilization signal, where radial growth increases in response to increasing atmospheric carbon dioxide (CO_2). This hypothesis has been debated, given the uncertainties regarding the radial growth of strip-bark trees (Graumlich 1991), and 20th century trend artifacts from the data treatment methods in the original study (Salzer et al. 2009). However, in many experimental environments, elevated CO_2 is shown to enhance photosynthesis and reduce stomatal conductance (e.g.,

Morison 1985, Ainsworth and Rogers 2007, Norby and Zak 2011). Yet in natural environments, while increases in intrinsic water-use efficiency (ratio of CO_2 assimilation to stomatal conductance) over the industrial period have been documented widely using carbon stable isotopes in tree rings, these increases do not coincide with improvements of radial growth rates (Andreu-Hayles et al. 2011, Peñuelas et al. 2011, Lévesque et al. 2014, Giguère-Croteau et al. 2019). Graybill and Idso (1993) hypothesized that strip-bark trees show a greater positive response to increasing atmospheric CO_2 because newly fixed carbon would be primarily allocated to the stem, whereas whole-bark trees might allocate more carbon to other sinks; for example, the root system on whole-bark trees could be a larger sink than that on a strip-bark tree. In terms of water-use efficiency inferred through tree-ring stable carbon isotopes, there was no significant difference between strip-bark and whole-bark bristlecone pine, though the question of potential differences in carbon allocation still remains open (Tang et al. 1999).

Another hypothesis for explaining the increasing ring-width trends observed in strip-bark trees might be that after cambial dieback occurs, the ratio between the crown (canopy) to active cambial area increases (Bunn et al. 2003). This could explain why strip-bark trees, with a smaller area of radial growth, have larger ring widths compared to whole-bark trees, which continue growing fully around the stem. However, this suggests that cambial dieback on the stem does not immediately result in a proportionate loss of canopy area, which opposes observations that active stem and canopy area remain relatively proportionate in strip-bark bristlecone pine (Wright and Mooney 1965).

Contributions of this dissertation to the existing literature

Better understanding the causes and physiology of partial cambial dieback will be essential for evaluating radial growth trends in strip-bark trees. If variance related to partial

cambial dieback is identified in tree-ring records, and is found to be unrelated to climate variability driving radial growth, then standardization methods should be established to account for and remove this additional variance. Ultimately, removing strip-bark biases in radial growth data will be essential for producing reliable estimates of past climate as many of the oldest trees at a site exhibit partial cambial dieback. In this dissertation, I decipher the complex climatic and morphological tree-ring signals contained within ancient strip-bark Siberian pine trees using tree-ring width and stable carbon and oxygen isotope records. Following these assessments, I develop statistical methods for attenuating strip-bark biases in tree-ring records for purposes of climate reconstruction.

The majority of this dissertation is focused on comparisons of strip and whole-bark Siberian pine from an ancient lava flow site ("Khorgo Lava") in central Mongolia. These trees have been instrumental for quantifying hydroclimatic variability over the Common Era, and provide significant insights on recent climatic changes in this region of arid Central Asia (Pederson et al. 2014, Hessl et al. 2018). We additionally evaluate strip-bark and whole-bark Great Basin bristlecone pine from two sites in the western United States (Mount Washington data shared by M. Salzer and A. Bunn, and Sheep Mountain data from Graybill and Idso, 1993) to test methods for reducing potential strip-bark biases in tree-ring data. This dissertation is formatted as follows:

Chapter 1 examines the timing and likely cause of partial cambial dieback in ancient Siberian pine from central Mongolia, and compares radial growth trends of strip-bark and whole-bark trees. Cambial dieback is common at this site during the cold, and somewhat dry, mid-19th century. It is hypothesized that cambial dieback is associated with cold-related stem injuries, especially on the southern side of tree stems, which are subjected to more intense solar radiation

and dramatic fluctuations in temperatures than other sides of the stem. After this 19th century period of widespread dieback, ring widths of strip-bark trees dramatically increase and diverge from ring widths of whole-bark trees. Thus, a causal link between cambial dieback and increasing ring widths in Siberian pine strip-bark trees is inferred.

Chapter 2 explores the potential physiological mechanisms behind the observed increases in strip-bark ring-width trends of Siberian pine relative to whole-bark trees. Using ring-width measurements and stable carbon and oxygen isotopes from annual tree rings, three hypotheses are tested: are increasing strip-bark ring widths associated with i) a different sensitivity to climate than whole-bark trees, ii) a different response to increasing atmospheric CO_2 than whole-bark trees, or iii) a sudden reduction in stem area after dieback occurs? Results from this chapter show that strip-bark and whole-bark trees respond similarly to increasing atmospheric CO_2 and climate variability, but dieback activity directly results in increasing ring widths and inferred stomatal closure in strip-bark trees. Based on these findings, it is hypothesized that cambial dieback leads to an increase in the ratio of leaf to sapwood (conducting) area in strip-bark trees. Cambial dieback events might periodically allow ancient trees to reduce their stem to a more 'sustainable' size and thus, might contribute to their impressive longevity.

As the first two chapters of this dissertation suggest that increasing ring-width trends in strip-bark Siberian pine are a direct manifestation of partial cambial dieback, it is important to remove such non-climatic variance from tree-ring series prior to reconstructing climate. Chapter 3 explores two standardization methods for reducing morphology-related biases in ring-width records of strip-bark trees. Here, these methods are tested on both Siberian pine from Mongolia and bristlecone pine from the western United States. Both methods successfully reduce low-frequency variability likely associated with cambial dieback, while retaining reliable low to

medium-frequency (inferred climate) variance found in whole-bark chronologies from each site. These newly developed standardization methods can be applied broadly to other sites or tree species, and can considerably improve the reliability of climate reconstructions estimated from sites where strip-bark biases are documented.

Chapter 1: Strip-bark morphology and radial growth trends in ancient *Pinus sibirica* from central Mongolia

Abstract

Some of the oldest and most important trees used for dendroclimatic reconstructions develop strip-bark morphology, in which only a portion of the stem contains living tissue. Yet the ecophysiological factors initiating strip bark and the potential effect of cambial dieback on annual ring widths and tree-ring estimates of past climate remain poorly understood. Using a combination of field observations and tree-ring data, we investigate the causes and timing of cambial dieback events in *Pinus sibirica* strip-bark trees from central Mongolia and compare the radial growth rates and trends of strip-bark and whole-bark trees over the past 515 years. Results indicate that strip bark is more common on the southern aspect of trees and dieback events were most prevalent in the 19th century, a cold and dry period. Further, strip-bark and whole-bark trees have differing centennial trends, with strip-bark trees exhibiting notably large increases in ring widths at the beginning of the 20th century. We find a steeper positive trend in the strip-bark chronology relative to the whole-bark chronology when standardizing with age-dependent splines. We hypothesize that localized warming on the southern side of stems due to solar irradiance results in physiological damage and dieback and leads to increasing tree-ring increment along the living portion of strip-bark trees. Because the impact of cambial dieback on ring widths likely varies depending on species and site, we suggest conducting a comparison of strip-bark and whole-bark ring widths before statistically treating ring-width data for climate reconstructions.

Citation:

Leland, C., Cook, E.R., Andreu-Hayles, L., Pederson, N., Hessl, A., Anchukaitis, K.J., Byambasuren, O., Nachin, B., Davi, N., D'Arrigo, R. and Griffin, K., 2018. Strip-Bark Morphology and Radial Growth Trends in Ancient *Pinus sibirica* Trees From Central Mongolia. *Journal of Geophysical Research: Biogeosciences*, *123*(3), pp.945-959. https://doi.org/10.1002/2017JG004196

1.1 Introduction

Many of the oldest living trees in the world, and those most useful for climate reconstructions, persist under extremely cold and dry environmental conditions (Schulman 1954, LaMarche 1969). Ancient trees living near the margin of their environmental tolerances can be exceptionally slow growing, and can have sinuous, stunted stems and limited foliage (Bailey 1970, Kelly et al. 1992, Swetnam and Brown, 1992, Stahle, 1996). Strip-bark morphology, also known as partial cambial dieback, is another characteristic common among old trees growing in harsh environments. In contrast to whole-bark trees with a complete living cambium, strip-bark trees have discontinuous radial growth, exhibit strips of dead and living tissue along the stem, and have eccentric growth patterns (Schulman 1954, LaMarche 1969, Esper 2000). Strip-bark morphology has been noted in *Pinus aristata* Engelm*, Pinus longaeva* Bailey, and *Pinus balfouriana* Grev. & Balf. in the Pinaceae family, and some *Thuja spp.* and *Juniperus spp.* in the Cupressaceae family, among others (Matthes et al. 2002).

Strip-bark morphology is initiated by a localized disruption in resource transport, which ultimately results in cambial dieback along a vertical axis of the tree (Larson et al. 1993, 1994, Matthes et al. 2002, Matthes and Larson 2009). Strip-bark *Thuja occidentalis* L., for example, has a sectored radial architecture where shoot segments are directly connected to particular roots (Larson et al. 1993, 1994). These vertical segments are independent from other portions of the stem. Thus, root mortality might only result in death of the corresponding shoot segment while the remainder of the tree continues to grow. This type of physiology, in which only vulnerable portions of the cambium die, could allow trees to survive in adverse sites with spatially variable or transitory resources (Larson et al. 1993, 1994, Matthes et al. 2002).

The factors initiating cambial dieback in trees likely depend on a suite of environmental hazards and physiological traits. Strong winds can cause localized injury to a stem via blowing ice or dirt particles that abrade leaves or shoots, or more directly through tree swaying and root mortality (LaMarche 1969, Beasley and Klemmedson 1973, Schauer et al. 2001, Boyce and Lubbers 2011). As a result, some high-elevation trees experience dieback along the side exposed to prevailing winds (Jacoby et al. 1996, Schauer et al. 2001). In cliff environments, rockfall and root exposure can cause root mortality and subsequent dieback along the spatially-connected shoot system (Kelly et al. 1992, Larson et al. 1993, Matthes et al. 2002). However, experiments revealed that root loss may not necessarily lead to sectored bark stripping, suggesting that other factors could trigger stripping events (Matthes and Larson 2009). Tree age, size, and cellular structure are also cited as attributes that can predispose trees to bark stripping on particular individuals or species (Kelly et al. 1992, Schauer et al. 2001, Matthes et al. 2002). Earlywood tracheid pits were larger in mature *T. occidentalis* trees relative to young trees, indicating that older trees might be at a higher risk of drought-induced sapwood cavitation and stem stripping (Matthes et al. 2002). Wood anatomy of ancient *P. longaeva*, however, did not change as a function of age (Connor and Lanner 1990). Although there are no universal factors that initiate partial cambial dieback across all sites and species, evidence suggests that strip bark is triggered by some degree of environmental and physiological stress.

The effect of localized cambial dieback on radial growth of the living portion of the stem, if any, remains uncertain across different species. Absolutely dated annual tree rings provide information on changes in radial growth rate through time and are valuable for reconstructing past climate when tree growth is limited by target climate variables (Fritts 1976, Cook and Kairiukstis 1990). Given that strip-bark trees can be found at sites targeted for dendroclimatic

studies, there is a need to determine whether partial cambial dieback in trees can alter the trajectory of radial growth of the living stem subsequent to cambial dieback events, and consequently alter estimates of past climate. Differences in radial growth rates between strip-bark and whole-bark trees could reflect morphological adjustments in strip-bark trees after dieback, where a reduction of operable stem circumference leads to higher growth rates along the remaining living axis. However, if the percentage of living cambium remains in proportion to the amount of foliage on the crown (Wright and Mooney 1965), or if root-shoot carbon allocation is different in trees with partial cambial mortality (Graybill and Idso 1993), the influence of dieback on annual growth of the remaining stem is uncertain.

Several studies have investigated radial growth rates of strip-bark and whole-bark trees over different time scales. Ring widths of *T. occidentalis*, for example, drastically increased in the few years following cambial dieback events (Kelly et al. 1992). Over longer timescales, Bunn et al. (2003) found that the growth rate of strip-bark *Pinus albicaulis* Engelm. trees exceeded whole-bark trees starting around 1875. Graybill and Idso (1993) compared standardized chronologies of strip-bark and whole-bark *P. longaeva* trees and reported more positive trends in strip-bark trees during the 20th century. However, using unstandardized (raw) ring width data, Salzer et al. (2009) found that the 20th century trends between the two populations were the same. Standardization removes or reduces biological trends in the raw tree-ring data, but these data processing techniques can introduce differences in recent strip-bark and whole-bark trends that are not evident in raw ring-width data (Salzer et al. 2009). Despite similar growth rates and trends in the modern period, comparatively larger raw ring-widths are evident in whole-bark *P. longaeva* trees in earlier centuries (Ababneh 2006, Salzer et al. 2009), which can be due to younger trees comprising the whole-bark population (Salzer et al. 2009), leading to

relatively steeper trends in strip-bark trees over the past several centuries. Other studies have also noted positive trends in raw ring-width data of strip-bark trees compared to whole-bark trees from the same site (Pederson et al. 2014, Yang et al. 2014).

The relationship between partial cambial dieback and radial ring width remains unclear, especially as it applies to different species or sites with different environmental stressors. Strip-bark morphology is a common feature in ancient Siberian pine (*Pinus sibirica* Du Tour) trees growing on the Khorgo lava field in central Mongolia (Figs. 1.1 and 1.2). These drought-sensitive trees are valuable for reconstructions of past hydroclimate, and some appear to contain long-term positive growth trends that may be related to strip-bark morphology (Pederson et al. 2014). However, radial growth comparisons of strip-bark and whole-bark trees from this site have not been explicitly tested using living trees known to have a partial or full cambium. To better understand strip-bark morphology and its effect on ring widths, here we determine the timing and potential cause of cambial dieback events on the Khorgo lava field, and compare radial growth rates and trends of living *P. sibirica* whole-bark and strip-bark trees. These findings will help improve our understanding of the environmental factors that stress long-lived trees, allow us to better identify morphology-related (non-climatic) signals in tree-ring data, and refine our reconstructions of past climate through reducing uncertainty in long-term radial growth variability and trends.

1.2 Materials and Methods

1.2.1 Field collection

We collected increment cores and field data from trees growing on the Khorgo lava field located in the northern Khangai Mountains of central Mongolia (Fig. 1.1; 48.16° N, 99.84° E, elevation: ~2060 m asl). The sampled study area has complex microtopography and hydrology

imposed by underlying basalt. The forest growing on Khorgo is dominated by widely-spaced *P. sibirica* and *Larix sibirica* trees, many of which show classic old-growth characteristics, such as stunted and twisted (spiral grain) morphology, spiked tops, and strip bark (Swetnam and Brown 1992, Pederson 2010; Fig. 1.2). Spiral grain due to cell reorientation is a common feature of old trees growing in rocky soils with heterogeneous resource supply, and facilitates the distribution of sap and sugar to multiple parts of a tree (Kubler 1991). In these spiral-grained individuals, dieback takes a winding path from the base to the crown following the tree grain. Some trees at Khorgo grow directly on exposed lava rock, while others inhabit "islands" of soil development, likely self-created by litter accumulation and root action. Whole-bark trees tended to grow in areas with thicker soils and were often spatially clustered, whereas strip-bark trees were found in both environments.

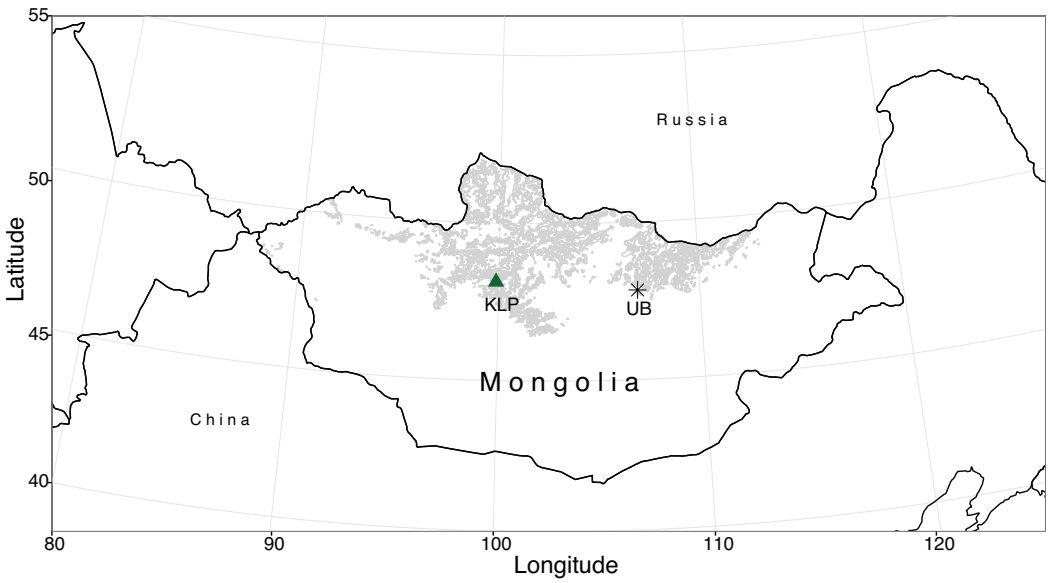

Fig. 1.1. Map of Mongolia showing the Khorgo lava field study site (green triangle, "KLP") and the capital Ulaanbaatar ("UB") 530 km to the east of KLP. The light gray shading illustrates forest cover in Mongolia.

We extracted increment cores from 45 strip-bark and 46 whole-bark *P. sibirica* trees. A tree was classified as strip-bark if cambial dieback could be traced along the entire vertical

length of the stem extending to the crown. For each strip-bark tree, we took an "A" and "B" core from breast height of the living side near the axis of dieback and opposite the side of dieback, respectively. A "D" (for "dead") core was collected from the dead side of strip-bark trees only to estimate the year of cambial dieback along the sampled axis. The percentage of dead cambium along the circumference of each tree at breast height was estimated and recorded. Additionally, we noted the range of aspects showing dieback (dead stem) along the circumference at the base and breast-height of each strip-bark tree. Dieback at both heights was documented to account for the spiral grain of some strip-bark trees (Fig. 1.2) and the possibility that environmental disturbances could initiate dieback along different heights of the stem. In terms of whole-bark trees, nearly all mature trees had some evidence of dead roots or isolated dieback at the crown, thus trees were only classified as whole-bark if ≥95% of the stem retained living cambium. We collected two cores per whole-bark tree, at opposing sides when possible, and perpendicular to the underlying slope of the terrain or lean of the tree (if present).

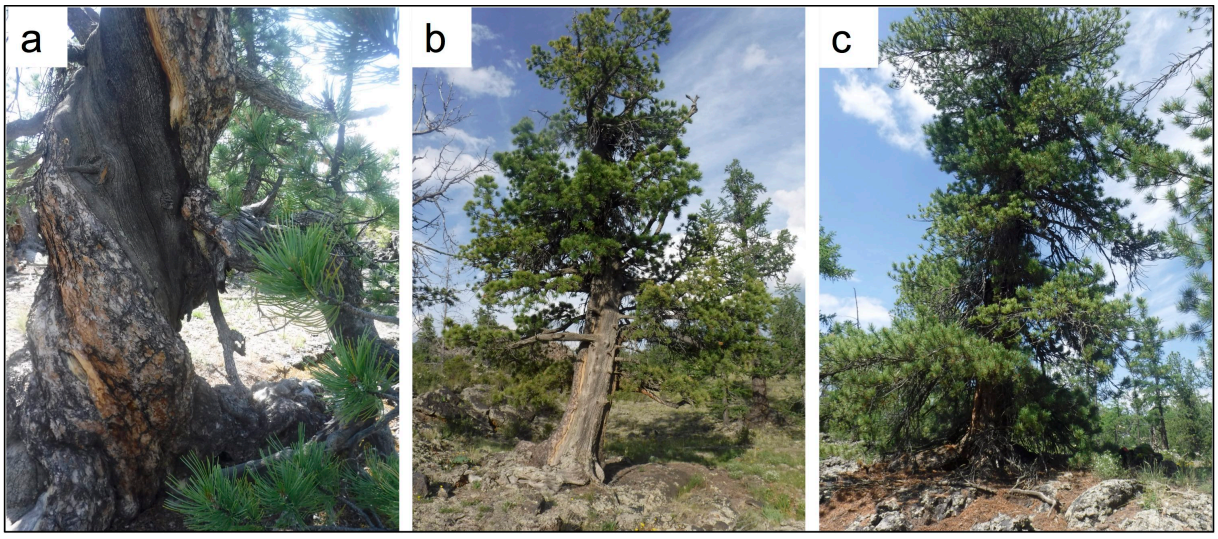

Fig. 1.2. Examples of *Pinus sibirica* trees sampled from Khorgo. Trees with strip-bark morphology had spiral (a) or straight (b) growth forms. Whole-bark trees (c) often had large, full canopies.

1.2.2 Laboratory methods

Increment cores were prepared for analysis using standard dendrochronological methods in the laboratory (Stokes and Smiley 1968). Cores were visually cross-dated, and the software program COFECHA was used to ensure accurate dating of each series (Holmes 1983). Many whole-bark samples came from younger, fast-growing trees, so cores with <315 rings (inner ring date after 1700 CE) were excluded from further analysis to reach a median tree series length comparable to the generally older strip-bark trees. All strip-bark trees were retained, including some cores with fewer than 315 rings; these cores came from trees that were visibly much older, but were rotten or hollow and thus were missing some inner growth rings. Some individual series were excluded due to gaps caused by rotten wood, the loss of outer rings during field collection, or in two cases, because extreme growth suppression precluded dating over several decades. However, all excluded strip-bark series had another core from the same tree that was included in our analysis. Additional analyses were conducted using exclusively strip-bark and whole-bark cores with >515 rings (at least back to 1500 CE) to evaluate growth patterns from the oldest trees.

In total, 45 strip-bark trees (78 series) and 35 whole-bark trees (60 series) were retained for analysis using the outlined criteria. The strip-bark series spanned the years 1022-2014 CE and retained a strong common signal back to 1215 (Expressed Population Signal, EPS >0.85 using 50-year windows with overlapping 25-years; (Wigley et al. 1984). The whole-bark series extended from 1297-2014 CE, and had an EPS > 0.85 back to 1315. The median series lengths of the strip-bark and whole-bark chronologies were 491 and 407 years, respectively.

1.2.3 Analysis

To ascertain the potential causes of strip bark at Khorgo, we determined the cardinal direction and timing of cambial dieback across all trees. Estimated cambial death dates were plotted through time to determine if dieback events clustered around a similar time period, were randomly dispersed, and/or occurred during particular climatic events. Only approximate dieback dates could be determined due to erosion and decay on the dead side of the tree over time leading to potential loss of outer growth rings. Additionally, a gradual spreading of strip bark across the tree over time might result from multiple successive stripping events (Bunn et al. 2003). The former uncertainty implies that dieback estimates will pre-date the occurrence year, whereas the latter uncertainty suggests that dieback estimates will be related to the coring location. The "D" cores were taken wherever we could attain a quality sample from the strip of dead cambium, which ranged from the center of the dead strip, to near the intersection with living cambium. These uncertainties preclude a direct year-to-year comparison between dieback dates and climate anomalies. Consequently, we analyze broader temporal associations between climatic conditions and large-scale dieback phenomenon. A June-July temperature reconstruction from the Ondor Zuun Nuruu site in Northern Mongolia (Davi et al. 2015) and a June-September self-calibrating Palmer Drought Severity Index (scPDSI) reconstruction derived from a separate and independent set of samples from Khorgo trees (Pederson et al. 2014) were used to investigate the climatic conditions during dieback events from 1500-2005 C.E. The scPDSI represents relative moisture availability, where negative (positive) values indicate drier (wetter) conditions (van der Schrier et al. 2013). The number of dieback events during a moving 30-year window was compared to the average reconstructed temperature and scPDSI for each corresponding window of time.

Strip-bark and whole-bark radial growth patterns and rates were first compared using raw ring-width data. Analyzing raw ring-width data is a common approach for dendroecological

studies seeking to evaluate radial growth patterns (Fritts and Swetnam 1989, Bunn et al. 2003) while preventing standardization-related artifacts in trends of tree-ring data (Cook and Peters 1997, Salzer et al. 2009, Briffa and Melvin 2011). First, the means and 95% bias-corrected and accelerated (BCa) bootstrap confidence intervals (Efron 1987) were computed for raw ring-width measurements of all strip-bark and whole-bark trees separately to compare radial growth rates between the two populations. This analysis was performed on all selected cores and a subset of cores with >515 rings from both groups (see section 1.2.2). Regional curves developed from age-aligned series (Briffa et al. 1992) were also produced for the strip-bark and whole-bark populations to compare growth trajectories with increasing cambial age. In this analysis, we only included cores that either reached pith, or appeared to have rings with clear curvature nearing pith.

We conducted multiple analyses on the strip-bark trees alone to evaluate the range of ring-width variability within this population. First, strip-bark samples were divided into terciles based on the percentage of cambial dieback along the stem, and mean ring widths and 95% BCa bootstrap confidence intervals were compared among the three groups. Then, bootstrapped means and 95% confidence intervals were calculated for the "A" and "B" strip-bark cores separately to determine if the position along the stem (i.e., near to or distant from the dieback axis) influences mean ring widths. Strip-bark trees with only a narrow strip of active cambium along the stem required us to collect the "B" core nearly adjacent to the "A" core, so these trees (n=17) were not included in this analysis.

We also compared whole-bark and strip-bark standardized chronologies to assess how residual trends in the populations differ after removing the overall allometric radial growth trends from the individual series. All series were standardized using signal free (SF) methods

(Melvin and Briffa 2008) with a time-varying spline (Melvin et al. 2007) with an initial stiffness of 50 years. This detrending method removes early allometric trends, and stiffens through time to retain longer-term trends at the end of series, which theoretically should be related to climate. SF indices were estimated as residuals of the power-transformed ring widths from the fitted detrending curves (Cook and Peters 1997), and final robust mean chronologies were produced using the RCSigFree program (http://www.ldeo.columbia.edu/tree-ring-laboratory/resources/software). The SF and residuals methods were selected to reduce the amount of bias and trend distortion that can occur as a result of standardization, particularly at the ends of tree-ring series (Cook and Peters 1997, Melvin and Briffa 2008). Trend distortion occurs when tree-ring variance related to climate affects the fitting of detrending curves used for removing non-climatic variance, and can therefore result in the distortion of some climate-related variance in the final tree-ring chronology (Melvin and Briffa 2008). SF standardization iteratively removes the common chronology signal from tree-ring measurements to improve fitted standardization curves and produce a robust mean chronology with reduced trend distortion relative to traditional or standard methods (Melvin and Briffa 2008).

A strip-bark and whole-bark chronology was computed using all series from each group, and we applied a non-parametric Mann-Whitney U test to determine whether there were significant differences in the indices over each century of analysis. Chronologies using a subset of series with >515 years from each group were also compared. Next, a dynamic linear regression using the Kalman filter (Kalman 1960, Visser and Molenaar 1988, Petris and An 2010, Visser et al. 2010) was employed to assess the time-dependent relationship between the whole-bark chronology as a "target" predictor variable, and the strip-bark chronology as the dependent variable. The whole-bark chronology, in this case, is assumed to be the control with

no (or negligible) influence of physiological dieback on ring-width variability. Through estimating time-varying regression coefficients, this method tests how the index values of strip-bark and whole-bark chronologies change relative to one another through time and can be used to determine whether there are periods of time in which their trends diverge. Chronology comparison and the Kalman filter analysis were also applied to strip-bark and whole-bark chronologies developed from standard (i.e. not SF) methods, otherwise using the same standardization scheme, to compare with our SF results.

1.3 Results

1.3.1 Cambial dieback

Cambial dieback occurred along all aspects of strip-bark trees, but was more frequent on the southern side of the stems (Fig. 1.3). South-facing dieback was particularly dominant along the base of all strip-bark trees, and for a subset of those with straight (i.e., not spiral-grained) strip-bark morphology. The breast-height measurements, which are different than basal measurements due to the spiral grain of some strip-bark trees, show more dieback along the south and west-facing aspects (Fig. 1.3). Approximate dieback dates were detectable for 40 of the 45 (89%) strip-bark trees studied. The remaining "D" (dead) cores had extremely suppressed rings at the modern end and could not be reliably dated. The dieback events were scattered throughout the 1500-2014 period, however, 45% of all cambial mortality events occurred in the 19th century (Fig. 1.4a, Supplemental Fig. A.1a). This peak in dieback events is also apparent when controlling for declining sample depth through time (Supplemental Fig. A.1b). The peak density of these events in the mid-1800s (Fig. 1.4a) follows two of the coldest (Davi et al. 2015; Fig. 1.4b) and one of the driest (Pederson et al. 2014; Fig. 1.4c) non-overlapping 30-year periods of summertime climate. Dieback events were more common during 30-year periods of below-

average temperatures, but there was no consistent pattern with moisture conditions (Fig. 1.4d, vertical and horizontal lines represent mean temperature and scPDSI, respectively, over the 1500-2005 common period).

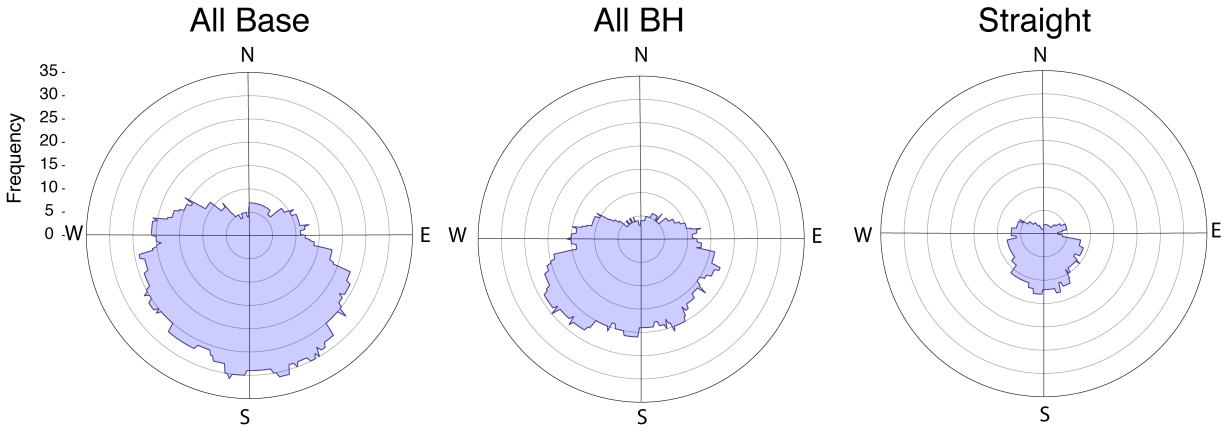

Fig. 1.3. Polar plots showing the frequency of trees (out of 45 total trees) with evidence of strip-bark morphology along all compass directions. Dieback at the base (left) and breast height (middle) of all strip-bark trees, and only those with straight strip-bark morphology (right), are shown. Each nested circle, moving outward from the center, represents an incremental increase of five trees showing dieback.

1.3.2 Comparison of mean ring-width trends

The mean ring-width chronologies of strip-bark and whole-bark trees are strongly coherent on interannual and decadal time scales from 1500 to 2014, but have differing centennial-scale trends. After prewhitening each chronology using the minimum Aikaike information criterion (AIC) to select the autoregressive (AR) model order (Akaike 1974), the chronologies are strongly and significantly correlated on the interannual scale ($r=0.90$, $p<0.001$). However, the strip and whole-bark chronologies have markedly different long-term growth trends from 1500 to 2014 (Figs. 1.5a and 1.5b). The whole-bark chronology has a persistent decreasing trend not shared by the strip-bark chronology. The mean ring width of strip-bark trees

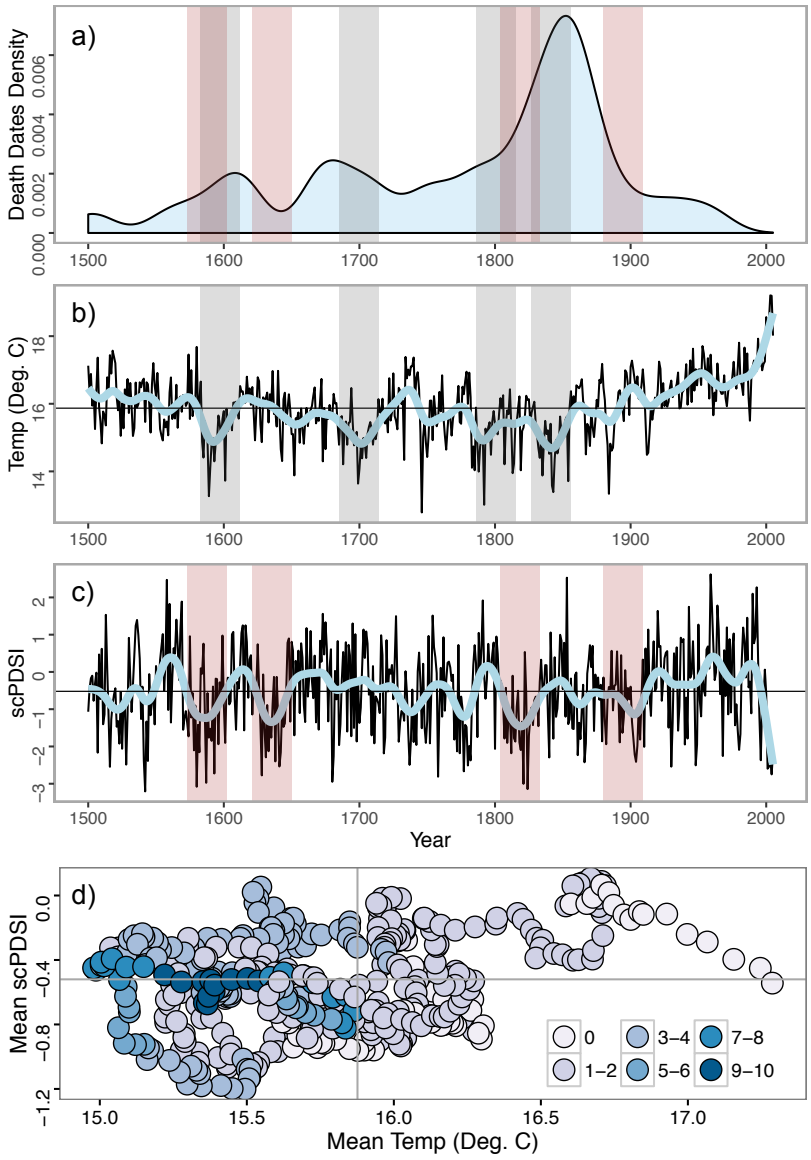

Fig. 1.4. Comparison of death date estimates with climate. a) Density of dieback dates from individual strip-bark trees over time; b) June-July temperature reconstruction from Ondor Zuun Nuruu in Northern Mongolia (Davi et al. 2015) with a 50-year smoothing spline in blue; c) June-September scPDSI reconstruction derived from independent Khorgo trees (Pederson et al. 2014), and a 50-year smoothing spline in blue; Gray bars highlight the four coldest 30-year periods based on non-overlapping windows, and pink bars represent the four driest 30-year periods. Panel d) shows the number of death dates occurring in each 30-year moving window, plotted against the mean temperature and drought index for each corresponding period. Vertical and horizontal grey lines in panel d represent the long-term common period (1500-2005) mean for temperature and scPDSI, respectively.

oscillates around 0.3 mm/year across the entire record until the early 20th century when it suddenly increases and significantly exceeds the whole-bark mean ring-width chronology (Figs. 1.5a and 1.5b). Moreover, when using series from older trees (with > 515 rings), strip-bark trees significantly exceed whole-bark trees starting in the mid-1800s (Supplemental Fig. A.2).

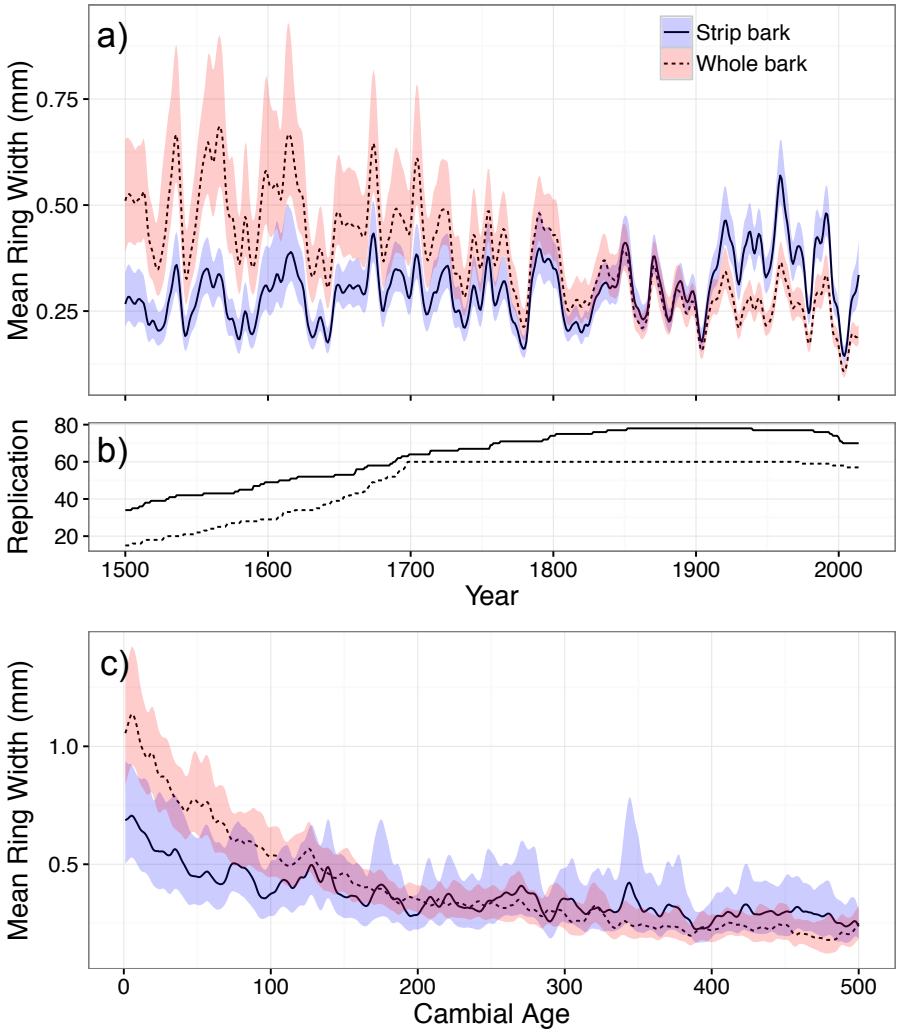

Fig. 1.5. Mean ring-width comparisons of strip-bark and whole-bark trees. a) A 10-year spline of strip-bark (solid line) and whole-bark (dashed line) mean ring-width chronologies from 1500-2014. The 95% BCa bootstrap confidence intervals around the mean are shown in blue and pink for strip-bark and whole-bark trees, respectively. b) The number of strip-bark (solid) and whole-bark (dashed) series over time corresponding to figure a. c) Age-aligned regional curves for strip bark (n=22) and whole bark (n=25) series, shown with 95% BCa bootstrap confidence intervals.

Regarding age-aligned regional curves, based only on series reaching or nearing pith, both strip-bark and whole-bark trees show a decreasing allometric ring-width trend. Strip-bark ring widths rapidly stabilize after a cambial age of ~200 years, whereas whole-bark trees have larger rings at a young cambial age and a more rapid ring-width decline that continues to decrease with increasing cambial age (Fig. 1.5c).

Separating the strip-bark trees into terciles based on percentage of cambial dieback yields low (7-23%; n=26 series), medium (23.1-40%; n=26 series), and high (40.1-81%; n=26 series) dieback groups. High dieback trees have larger mean ring widths across some periods of time, particularly in the early 1600s and mid-to-late 1900s, followed by the medium, and low dieback trees, though these differences are not consistent (Fig. 1.6a). In comparing "A" and "B" cores of strip-bark trees (Fig. 1.6b), the "A" cores near the region of cambial dieback have a higher positive slope from 1500 to 2014 ($\beta = 0.00028$, in units of mm/year, $p<0.001$) relative to the "B" cores ($\beta = 0.00007$, $p<0.001$). The "A" cores had smaller mean ring widths than "B" cores until the 20th century, though the 95th percentile confidence interval of "A" cores also exceeded the same confidence limit for "B" cores during the early 1600s. Even though the "B" cores had a smaller positive slope than "A" cores, the mean ring widths of "B" cores alone still significantly exceeded whole-bark ring widths starting in the 20th century ($p<0.05$, Supplemental Fig. A.3).

1.3.3 Comparison of standardized chronologies

The SF standardized chronologies of strip-bark and whole-bark trees show differing trends over the past several centuries. The strip-bark standardized chronology has lower or equivalent index values relative to the whole-bark standardized chronology until the mid 19th to early 20th century (Fig. 1.7a). The strip-bark and whole-bark chronologies have significantly different index values only in the 16th ($W= 4027$; $P_{wilcox} = 0.0180$), and 20th ($W= 7047$; $P_{wilcox} =$

<0.001) centuries (Supplemental Table A.1). Further, the strip-bark chronology has a higher slope over the full 1500 to 2014 period relative to the whole-bark chronology (β = 0.00093 and 0.00019, in units of index value/year, respectively). Results are similar when using standard chronologies developed with traditional methods rather than SF methods; the strip-bark chronology slope is higher than that of whole-bark trees (β = 0.00061 and 0.00005, respectively; Supplemental Fig. A.4c). However, differences between strip-bark and whole-bark standard indices are significant only in the 20th century (W=6713; P_{wilcox}<0.001; Supplemental Table A.1.)

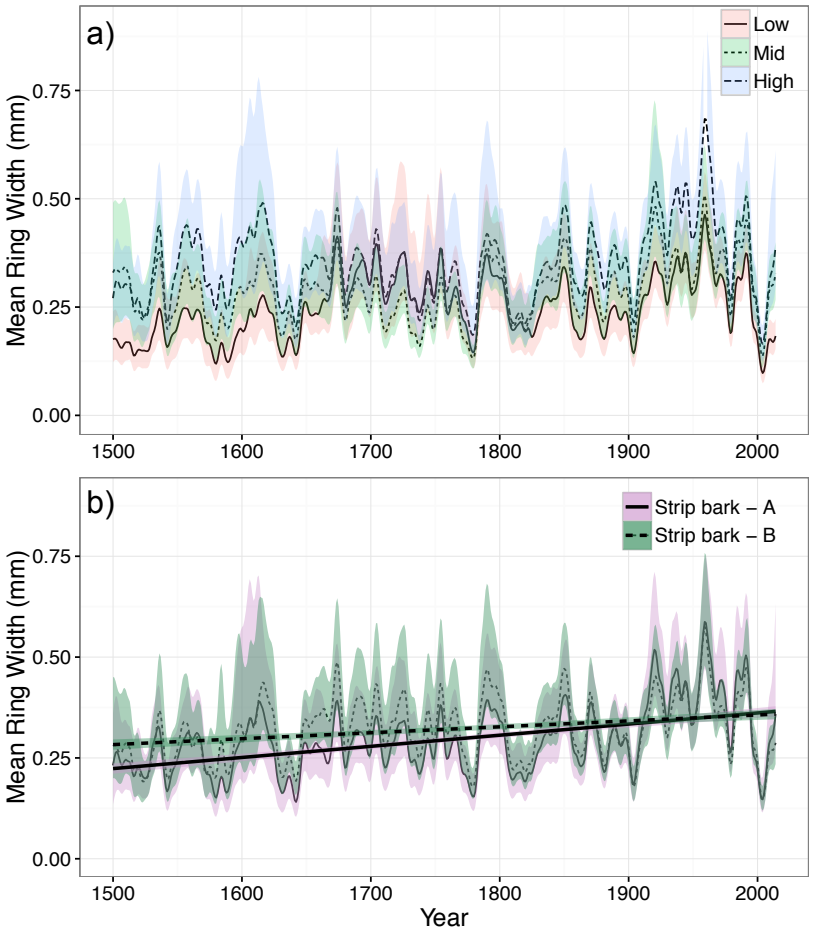

Fig. 1.6. Mean ring-width comparisons between and within strip-bark trees. a) Mean ring width of all series for trees with a low (7-23%), medium (23.1-40%), and high (40.1-81%) percentage of cambial dieback, with 95% BCa bootstrap confidence intervals (pink, green, and blue, respectively). b) Mean and 95% BCa bootstrap confidence intervals for "A" (solid, purple) and "B" (dashed, green) cores from strip-bark trees. "A" cores were taken near the dead strip and "B" cores were taken opposite of the dead strip.

There is an overall positive trend in dynamic regression slope between strip-bark and whole-bark SF chronologies from 1500 to 2014 (Fig. 1.7b), indicating that strip-bark indices are steadily increasing relative to whole-bark indices. However, this general trend is punctuated by

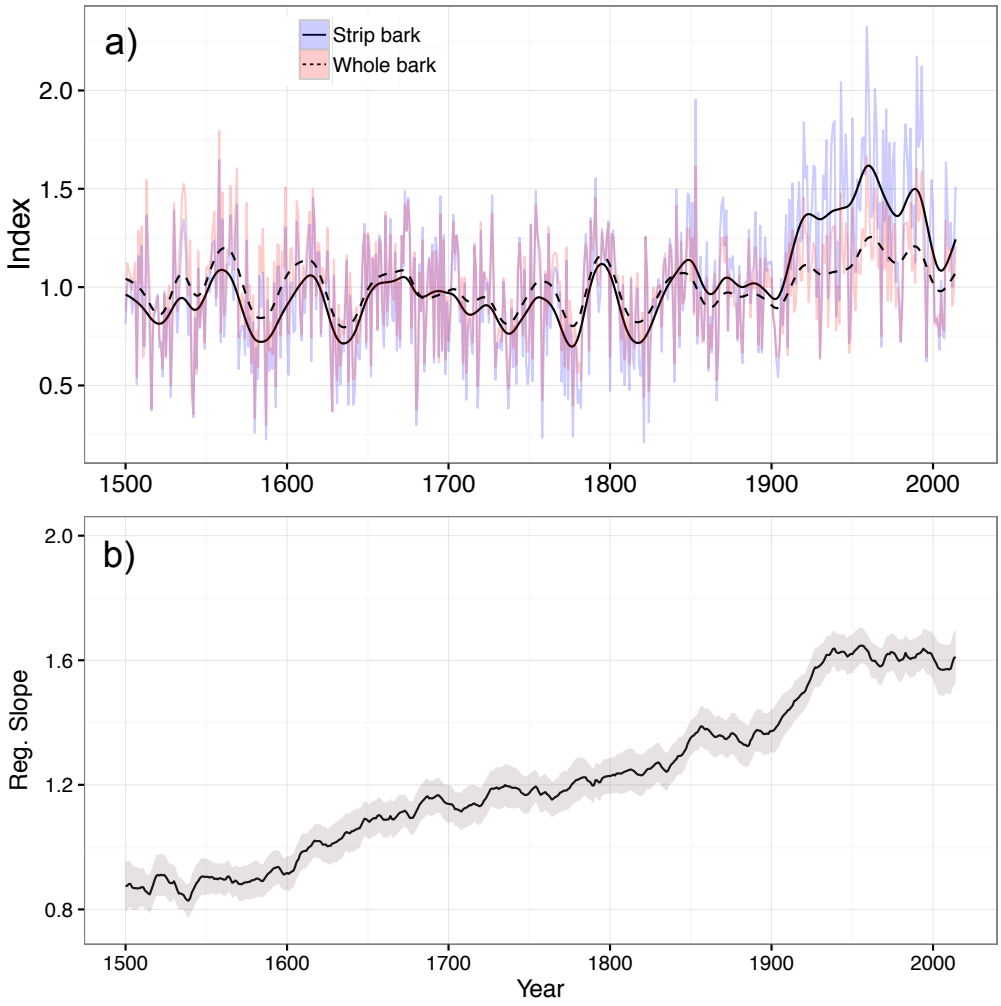

Fig. 1.7. Standardized chronologies of strip-bark and whole-bark trees and their relationship over time. a) Strip-bark (blue with solid 30-year spline) and whole-bark (pink with dashed 30-year spline) signal free chronologies for all cores. b) Dynamic regression coefficients for a model relating Khorgo strip-bark and whole-bark chronologies, with gray shading representing a 95% confidence interval. The increase in regression slope through time indicates a gradual increase in the index values of strip-bark trees relative to whole-bark trees.

periods of rapid increases, steady plateaus, and short-term decreases in the coefficients through time. Notably, the early 1600s, mid-1800s, and early 1900s, following cold and dry periods (Figs. 1.4b and 1.4c) show a rapid increase in regression coefficients, indicating a sudden surge in the strip-bark chronology compared to the whole-bark chronology. While there is a particularly sudden and steep increase in regression coefficients during the early 20th century when using all cores to develop the chronologies (Fig. 1.7b), this effect is more gradual when only including the longest cores (>515 rings) (Supplemental Figs. A.4a and A.4b). These temporal patterns of dynamic regression coefficients between strip-bark and whole-bark chronologies are also evident with standard chronologies (Supplemental Figs. A.4c and A.4d).

1.4 Discussion

In this study, we investigate the cause and timing of partial cambial dieback in *P. sibirica* trees from central Mongolia and evaluate whether dieback can affect tree-ring widths on the remaining portion of stems. Our results indicate that cambial dieback was most abundant on the southern side of stems and occurred most frequently during the 19th century, when there were periods of unusually cold growing-season conditions. Following this period, ring widths of strip-bark trees significantly exceeded whole-bark trees, indicating a potential link between tree morphology and radial growth trends. These findings have important implications for the use of *P. sibirica*, or other trees with morphology-related growth trends, in climate reconstructions.

1.4.1 Proposed cause and timing of dieback

The causes of cambial dieback leading to strip-bark morphology are not well understood across a range of different tree species and environments. Trees on the Khorgo lava field in central Mongolia are exposed to a number of environmental hazards throughout the year, many of which could cause cambial dieback. The predominance of cambial dieback on the southern

side of trees suggests that the primary environmental drivers of strip bark are unidirectional. One key driver might be solar radiation, which can cause the sunlit (southern) side of the tree to warm several degrees more than the northern side of the tree during mid-day (Harvey 1923, Sakai 1966), particularly in locations such as Khorgo, where trees are exposed and have little relief from direct sun.

There are several ways in which differential radiation and warming could result in physiological damage and subsequent dieback on the southern side of stems. Freeze-thaw dynamics can cause severe and localized physiological injuries to trees. For example, in the eastern United States, freeze-thaw dynamics, in combination with direct sublimation or evaporation from xylem units, were shown to result in localized emboli formation on the southern side of *Acer saccharum* trees during the winter (Sperry et al. 1988). While conifers have anatomical features that can increase resistance to xylem cavitation relative to some woody angiosperms, often resulting in lower rates of embolism (Sperry and Sullivan 1992, Sperry et al. 2006), severe freeze-thaw embolism has been reported in many coniferous species, particularly under severe drought conditions (Mayr et al. 2002, 2003) or during periods with reduced insulating snow cover (Beier et al. 2008). If warmer localized temperatures initiate earlier cambial reactivation of trees (Oribe and Kubo 1997, Oribe et al. 2003, Begum et al. 2008) and earlier cambial division on the southern side of stems, this region could be even more vulnerable to cavitation and hydraulic disruption. Many conifers can sufficiently recover from wintertime hydraulic stress via tracheid refilling (Sperry et al. 1994, Mayr et al. 2014); however, concurrent drought conditions or high embolism rates might make recovery more difficult.

Sunscald is another unidirectional and sun-related injury where cambium and bark can separate from the wood (Sakai and Larcher 1987). Solar radiation can warm, and prematurely

deharden the southern side of trees in early spring, effectively decreasing the freezing tolerance of tissues (Kramer and Koslowski 1979, Harvey 1923, Sakai and Larcher 1987). If re-freezing occurs, cambial death on the south side of trees can follow, and phloem tissue can be damaged; this blocks sugar translocation along the stem, and bark peeling and exposure can introduce pathogens, which can lead to additional deterioration on the injured side of the stem (Kramer and Koslowski, 1979). Therefore, it is possible that injuries related to solar radiation and direct heating of the southern side of stems could have initiated localized mortality and strip-bark morphology on the *P. sibirica* stems studied here.

The peak of dieback events occurred during the 19th century, when central Mongolia experienced extremely cold conditions in addition to some severe droughts (Pederson et al. 2014, Davi et al. 2015). We can only comment on past summer climatic conditions because the tree-ring based reconstructions estimate June-July temperature and June-August scPDSI. However, the June-August period represents the vast majority of the growing season in this region (Davi et al. 2006, De Grandpré et al. 2011). Although we do not have paleoclimatic information specifically for the earliest portion of the growing season, when trees might be especially susceptible to freezing injuries, we hypothesize that trees during the 19th century were exposed more often to inhospitable temperatures during all periods of radial growth. If cold temperatures were combined with dry (and possibly sunny) conditions, as identified during some periods of the 1800s, trees might have been at a higher risk of unidirectional stem injury. In contrast to the high dieback rate in the 1800s, there were only three of 40 recorded dieback events in the 20th century, a period of relatively warmer and wetter climatic conditions (Davi et al. 2006, Pederson et al. 2014).

Although variation in solar radiation and climate could have contributed to the strip-bark phenomenon due to the prevalence of south-facing dieback, some trees experienced dieback exclusively on other sides of the stem indicating that other environmental factors could be important as well. In particular, some of the spiral-grained trees had dieback along south-west facing aspects at breast height. Spiral-grain morphology leads to an additional complication when determining cause of dieback initiation because ribbons of dieback migrate around the stem with height. It is possible that blowing ice particles and dust from surface winds, which arrive primarily from the west at Khorgo (Supplemental Fig. A.5; Rienecker et al. 2011, Molod et al. 2015) could have contributed to west-facing dieback near breast height on some of these stems. Differing local and/or seasonal wind directions could have affected other sides of some trees as well. Jacoby et al. (1996) noted partial cambial dieback on the northern side of Siberian pines from a tree-line site in the Tarvagatay Mountains of Central Mongolia and suggested that northerly winds were the likely driver of dieback on these trees, which were growing on a north-facing slope. Prevailing surface wind was also found to be a dominant contributor to dieback in *P. aristata* trees from other environments (Schauer et al. 2001, Boyce and Lubbers 2011). Regardless, the preponderance of dieback on the southern base of trees with and without spiral grain suggests that the dominant stressor affects primarily the south-facing side of trees. Further, the clustering of dieback events through time might indicate that temporally variable environmental factors, such as climate, are likely important contributors of dieback.

Microsite characteristics on the lava, such as underlying soil conditions or topography, or variation in snow depth or relative moisture, may put particular individuals at risk of cambial mortality. Initial observations at Khorgo suggest that strip-bark trees tend to grow on more stressed microsites, with thinner soil development. Bunn et al. (2003) found that the topographic

convergence index (a soil moisture proxy) can explain some of the spatial patterning of strip-bark *P. albicaulis* trees; however, they suggest that strip-bark trees might cluster on wet sites because these individuals might not survive on more adverse sites. Future research should further evaluate the microsite conditions of strip-bark and whole-bark trees at Khorgo and other locations to determine the extent to which local abiotic characteristics are related to tree morphology.

1.4.2 Differences in radial growth trends

Our study shows that strip-bark *P. sibirica* trees in central Mongolia have different long-term growth trends than trees with a fully active cambium. The whole-bark mean (raw) ring-width chronology has a clear and persistent decline over time. This decline, referred to here as the allometric growth trend, is due to the geometry of trees in which a similar volume of wood is placed around an ever-increasing cylinder (Fritts 1976). Allometric radial growth trends are prominent in trees growing under open-canopy conditions, free of direct tree-to-tree competition, such as those at Khorgo. In contrast, this allometric growth trend was not apparent in the mean ring-width strip-bark chronology. However, the regional curves of age-aligned series, based only on tree-ring series reaching or nearing pith, illustrate that the allometric growth trend is present but relatively muted in strip-bark trees compared to whole-bark trees. Strip-bark ring widths stabilized with increasing cambial age, and strip-bark trees had a lower initial growth rate than whole-bark trees at young cambial ages. Slow early growth rates indicate that strip-bark trees might have been disadvantaged from a juvenile stage, due to either the microsite environment or genetics, and such disadvantages might have predisposed these trees to dieback events. The stabilization of strip-bark radial growth over time suggests that these trees can reduce their

biomass to a sustainable level for continued radial growth (Matthes et al. 2002), perhaps allowing them to live under and adapt to unfavorable conditions for longer periods of time.

The prominent growth increase starting around the beginning of the 20th century in the strip-bark chronology was largely absent in the whole-bark mean chronology. A similar pattern was observed in *P. albicaulis* from Montana, where strip-bark and whole-bark trees had similar growth rates until about 1875, after which the strip-bark trees showed a step-change increase compared to whole-bark trees (Bunn et al. 2003). While strip-bark and whole-bark *P. longaeva* trees from the White Mountains in California have similar growth rates and trends over the industrial period, the strip-bark trees have steeper increasing linear trends in mean ring widths relative to whole-bark trees over several centuries (Ababneh 2006, Salzer et al. 2009). This steeper trend may occur because strip-bark trees were older and initially slower growing, similar to the trees analyzed in our study, but showed the same modern growth rate increase as whole-bark trees (Salzer et al. 2009).

Within strip-bark trees alone, we found notable variability in growth rates where there is a positive association between dieback extent and mean ring width. Across much of the record, a higher percentage of cambial dieback occurring on a stem results in higher mean ring widths on the remainder of the living stem. These findings, in addition to our comparison of strip-bark and whole-bark trees, support the notion that strip-bark events and subsequent morphological changes can directly cause an increase in radial growth rate along the living part of a stripped tree. Drastic short-term growth increases have been reported after strip-bark events in *T. occidentalis* trees (Kelly et al. 1992); however, we did not see a clear association between specific dieback events and growth rates of individual trees (results not shown). This might be due to inherent error in estimates of dieback dates, or the ability to capture only one of many

possible dieback events through time (Bunn et al. 2003). However, we observed a combination of multiple step changes and gradual growth increases in individual strip-bark series, suggesting that multiple dieback events can occur across the bole of a tree and continually influence growth rates of strip-bark trees.

In addition to between-tree variability, we document pronounced within-tree differences in ring-width trends between two cores of the same strip-bark tree. Cores taken near the axis of cambial dieback ("A" cores) displayed marginally slower growth rates before the 20th century than those distant from strip ("B" cores) and thus had a steeper positive trend in ring width through time. Physical injuries to tree stems can have an important impact on ring-width variability across the stem, which is useful for identifying past geomorphic or ecological processes (Stoffel and Bollschweiler 2008). Features such as overgrowing callus tissue and distorted tree rings near the injured axis can contribute to eccentricity and different ring-width trends along the stem. Based on observations in the field, lobate protrusions of the stem near the axis of dieback were common. Lobate growth morphology in other species prone to partial cambial dieback has also been reported (Kelly et al. 1992, Esper 2000). As such, larger modern ring widths near the strip were not particularly surprising and indicated that cambial injury might have a more dramatic impact on ring-width patterns nearest the injured region.

After detrending all tree-ring series using an age-dependent spline, the gradual positive trend, and the sudden increase in tree-ring indices particularly near the beginning of the 20th century remained in the strip-bark standardized chronology. This further supports a significant distinction between radial growth trajectories of strip-bark and whole-bark *P. sibirica* trees at Khorgo, even after removing biological trends related to tree allometry. However, it is important to note that the standardization method applied to tree-ring series can influence the relative

difference between recent trends of strip-bark and whole-bark standardized chronologies (Salzer et al. 2009; see section 1.4.4).

1.4.3 Linking the mechanisms and timing of strip-bark growth trends

The large increase in radial growth rate of strip-bark trees starting around the early 20th century, in both the mean ring-width and standardized chronologies, follows a high proportion of cambial dieback events identified in the 19th century. Frequent dieback events during that time, perhaps due to unfavorable climatic conditions, might have reduced the area of active cambium across many individual trees on the landscape, and affected subsequent growth rates on the remaining part of the stems. Following the late 1500s, another cold and dry period, there is a small jump in dynamic regression coefficients between strip-bark and whole-bark trees, and cores taken near the cambial injury have a sudden growth increase relative to those taken from farther away. However, there are fewer estimated dieback dates during the 16th and 17th centuries, and the sample size of living trees is much lower during that time.

The mechanisms behind increasing ring widths of strip-bark trees after cambial dieback events are not well understood. The sectored radial architecture of some strip-bark trees suggests that xylem units are independent; the loss of functioning on one side of the tree, due to catastrophic environmental hazards and loss of resource acquisition, would not necessarily impact other sides of the tree (Larson et al. 1993). Wright and Mooney (1965) similarly noted that the amount of living stem on *P. longaeva* seems in proportion to that of the living crown. Under these conditions, decreasing photosynthetic capacity of the crown might be matched by a decrease in non-photosynthetic stem tissue. A proportional equilibrium between photosynthetic and non-photosynthetic tissue in a tree might suggest that ring widths on the independent, living

portion of the stem would not necessarily change as a function of dieback given acquisition of other resources remains proportional.

A prevailing theory is that strip-bark trees might grow wider annual rings as a similar amount of growth is applied to a decreasing area of active stem (Salzer et al. 2009). Thus, a change in tree geometry, but not necessarily carbon allocation and total growth along the stem, would cause changes in ring widths on the remaining living axis of stem. Considering a "pool" of resources available to a strip-bark tree could also explain why a persistent growth increase could be evident after the loss of part of the tree. In a conceptual model of stem stripping, Matthes et al. (2002) discuss how a sudden decline in resource pool size (e.g., physical damage to part of a tree such that some resources can no longer be accessed) would result in stem stripping on one side of the tree; death along one axis allows the living remainder of the plant to maintain growing conditions despite a net reduction in resources. This model explains why strip-bark trees are able to survive in sites with spatially heterogeneous resources (Matthes et al. 2002). However, if a portion of the tree dies, additional resources within a common below-ground pool might become available to the living remainder of the plant. For example, if a severe drought reduces water availability particularly to one axis of a tree, resulting in unidirectional dieback, a return to wet conditions would mean the living part of the tree would directly benefit from the loss of the other side and have more resources available to it (i.e., resources become available to a smaller region of active growth in strip-bark trees). This hypothetical mechanism could explain the larger ring widths we identified in the strip-bark trees during the relatively wet (Pederson et al. 2014) and warm (Davi et al. 2015) 20th century in Mongolia following inhospitable climate and frequent dieback events in the 19th century.

Previous reports have suggested that changes in water-use efficiency (WUE) could also play an important role in radial growth increases seen in strip-bark individuals (Graybill and Idso 1993, Bunn et al. 2003). Graybill & Idso (1993) argued that the physiological response of trees to increasing atmospheric carbon dioxide might be more apparent in radial growth rates of strip-bark trees relative to whole-bark trees. They proposed that the two growth forms might have different allocation strategies, where strip-bark trees direct new carbon primarily to cambial growth, while whole-bark trees allocate more carbon to a larger root system, reproduction, and foliage (Graybill and Idso 1993). Bunn et al. (2003) suggested that an increase in relative strip-bark *P. albicaulis* growth rates only after 1875, despite evidence of cambial dieback well before that period, could indicate that increased WUE due to increased atmospheric CO_2 is a driver of these changes, although it was not explicitly tested. In contrast, Tang et al. (1999) found similar increases in WUE for both strip-bark and whole-bark *P. longaeva* trees over the past two centuries. Detailed physiological (including $\delta^{13}C$ and intrinsic WUE) and allometric measurements will be necessary to fully understand the factors causing the increasing ring-width trends identified in strip-bark trees at Khorgo.

1.4.4 Considerations for dendroclimatic interpretations

The distinct long-term growth trends in *P. sibirica* trees due to stem morphology have important implications for climate reconstructions using both strip-bark and whole-bark trees. Based on our strip-bark and whole-bark chronology comparison for Khorgo, and knowledge of the drought sensitivity of these trees (Davi et al. 2006, Leland et al. 2013, Pederson et al. 2014), we can infer that a hydroclimatic reconstruction using the standardization methods and strip-bark chronology presented here would indicate a wetter 20th century and a more positive trend in moisture through time, relative to a reconstruction derived from the whole-bark chronology.

While morphology-related growth trends may not be present at other sites or with other species prone to strip-bark, we recommend several precautionary steps before using strip-bark trees for climate reconstruction. First, we recommend taking thorough notes in the field regarding the presence or absence of strip bark. Researchers might take samples from documented living strip-bark and whole-bark trees to determine whether differences in radial growth or trends occur between the growth forms at their particular study sites. Further, if a larger biological effect on ring widths occurs near the zone of injury, as supported by our results, tree-ring samples should be taken as far away from the injury as possible to avoid any additional bias.

If distinct strip-bark and whole-bark trends in ring-width data are identified, researchers should proceed with informed and cautious statistical data treatment and should compare standardized strip-bark and whole-bark chronologies prior to combining them for climate reconstruction. For example, a common detrending method is to use a fitted linear or exponential curve that is constrained to be negative or have a slope of zero in order to conservatively remove only the expected allometric growth trend (Cook and Kairiukstis 1990). In the case of this study, such a method would retain the positive morphology-related (not climate) trends unique to strip-bark trees. A few studies have recognized the uncertainty associated with strip-bark morphology on growth trends and took steps to avoid bias in climate reconstructions due to tree morphology. Using independent living and dead trees from the same site as this study, Pederson et al. (2014) allowed for straight-line detrending with positive slopes and found no significant difference between chronologies of living and dead trees inferred to have strip and whole-bark forms. Yang et al. (2014) also noted strip-bark forms in ancient *Juniperus przewalskii* Kom from the northeastern Tibetan Plateau, and thus allowed for increasing RCS curves for trees older than 1500 years; no strip-bark bias was found in trends of indices over the past 1000 years. These

methods, or more flexible detrending curves, can effectively reduce or remove the potential influence of tree morphology on ring-width trends and better isolate long-term climate variability in tree-ring data.

The use of SF versus traditional methods should also be further explored to determine the extent to which these two forms of standardization, when applied to raw tree-ring data, might influence trends in the chronologies of strip-bark and whole-bark populations. In both cases, we found here that the strip-bark chronology had a higher positive slope relative to the whole-bark chronology. However, the slope difference between the two chronologies was slightly greater when using the SF approach. As SF methods are designed to better preserve common medium-frequency variability through reducing trend distortion (Melvin and Briffa 2008), it may be the case that common growth variability among strip-bark trees is better retained using this method. Future research should focus on testing different standardization and detrending methods on trees with morphology-related growth trends in order to reduce potential bias in climate reconstructions.

Chapter 2: Physiological responses of ancient pine trees to partial stem dieback and environmental changes

Abstract

Partial cambial dieback, or 'strip bark', is a form of localized stem mortality commonly attributed to harsh environmental conditions. Strip bark is a common morphological feature in ancient trees that might contribute to their longevity. Some studies demonstrate that strip-bark trees have increasing ring-width trends relative to trees without dieback ('whole-bark' trees), yet the physiological mechanisms behind these increasing trends are not well understood. We investigated whether a divergence in strip-bark and whole-bark ring-width trends could be related to a (i) differing climate sensitivity, (ii) differing response to increasing atmospheric CO_2 concentration, or (iii) a reduced cambial area for growth in strip-bark trees after dieback events. To test these hypotheses, we analyzed annual time series of tree-ring widths and stable carbon and oxygen isotopes ($\delta^{13}C$ and $\delta^{18}O$) from 1830-2011 in Siberian pine trees from Mongolia. Strip-bark and whole-bark trees had similar climate sensitivities, showing reduced growth and inferred stomatal closure in response to drought. Both strip-bark and whole-bark trees also responded similarly to recent increases in atmospheric CO_2 through maintaining a constant ratio of intercellular to atmospheric CO_2. In contrast, strip-bark and whole-bark trees had differing behavior following a period of extensive cambial dieback. Strip-bark trees exhibited relatively higher ring widths and enriched $\delta^{13}C$ after a cambial dieback period in the early-to-mid-1800s, whereas ring-width and $\delta^{13}C$ of whole-bark trees remain comparatively stable through the 19th and 20th centuries. We postulate that partial cambial dieback increases the leaf area to sapwood area ratio in strip-bark trees, which alters leaf-level behavior and contributes to increasing ring-width trends compared to whole-bark trees. An increase in the leaf area to sapwood area ratio

might relieve Siberian pine trees from a carbon imbalance and contribute to their long-term survival in adverse environments.

2.1 Introduction

Forest dieback and mortality are increasing in frequency across many regions of the world in response to extreme climatic and ecological conditions, notably severe drought and heat stress, and are projected to increase concurrent with future warming and drying (Allen et al. 2010, 2015, Williams et al. 2013). A sufficiently intense and/or extended period of environmental stress can lead to a sudden or gradual growth decline, followed by eventual mortality (McDowell et al. 2008). Yet many of the oldest living conifers in the world, such as the Great Basin bristlecone pine (*Pinus longaeva* Bailey), Qilian juniper (*Juniperus przewalskii* Kom.), and Northern white cedar (*Thuja occidentalis* L.), can persist for millennia under extreme environmental conditions (Schulman 1954). Many of these long-lived conifers are exposed to severe water limitation, intense winds, and cold temperatures. Harsh environmental conditions coupled with infrequent stand-wide disturbances can similarly promote slow growth and longevity in broadleaf deciduous trees (Di Filippo et al. 2015). The environmental pressures that ancient trees undergo are clearly evident in their contorted, twisted, and stunted morphologies (Swetnam and Brown 1992, Stahle 1996, Huckaby et al. 2003, Pederson 2010).

The ability of some trees to live for several millennia despite their challenging growth environment is multifactorial. Some physiological traits, such as a slow growth rate, great mechanical strength, and resistance to pathogens, allow trees to withstand extreme environmental conditions and increase their chances of survival over long periods of time (Larson 2001). A common indicator of longevity, particularly in ancient slow-growing conifers found on exposed and xeric sites, is partial cambial dieback along the tree stem (LaMarche

1969). This so-called ‘strip-bark morphology’ occurs when one or multiple vertical axes of the stem die in response to environmental stress or a localized loss of resources, while the remainder of the tree continues to add annual growth layers. The factors causing stem dieback vary, but can include damage from wind-blown ice or dirt particles (Schauer et al. 2001, Boyce and Lubbers 2011), root mortality from rock fall or severe drought (Larson 2001, Matthes et al. 2002), or possibly, physiological damage associated with cold and dry conditions, coupled with extreme temperature fluctuations from localized solar radiation (Leland et al. 2018).

Research suggests that partial cambial dieback is due to a highly sectored xylem architecture on water-limited plants, as shown experimentally on cliff-dwelling *T. occidentalis* (Larson et al. 1993, 1994). Stem sectorality may be advantageous for trees growing on adverse sites because physiological damage and mortality from environmental hazards will be isolated to one part of the stem with little or no effects on other portions of the stem (Mathaux et al. 2016). After a catastrophic loss of resources available to a tree, due to severe drought for example, partial cambial dieback may help trees effectively ‘shrink’ in size, and recover a sustainable level of tree biomass (Matthes et al. 2002). In some cases, such a large reduction in conducting area might not strongly impact carbon-water relations at the canopy level (Dietrich et al. 2018). Further, gradual cambial dieback through time might constrain the continual accumulation of biomass of aging trees, thus reducing geometric pressures and allowing trees to continue growing in resource-limited environments (LaMarche 1969, Mathaux et al. 2016). Partial cambial dieback, therefore, is a consequence of an adverse growing environment, but might also contribute to tree longevity.

Some studies suggest that strip-bark *P. longaeva* trees maintain a relatively constant ratio of canopy to stem area through time as dieback spreads across the stem (Wright and Mooney

1965, LaMarche 1969), possibly allowing for long-term stability in radial growth from the living portion of strip-bark trees (Fritts 1969). However, studies have shown that strip-bark whitebark pine (*Pinus albicus* Engelm.) and Siberian pine (*Pinus sibrica*) have steeper positive trends in radial increment during recent decades or centuries relative to trees with a full cambium ("whole-bark" trees). The physiological drivers behind diverging ring-width trends are currently unknown. One possibility is that strip-bark trees apply a similar amount of radial growth as whole-bark trees, but with a reduced area for stem expansion, resulting in wider rings. This hypothesis suggests that the ratio of leaf (photosynthetic) to stem (conductive) area might increase after stem dieback, though the duration of this potential effect is unknown. Alternatively, Graybill and Idso (1993) suggested that increasing growth trends of strip-bark bristlecone pine could reflect a carbon fertilization signal, where strip-bark trees allocate newly acquired carbon to stem growth, while whole-bark trees allocate a higher proportion of carbon to root and reproductive growth. However, later comparisons of strip-bark and whole-bark bristlecone pine ring-widths from the original Graybill and Idso (1993) samples and additional collections were not significantly different during the 20^{th} century, suggesting a recent bias from detrending methods in the Graybill and Idso (1993) study (Salzer et al. 2009). Further, water-use efficiency trends over the past 200 years were not significantly different between strip-bark and whole-bark bristlecone pine trees (Tang et al. 1999). If strip-bark trees exhibit differences in the ratio of leaf-to-sapwood area after dieback, or respond differently to increasing atmospheric CO_2 or climatic changes, we might expect gas-exchange at the leaf level, regulated by stomatal conductance, to differ in these trees relative to whole-bark trees growing under the same conditions.

Stable carbon ($\delta^{13}C$) and oxygen ($\delta^{18}O$) isotope ratios in tree-ring cellulose record multiple physiological processes occurring within trees, but mainly reflect an overall measure of gas-exchange at the leaf level (McCarroll and Loader 2004, Gagen et al. 2004), and can complement or provide different information than radial growth data on how trees adjust to changing environmental conditions. Tree-ring $\delta^{13}C$ reflects the carbon-water relations of a tree, principally linked to variation in the ratio between intercellular and ambient CO_2 concentrations (c_i/c_a), which is influenced by assimilation rate (A) and stomatal conductance (g_s). These factors can be influenced by climate, sunlight, atmospheric CO_2 concentration, and changes in leaf or stem morphological factors that affect hydraulic resistance or demand, such as tree height or leaf area to sapwood area ratio (Farquhar et al. 1989, McCarroll and Loader 2004, Klesse et al. 2018 and references therein). The $\delta^{18}O$ of tree-ring cellulose is predominantly influenced by the $\delta^{18}O$ of source water, such as direct precipitation or ground water, with modification due to evaporation at the soil and/or leaf-level (partially driven by temperature), and through exchange with xylem water (McCarroll and Loader 2004, Barbour 2007). A combined analysis of changes in $\delta^{13}C$ and $\delta^{18}O$ (the "dual-isotope approach") has been used to disentangle the primary driver of c_i variability (i.e., A or g_s), under the assumption that $\delta^{18}O$ is a stable recorder of primarily stomatal conductance and changes in leaf water enrichment (Scheidegger et al. 2000, Roden and Siegwolf 2012). As a result, tree-ring stable isotope data, especially in combination with measures of radial growth, have been useful for assessing carbon-water relations of healthy trees compared against those that show canopy dieback or eventual mortality (Voltas et al. 2013, Hereş et al. 2014, Camarero et al. 2016). However, we only know of one study, Tang et al. (1999) that has used tree-ring stable isotopes to better understand the leaf-level physiology of strip-bark trees relative to whole-bark trees.

In this study, we analyze potential differences in growth and inferred gas-exchange behavior of strip-bark (SB) and whole-bark (WB) Siberian pine (*Pinus sibirica* Du Tour) trees using a combined analysis of annual measurements of tree-ring width, $\delta^{13}C$ and $\delta^{18}O$. Previous studies show that strip-bark Siberian pine from an ancient lava flow site in central Mongolia have increasing positive trends relative to whole-bark trees (Pederson et al. 2014, Leland et al. 2018), especially since the turn of the 20th century, following a large-scale episode of stem dieback in the mid-19th century (Leland et al. 2018). Understanding the carbon-water relations of SB and WB trees might provide insight on whether unique leaf-level physiological behavior in terms of gas exchange could contribute to differences seen in ring-width trends observed over the last two centuries. Here, we assess whether SB and WB trees are responding differently to changes in climate and atmospheric CO_2 concentration, and whether stem dieback events are directly associated with changes in tree physiological behavior at the leaf level.

2.2 Materials and Methods

2.2.1 Sample collection and preparation

Increment cores for isotopic analysis were collected from three SB and three WB *P. sibirica* trees from the Khorgo lava field located in central Mongolia (48.16° N, 99.84° E, elevation: ~2060 m asl; Fig. 2.1, Table 2.1). The SB trees exhibited dieback along the entire vertical length of the stem but had varying degrees of dieback severity (see "Percent Dieback" in Table 2.1, estimated as the percentage of stem circumference that was dead). The WB trees had a fully living cambial band around the stem. A dieback date estimate is available for two of the analyzed SB trees, which was based on determining the outer ring year from a single core taken from the dead side of the stem (Table 2.1; Leland et al. 2018). Though only one dieback date was estimated from individual trees, SB trees likely experience multiple cambial dieback events as

stripping spreads around the stem (Bunn et al. 2003). Trees selected for analysis were open-grown, with little to no competition from surrounding trees, in order to circumvent potential trends in stable isotope ratios associated with light competition (Buchmann et al. 1997, Brienen et al. 2017, Klesse et al. 2018). Exact tree ages could not always be precisely determined because many trees had rotten interiors, but sampled SB trees were older than WB trees on average (Leland et al. 2018). To avoid the well-known juvenile effect on stable isotope ratios, which can be particularly common in the first few decades of tree growth (Francey and Farquhar 1982, Duquesnay et al. 1998, Gagen et al. 2007), all trees were at least 100 years old prior to the first analyzed ring.

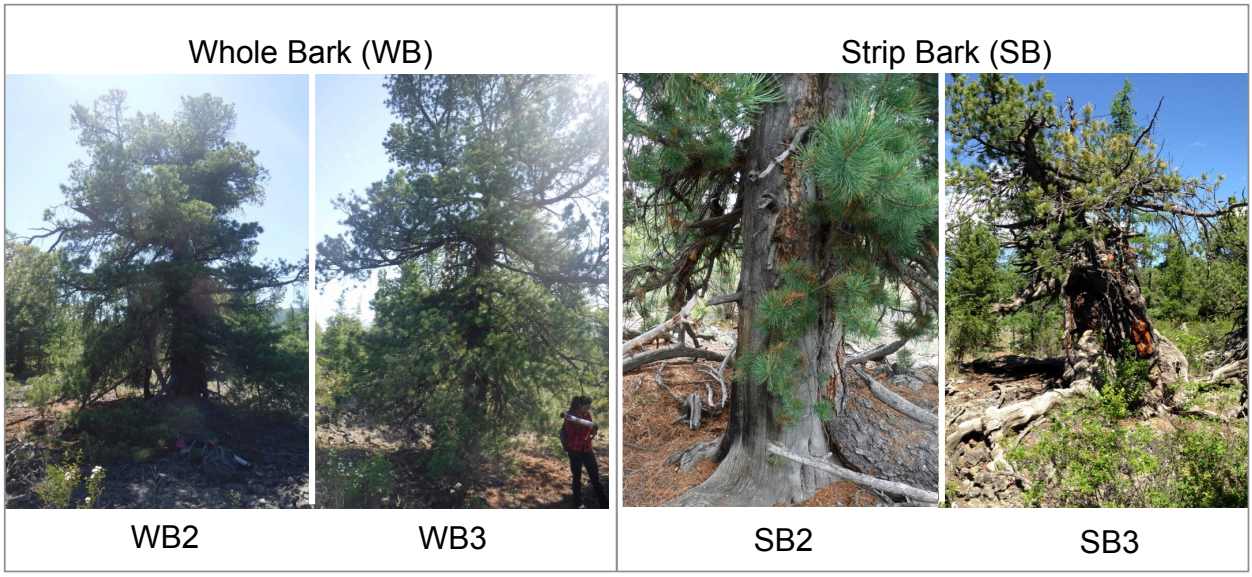

Fig. 2.1. Four of six sampled and analyzed whole-bark (WB) and strip-bark (SB) trees from the Khorgo lava field. Pictures of WB1 and SB1 are not available.

Table 2.1. Analyzed tree-ring samples, their cambial status (SB or WB) and time span of ring-width record. An asterisk indicates that the core sample reached near pith. The percent of stem showing cambial dieback and the estimated dieback date (Leland et al. 2018), if available, are also provided for each strip-bark tree.

Label	Sample ID	Cambial Status	RW Time Span	Percent Dieback	Estimated Dieback Date
WB1	KLP0111	Whole	1627-2013	--	--
WB2	KPW036	Whole	1704-2014*	--	--
WB3	KPW077	Whole	1639-2014*	--	--
SB1	KLP058	Strip	1490-2011	Unknown	Unknown
SB2	KPS006	Strip	1662-2014	45%	1788
SB3	KPS037	Strip	1356-2014	57%	1853

2.2.2 Laboratory

Increment cores were sanded following standard dendrochronological procedures (Stokes and Smiley 1968). All cores were visually crossdated and compared against an existing Khorgo Lava *P. sibirica* chronology (Pederson et al. 2014) and ring widths were measured to 0.001 mm precision with a Velmex measuring system. Individual annual growth rings were cut from increment cores using a scalpel under a stereoscope for the years 1830 to the most recent year of growth.

We extracted α-cellulose from each ring of each core (i.e., no pooling). The α-cellulose was isolated to prevent the effect of varying proportions of other wood components, such as lignin and hemicellulose, on stable isotope ratios of each sample (Loader et al. 2003). Wood from each year was subjected to chemical rinses of sodium hydroxide for solubilizing hemicelluloses and sodium chlorite/acetic acid for removing lignin (Loader et al. 1997, Andreu-Hayles et al. 2019). The remaining α-cellulose was homogenized using an ultrasonic bath and

freeze-dried, and then 250ug (+-10ug) of α-cellulose were weighed from each ring and encapsulated in silver capsules for analysis.

The $\delta^{13}C$ and $\delta^{18}O$ were measured simultaneously through high-temperature pyrolysis of each sample into carbon monoxide using a High Temperature Conversion Elemental Analyzer (TC/EA) interfaced with an isotope ratio mass spectrometer (IRMS) following methods described in Andreu-Hayles et al. (2019). Several studies show that $\delta^{13}C$ measurements produced via this method agree with those produced using the traditional Elemental Analysis (EA) approach with conversion of cellulose to CO_2 through combustion (e.g., Knoller et al. 2005, Andreu-Hayles et al. 2019). The $\delta^{13}C$ and $\delta^{18}O$ ratios of each sample are expressed as delta (δ) values with reference to a known standard, Vienna Pee Dee Belemnite (VPDB) for carbon and Vienna-Standard Mean Ocean Water (VSMOW) for oxygen, using the equations below.

$$\delta^{13}C_{sample} = \left[\frac{(^{13}C/^{12}C)_{sample}}{(^{13}C/^{12}C)_{VPDB}} - 1\right] x1000 \qquad \delta^{18}O_{sample} = \left[\frac{(^{18}O/^{16}O)_{sample}}{(^{18}O/^{16}O)_{VSMOW}} - 1\right] x1000$$

To obtain these values, raw $\delta^{13}C$ and $\delta^{18}O$ were computed relative to CO reference gas (grade 4.7, Praxair) in the IRMS, and we then used a two-point calibration to correct raw $\delta^{13}C$ and $\delta^{18}O$ measurements using reference standards from the International Atomic Energy Agency (IAEA-CH6 and IAEA-C3 for $\delta^{13}C$, IAEA-601 and IAEA-602 for $\delta^{18}O$). The precision of the measurements was checked with working standards (IAEA-CH6, IAEA-C3 and USGS-54 for $\delta^{13}C$, Sigma Sucrose and Sigma Alpha-cellulose for $\delta^{18}O$). See Andreu-Hayles et al. (2019) for additional details.

2.2.3 Data correction

Changes in the concentration and stable isotopic composition of atmospheric CO_2 since industrialization have impacted $\delta^{13}C$ of tree-ring cellulose in two ways. First, the gradual $\delta^{13}C$ depletion of atmospheric CO_2 due to the burning of fossil fuels is incorporated in tree-ring cellulose and imparts a decreasing trend in tree-ring $\delta^{13}C$ that is not related to physiological changes in the plant or its responses to climate (i.e., the Suess Effect). To correct for this Suess Effect trend, we mathematically corrected each tree-ring $\delta^{13}C$ series ($\delta^{13}C_{corr}$) by subtracting the observed changes in $\delta^{13}C$ of atmospheric CO_2 using a linear interpolation of ice core and atmospheric CO_2 records (Leuenberger 2007). A second correction is often applied to remove changes in tree-ring $\delta^{13}C$ due to physiological responses of plants to an increase in atmospheric CO_2 concentration, the so-called preindustrial (PIN) correction (McCarroll et al. 2009). While the PIN correction is important for paleoclimatic reconstructions, we did not apply this correction here because our objective was to discern whether SB and WB trees respond differently to increasing atmospheric CO_2.

2.2.4 Temporal changes in tree-ring parameters

We evaluated changes in tree growth and stable isotope records in the context of four periods of time with distinct climatic conditions and atmospheric CO_2 concentrations, as well as stand-level stem dieback histories (Fig. 2.2; P1: 1830-1884; P2: 1885-1939; P3: 1940-1995; P4: 1996-2011). By comparing tree responses across the different periods, we aimed to isolate potential drivers behind the physiological behavior of SB and WB trees. All periods cover a roughly equal amount of time (n=54 or 55 years), except for the shorter P4 (n=16 years) which covers a remarkable drought recorded in both the instrumental and paleoclimate records (Pederson et al. 2014, Hessl et al. 2018). P1 is defined by cold conditions and a high occurrence

of stem dieback activity across the site as reported in an earlier study (Leland et al. 2018). P2 is intermediate in terms of temperature, moisture, and atmospheric CO_2 concentrations relative to other periods, and P3 is defined by significantly warmer conditions, with rapidly increasing atmospheric CO_2 concentrations (Fig. 2.2).

To discern changes in SB and WB trees over the four periods, we evaluated their relative changes in ring widths, $\delta^{13}C_{corr}$, and $\delta^{18}O$. Here, we used detrended ring-width (RW_{dt}, i.e., dimensionless indices) in order to remove negative ring-width trends associated with the increasing size of trees as they age (Fritts 1976). RW_{dt} was calculated by taking the residuals of power-transformed ring-width series from fitted detrending curves (Cook and Peters 1997). We fit a negative exponential curve or linear function to each series, only allowing for a negative slope or horizontal line. Though we opted for the 'residuals method' to avoid inflationary biases in indices (Cook and Peters 1997), results were similar when calculating indices using the traditional 'ratios method' (Fritts 1976). All detrending was performed in program Arstan (Cook and Krusic 2014).

In order to better compare and assess SB and WB trends through time, we then scaled each RW_{dt}, $\delta^{13}C_{corr}$, and $\delta^{18}O$ series to a standard normal distribution (zero mean, unit variance), as some trees had notably different means, especially regarding the $\delta^{13}C_{corr}$ records. The scaled $RW_{dt,}$ $\delta^{13}C_{corr}$, and $\delta^{18}O$ records from adjacent periods (P1 vs. P2, P2 vs. P3, and P3 vs. P4) were compared for SB and WB trees at the group level and tested for significant differences using the non-parametric Wilcoxon signed-rank test ($\alpha \leq 0.05$). Differences between these periods at the group level were considered in terms of climate sensitivity, atmospheric CO_2 response, and morphological changes, and complement individual tree analyses described in the following sections.

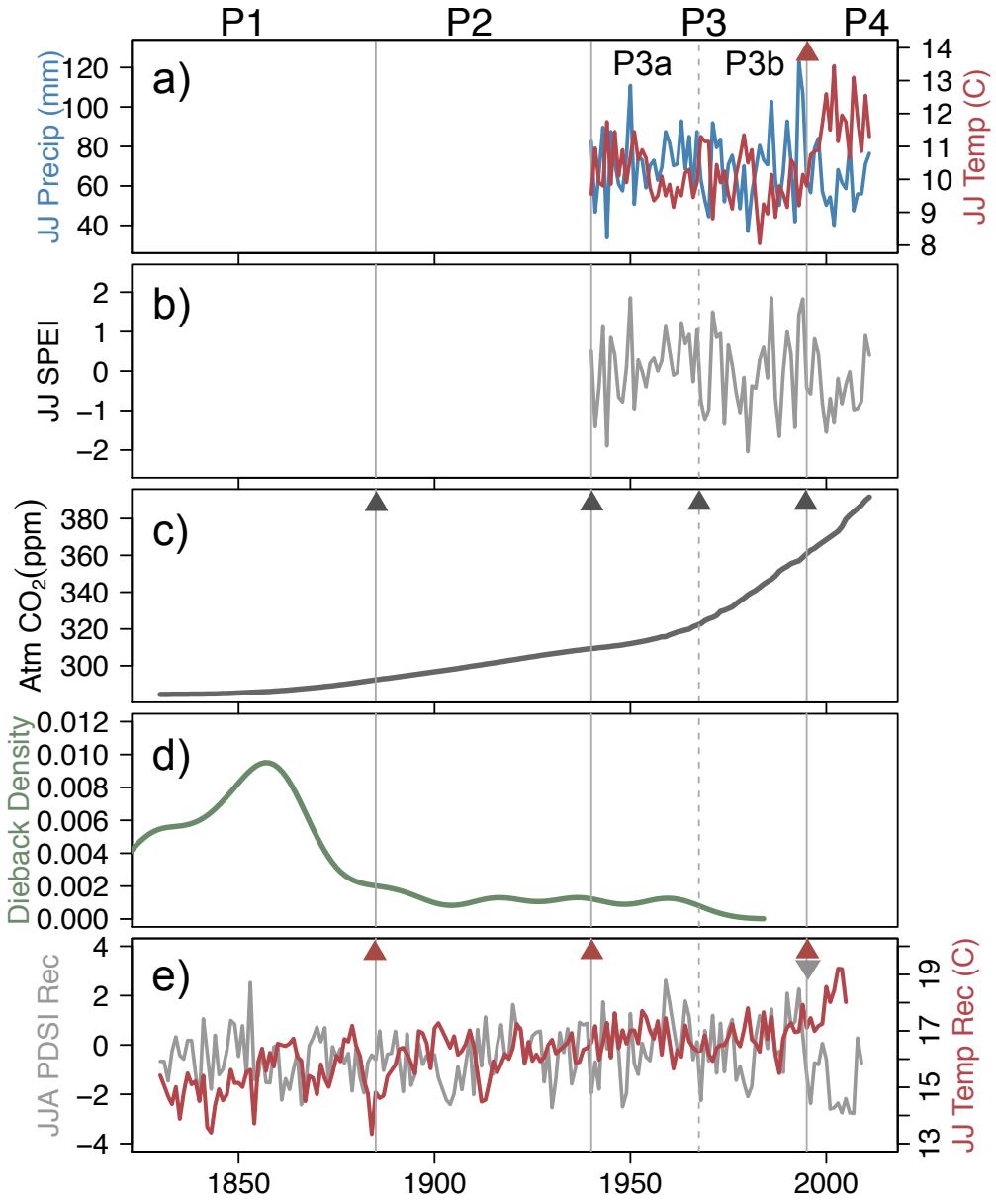

Fig. 2.2. Climate and environmental records across four periods of time (P1: 1830-1884; P2: 1885-1939; P3: 1940-1995; P4: 1996-2011), and two sub-periods within P3 (P3a: 1940-1967, P3b: 1968-1995). (a) June-July average CRU precipitation (blue) and temperature (red) and (b) SPEI from a grid point nearest to Khorgo. (c) Atmospheric CO_2 concentrations derived from Robertson et al. (2001) until 1993, and then updated with mean annual values from Mauna Loa until 2011. (d) Smoothed density estimates of dieback occurrence from SB Siberian pine trees at Khorgo Lava (Leland et al. 2018). (e) June-August self-calibrated Palmer's Drought Severity Index (scPDSI) reconstruction based on Siberian pine from Khorgo (gray; Pederson et al. 2014), and June-July temperature reconstruction from Northern Mongolia (red; Davi et al. 2015). Triangles represent points of significant changes in climate and CO_2 records when comparing adjacent periods. Up-facing triangles indicate significant increases, and down-facing triangles represent significant decreases for each color-coded record ($p \leq 0.05$).

2.2.5 Climate response

To compare the sensitivities of SB and WB trees to climate, we computed correlations of RW_{dt}, $\delta^{13}C_{corr}$, and $\delta^{18}O$ records with monthly climate variables. Meteorological records in the region are sparse during the early 20th century, so the period covering 1940 to 2011 (P3 and P4; Fig. 2.2) was used for climate analyses. Pearson correlation coefficients were calculated between the tree-ring parameters and monthly precipitation and average temperature from the Climatic Research Unit (CRU version 4.01) dataset (Harris et al. 2014), and a 1-month Standardized Precipitation-Evapotranspiration Index (SPEI-1; (Vicente-Serrano et al. 2010) from the grid point nearest to Khorgo Lava (48.25° N, 99.75° E; Fig. 2.2a,b). First, climate correlations were calculated using a robust mean chronology of RW_{dt}, $\delta^{13}C_{corr}$, and $\delta^{18}O$ based on series developed from all trees regardless of stem morphology. These chronologies (RW_{dt}, $\delta^{13}C_{corr}$, $\delta^{18}O$) have a stronger common signal due to the inclusion of a higher number of trees (n=6), allowing for a more robust determination of general relationships between climate and the tree-ring parameters (Fritts 1976). Then, a climate response on individual trees was conducted to determine whether SB and WB trees have a systematically different sensitivity to modern climate. Given the limitations associated with analyzing few individual records from this study, we also performed a climate response on RW_{dt} of all individual SB and WB series from a previous study (series n=78 SB; n=60 WB; Leland et al. 2018). All climate correlations were computed in R package 'treeclim' (Zang and Biondi 2015), and correlation coefficients were tested for significance at the $\alpha \leq 0.05$ level.

We also assessed whether SB and WB trees had a differing physiological response to a recent drought in central Mongolia in the early 21st century (Pederson et al. 2014, Hessl et al. 2018). We compared changes in RW_{dt}, $\delta^{13}C_{corr}$, and $\delta^{18}O$ from P3, a relatively wet period (1940-

1995) to P4, encompassing the recent drought (1996-2011; Fig. 2.2) at the individual tree level, where changes in tree-ring parameters were interpreted in three ways. First, changes in RW_{dt} and $\delta^{13}C_{corr}$ provided information on radial growth over the active stem area and intrinsic water-use efficiency (WUE_i), the ratio of CO_2 assimilation to stomatal conductance, respectively. Second, changes in $\delta^{13}C_{corr}$ and $\delta^{18}O$ were used in a simplified dual-isotope approach to evaluate the status of g_s in association with changes observed in WUE_i. Lastly, the $\delta^{13}C_{corr}$ and $\delta^{18}O$ plot was used in the classic dual-isotope framework for assessing concurrent changes in g_s and A from P3 to P4 (Scheiddeger et al. 2000). There are several caveats in the dual-isotope method for interpreting changes in g_s and A that must be taken into consideration (Roden and Siegwolf 2012). Importantly, the conceptual model assumes that $\delta^{18}O$ primarily reflects changes in g_s, and is not influenced by other environmental factors that can impact cellulose $\delta^{18}O$, such as changes in source water or precipitation $\delta^{18}O$, leaf temperatures, or the exchange of leaf-water with bole-water (Roden et al. 2000, Roden and Siegwolf 2012). As an initial step, for both $\delta^{13}C_{corr}$/$\delta^{18}O$ interpretations, we demarcate trees that do not have significant, positive correlations between $\delta^{18}O$ and SPEI during the instrumental period, suggesting that $\delta^{18}O$ variations might not clearly be linked with g_s and evaporative enrichment during P3 and P4. Over longer time scales, the ability of $\delta^{18}O$ records in these trees to primarily reflect long-term trends or variations in g_s is unknown, warranting caution in the dual isotope interpretation.

2.2.6 Atmospheric CO_2 response

Before comparing SB and WB responses to increasing atmospheric CO_2, we evaluated site-level changes in the ratio of intercellular to atmospheric CO_2 (c_i/c_a) and intrinsic water-use efficiency (WUE_i) over the full period of analysis (1830-2011). The c_i/c_a ratio provides an inferred measure of gas exchange in trees, and is useful for interpreting plant response to

increasing c_a. The raw $\delta^{13}C$ values can be used to calculate c_i/c_a for each tree using a series of equations (Farquhar et al. 1982). First, we calculated carbon isotope discrimination against ^{13}C (Δ) as follows:

$$\Delta = \frac{\delta^{13}C_{air} - \delta^{13}C_{tree}}{1 + \delta^{13}C_{tree}/1000}$$

Then, c_i/c_a was calculated using the following equation:

$$\frac{c_i}{c_a} = \frac{\Delta - a}{b - a}$$

where the constant *a* represents fractionation associated with diffusion of CO_2 through stomata (4.4‰), and *b* is the discrimination against $^{13}CO_2$ by Rubisco during carboxylation (~27‰). The average c_i/c_a ratio was calculated across all trees from 1830-2011 and compared against simulated c_i/c_a values corresponding to three gas-exchange CO_2 response scenarios proposed by Saurer et al. (2004): i) intercellular CO_2 concentration remains constant (constant c_i), ii) intercellular CO_2 increases proportional to atmospheric CO_2 concentration (constant c_i/c_a) and iii) intercellular CO_2 increases parallel to atmospheric CO_2 concentration (constant c_a-c_i). The simulations were initiated with an average of the first 5 years of c_i values (1830-1834), and then were extended to 2011, similar to methods implemented by Voltas et al. (2013).

The WUE_i is another important metric for understanding how trees respond to increasing c_a, as it captures the ratio between carbon assimilation (A) and stomatal conductance (g_s) in leaves. To evaluate site-level trends in WUE_i from 1830-2011, we calculated annual WUE_i as follows:

$$WUE_i = \frac{c_a \cdot (b - \Delta)}{1.6 \cdot (b - a)}$$

Growing season climate, in addition to changes in CO_2, can influence the WUE_i and c_i/c_a of trees through time. Here, to evaluate and compare the response of SB and WB trees to increasing c_a without the confounding effect of climate variability, we analyzed c_i/c_a for individual trees during the period 1940-1995 (P3). Within P3, we compared c_i/c_a of two 28-year sub-periods, 1940-1967 (P3a) and 1968-1995 (P3b), during which June-July precipitation, average temperature, and SPEI were statistically stable (Wilcoxon Signed Rank Test, $p>0.05$ for all climate variables, Supplemental Table B.1), but atmospheric CO_2 concentrations significantly increased ($p\leq0.01$; Supplemental Table B.1, Fig. 2.2a-c). For this reason, we chose to also avoid the recent drought period (P4), even though atmospheric CO_2 concentrations rapidly increased during that time (Fig. 2.2).

Changes in c_i/c_a of SB and WB trees during P3 were analyzed in two ways. First, non-parametric Wilcoxon signed rank tests were used to determine whether there was a significant change in c_i/c_a from P3a to P3b. Second, we once again compared c_i/c_a during P3 against the three scenarios of gas-exchange in relation to increasing atmospheric CO_2 (Saurer et al. 2004). In this analysis, the simulations were initiated with an average of the first 5 years of c_i values during P3 for each tree (1940-1944), and then were calculated to the end of P3 (1995). We compared

actual c_i/c_a measurements versus each of the three scenarios using the root mean square error (RMSE) to determine which scenario best fit the actual c_i/c_a values.

2.2.7 Physiological response to morphological changes

We assessed whether partial cambial dieback influences tree gas exchange by comparing relative changes in tree-ring parameters of WB and SB trees following dieback events in the past. In addition to comparing group-level responses from P1 (the extensive dieback period, Fig. 2.2) to following periods, we evaluated the physiological behavior of SB3 compared to other trees. SB3 was the only analyzed tree with a known dieback event during our period of analysis (year 1853; Table 2.1). For this tree, we computed changes in mean RW_{dt}, $\delta^{13}C_{corr}$, and $\delta^{18}O$ from 10 years prior (1843-1852) to 10 years after the known dieback event (1854-1863), and compared these changes against all other SB and WB trees for the same time period. Similar to methods described above (see *Climate Sensitivity*), we evaluated changes in all tree-ring parameters to infer potential effects of cambial dieback on radial growth, WUE_i, A and g_s.

2.3 Results

2.3.1 Tree-ring series

All RW_{dt}, $\delta^{13}C_{corr}$ and $\delta^{18}O$ records (Fig. 2.3) showed similar interannual variability. The Expressed Population Statistics (EPS; Wigley et al. 1984) for RW_{dt}, $\delta^{13}C_{corr}$, and $\delta^{18}O$ records developed from all trees are 0.91, 0.82 and 0.93, respectively, indicating strong coherence for all parameters. When calculating the EPS of SB and WB trees separately (n=3 per group), RW_{dt} and $\delta^{18}O$ are >0.85, but the EPS of $\delta^{13}C_{corr}$ decreases to 0.71 and 0.66 for SB and WB trees, respectively. The mean of SB and WB series are significantly correlated ($p \leq 0.05$) with r=0.77 for RW_{dt}, r=0.72 for $\delta^{13}C_{corr}$, and r=0.88 for $\delta^{18}O$ (Fig. 2.3) over the entire 1830-2011 period.

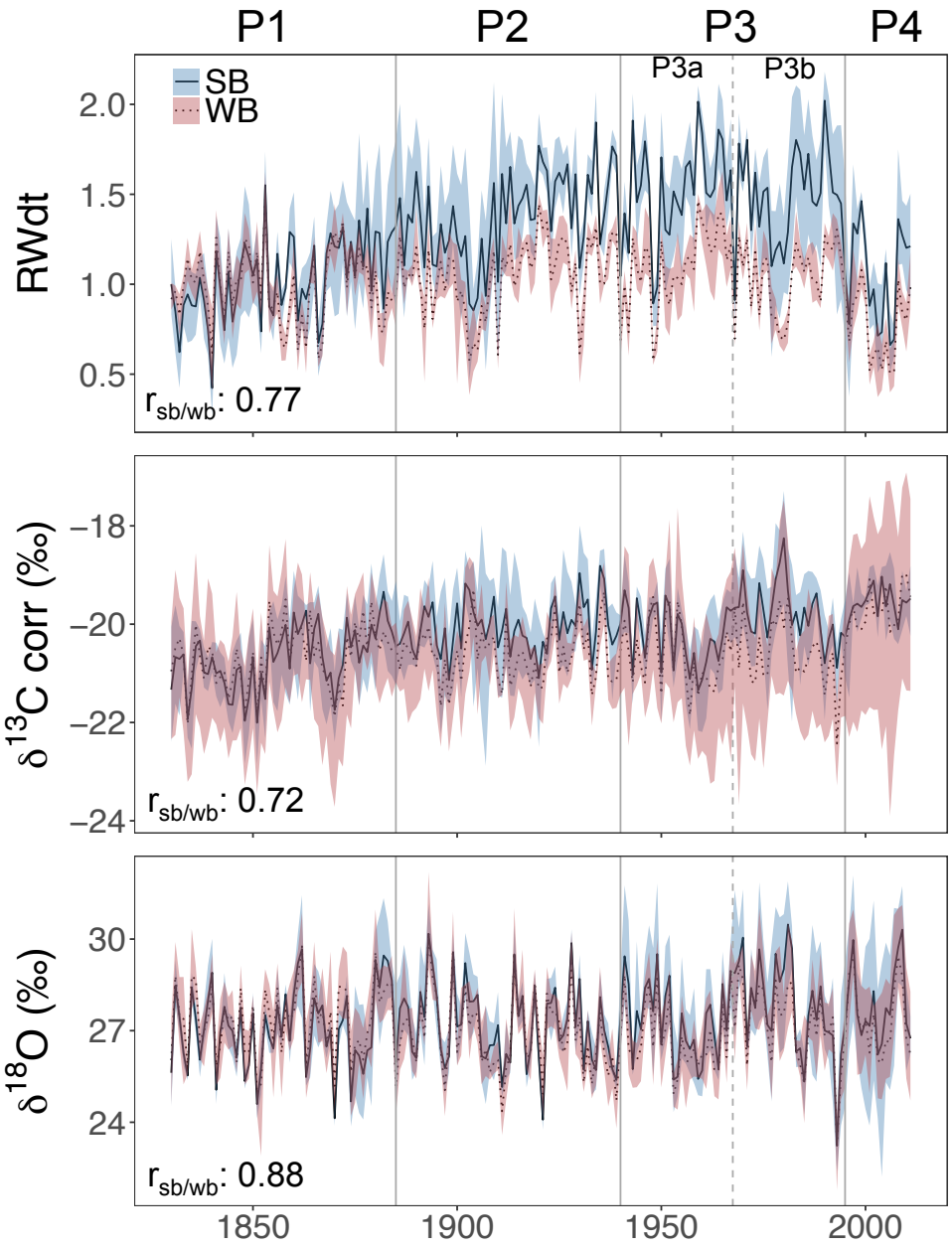

Fig. 2.3. Annual detrended ring-width (RW_{dt}), $\delta^{13}C$ corrected for the Suess Effect ($\delta^{13}C_{corr}$), and $\delta^{18}O$ records from three SB trees (mean: solid black line, range: blue shading) and three WB trees (mean: dotted line, range: red shading). The environmental periods (P1-P4) of interest are shown for each plot. Correlations between the mean of SB and the mean of WB series are shown at the bottom left of each plot.

2.3.2 Tree-ring parameter changes over time

SB and WB tree-ring parameters exhibited similar changes across some periods, but differing behavior across other periods (Fig. 2.4, Supplemental Table B.2). Progressing from P3

to P4, when an abrupt increase in temperature and drought-like conditions occurred (Fig. 2.2a,b,e), RW_{dt} significantly declined and $\delta^{13}C_{corr}$ significantly increased in both WB and SB trees at the group level. The most notable difference between WB and SB trends occurred following P1 (Fig. 2.4). WB trees maintained relatively stable RW_{dt} and $\delta^{13}C_{corr}$ from P1-P2, but $\delta^{18}O$ significantly decreased. Conversely, SB trees showed significantly increasing RW_{dt} and $\delta^{13}C_{corr}$ and stable $\delta^{18}O$ from P1 to P2 (Fig. 2.4, Supplemental Table B.2).

2.3.3 Modern climate sensitivity

Chronologies of RW_{dt}, $\delta^{13}C_{corr}$, and $\delta^{18}O$ developed from all trees showed strong sensitivity to climate, especially during spring and summer months (Supplemental Fig. B.1). The RW_{dt} chronology had a significant positive correlation to June precipitation ($r=0.49$, $p\leq0.05$) and SPEI-1 ($r=0.51$, $p\leq0.05$), and a significant negative correlation to temperature during current year June-August ($r=-0.50$, -0.40, and -0.22, respectively, $p\leq0.05$). A weaker sensitivity to prior year moisture conditions (SPEI-1) during the growing season is also evident. The $\delta^{13}C_{corr}$ chronology had a significant and negative correlation with precipitation and SPEI-1 during the growing season, especially June and July (precipitation: $r=-0.55$, -0.46 ($p\leq0.05$) and SPEI-1: $r=-0.51$ and -0.48, $p\leq0.05$), as well as a significant and positive correlation with average temperature during June and July ($r= 0.46$ and 0.48, $p\leq0.05$). While the $\delta^{18}O$ chronology was significantly and negatively correlated with current-year June and July SPEI-1 ($r=-0.27$ and -0.31, respectively), these correlations were weaker than those calculated for RW_{dt} and $\delta^{13}C_{corr}$. However, the $\delta^{18}O$ chronology had a stronger sensitivity to temperature in the early growing season, with significant and positive correlations to April and May temperatures ($r=0.32$ and 0.29, $p\leq0.05$).

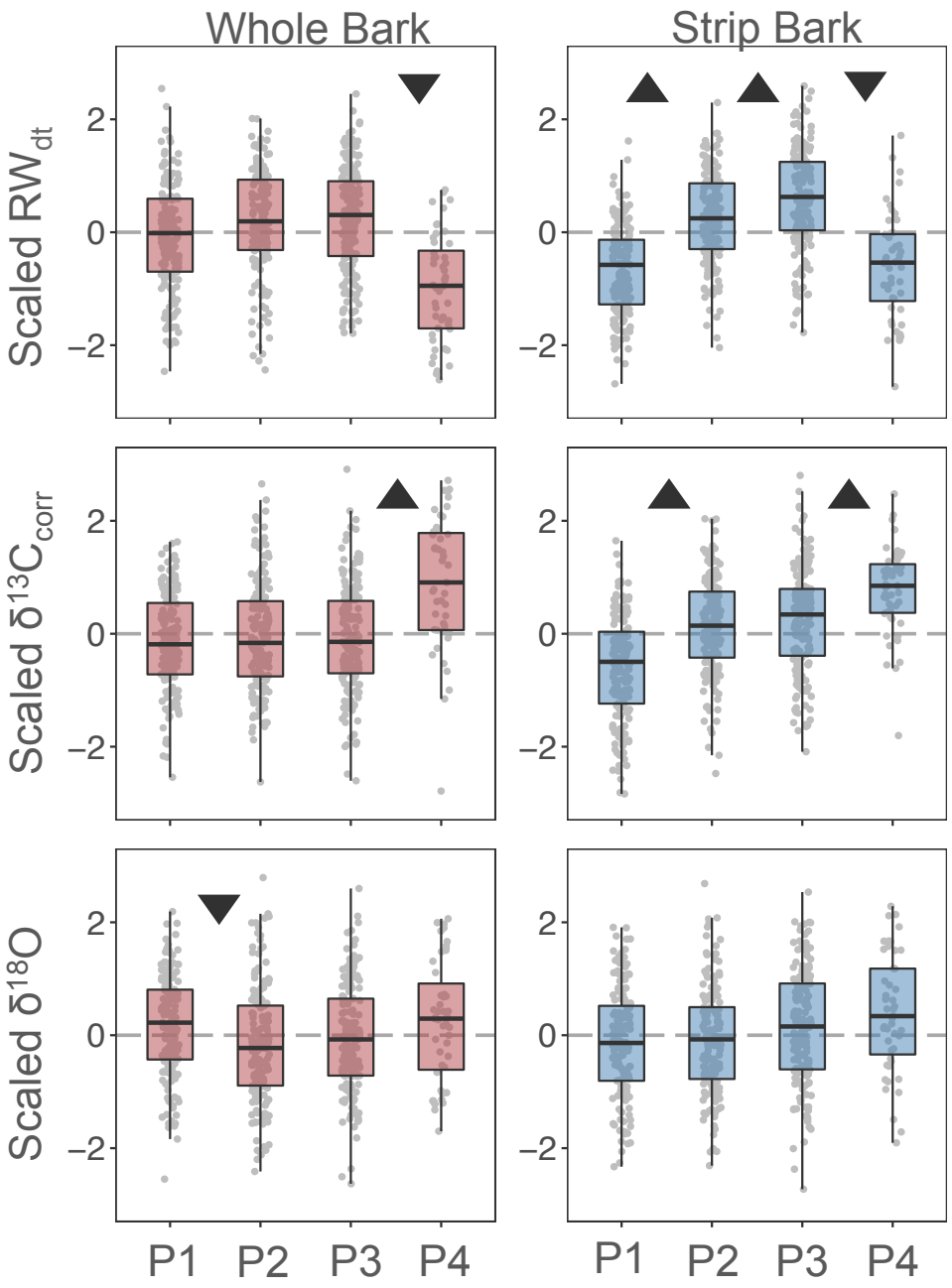

Fig. 2.4. Normalized values of RW_{dt} (top), $\delta^{13}C_{corr}$ (middle), and $\delta^{18}O$ (bottom) for WB (left) and SB (right) trees. Each boxplot corresponds to a different period (P1: 1830-1884; P2: 1885-1939; P3: 1940-1995; P4: 1996-2011). The triangle indicates that there is a significant difference between the two periods on either side ($p \leq 0.05$; Supplemental Table B.2).

For assessing the climate sensitivity of individual trees, we focused on April through July, which are the months corresponding to the highest correlations with all tree-ring parameters based on the full chronology climate response (Supplemental Fig. B.1). Overall, SB and WB

trees did not show consistently different sensitivities to climate (Fig. 2.5). All individual RW_{dt} records from this study (Fig. 2.5), as well as from the Leland et al. (2018) larger dataset (series n=78 SB; n=60 WB; Supplemental Fig. B.2), showed coherent positive correlations to precipitation and SPEI, and negative correlations with average temperature from June to July. Compared to RW_{dt} climate correlations, individual-tree $\delta^{13}C_{corr}$ and $\delta^{18}O$ records showed a wider spread of responses (Fig. 2.5). Some individual trees showed weak and insignificant $\delta^{13}C_{corr}$ and $\delta^{18}O$ correlations with climate from April through July, however, the sign of the response was typically the same across all trees. The individual $\delta^{13}C_{corr}$ and $\delta^{18}O$ records generally correlated negatively with summer precipitation and SPEI-1, and positively with summer temperature. Regarding $\delta^{18}O$, some individual records showed a significant positive correlation with spring temperature. There was a particularly large spread in correlations between $\delta^{18}O$ and both June-July precipitation and SPEI, where some trees had a weak or negligible response. Only two SB trees (SB1 and SB3) and one WB tree (WB3) showed a significant correlation between $\delta^{18}O$ and June-July SPEI.

2.3.4 Response to 21st century drought

In terms of a physiological response to the recent 21st century drought period (P4, 1996-2011: Fig. 2.2a,b), SB and WB trees shared a common response (Fig. 2.4). Both groups shared a significant decrease in RW_{dt} and an increase in $\delta^{13}C_{corr}$ from P3 to P4. These results are in agreement with observations at the tree level, in which all SB and WB trees showed a decline in

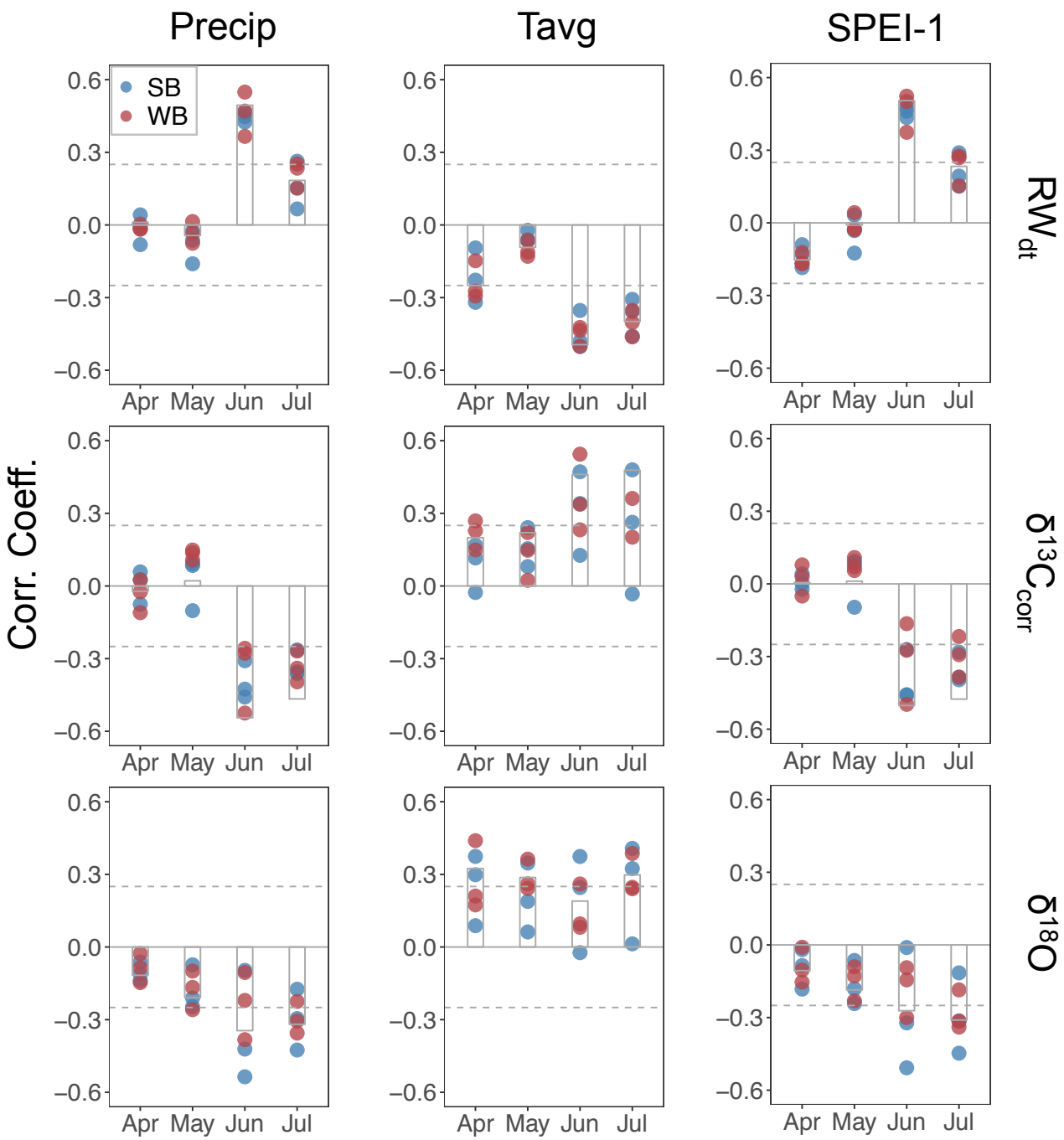

Fig. 2.5. Pearson's correlation coefficients between current April-July monthly climate variables (CRU TS 4.01 precipitation and average temperature, and SPEI-1) and RW_{dt} (top), $\delta^{13}C_{corr}$ (middle), and $\delta^{18}O$ (bottom) from individual trees for the period 1940-2011. Blue dots represent correlation coefficients for individual SB trees, red dots represent WB trees, and the gray bars indicate the correlation for the mean chronology (i.e. combining all series; Supplemental Fig. B.1). Positive/negative correlation coefficients above/below the gray dashed line are statistically significant ($p<0.05$).

RW_{dt} and four trees showed an enrichment in $\delta^{13}C_{corr}$ (Supplemental Fig. B.3a). Regarding the $\delta^{18}O$ response to drought from P3 to P4, we observed an enrichment at the SB and WB group level, albeit not significant (Fig. 2.4). Only three $\delta^{18}O$ records correlated significantly with June-July SPEI (Fig. 2.5), and expressed enriched values associated with the 21st century drought (Supplemental Fig. B.3b), indicating that some caution should be taken when interpreting an evaporative enrichment signal in $\delta^{18}O$.

2.3.5 Tree responses to atmospheric CO_2

At the site level, we found that the average c_i/c_a of all trees fell between the simulation of Scenario 2 (constant c_i/c_a), and Scenario 1 (constant c_i), with a slightly closer association with the latter (RMSE= 0.040 and 0.036, respectively), from 1830-2011 (Supplemental Fig. B.4, Supplemental Table B.3). The average WUE_i of all trees increased by 0.21 μmol mol^{-1} yr^{-1} from 1830-2011, with the largest increase in WUE_i during P4 (1.02 μmol mol^{-1} yr^{-1}; Supplemental Fig. B.4, Supplemental Table B.4). During the 20th century, average WUE_i at our study site increased by 18.85%, when percent change is calculated between the WUE_i mean from 1901-1910 and 1991-2000. Refer to Supplemental Table B.4 for more detailed information on WUE_i changes on different periods of time and comparisons with other studies.

To compare the impact of CO_2 concentration on SB and WB trees, while reducing impacts from changes in climate on c_i/c_a, we analyzed changes in c_i/c_a between P3a (1940-1967) and P3b (1968-1995). There was no significant difference in c_i/c_a from P3a to P3b for all trees, except for SB3, which showed a significant decline of c_i/c_a ($p \leq 0.01$; Fig. 2.6, Supplemental Table B.5). We also compared c_i/c_a values of each tree relative to the gas-exchange scenarios during P3, and found that two SB (SB1 and SB2) and two WB trees (WB1 and WB3) had a

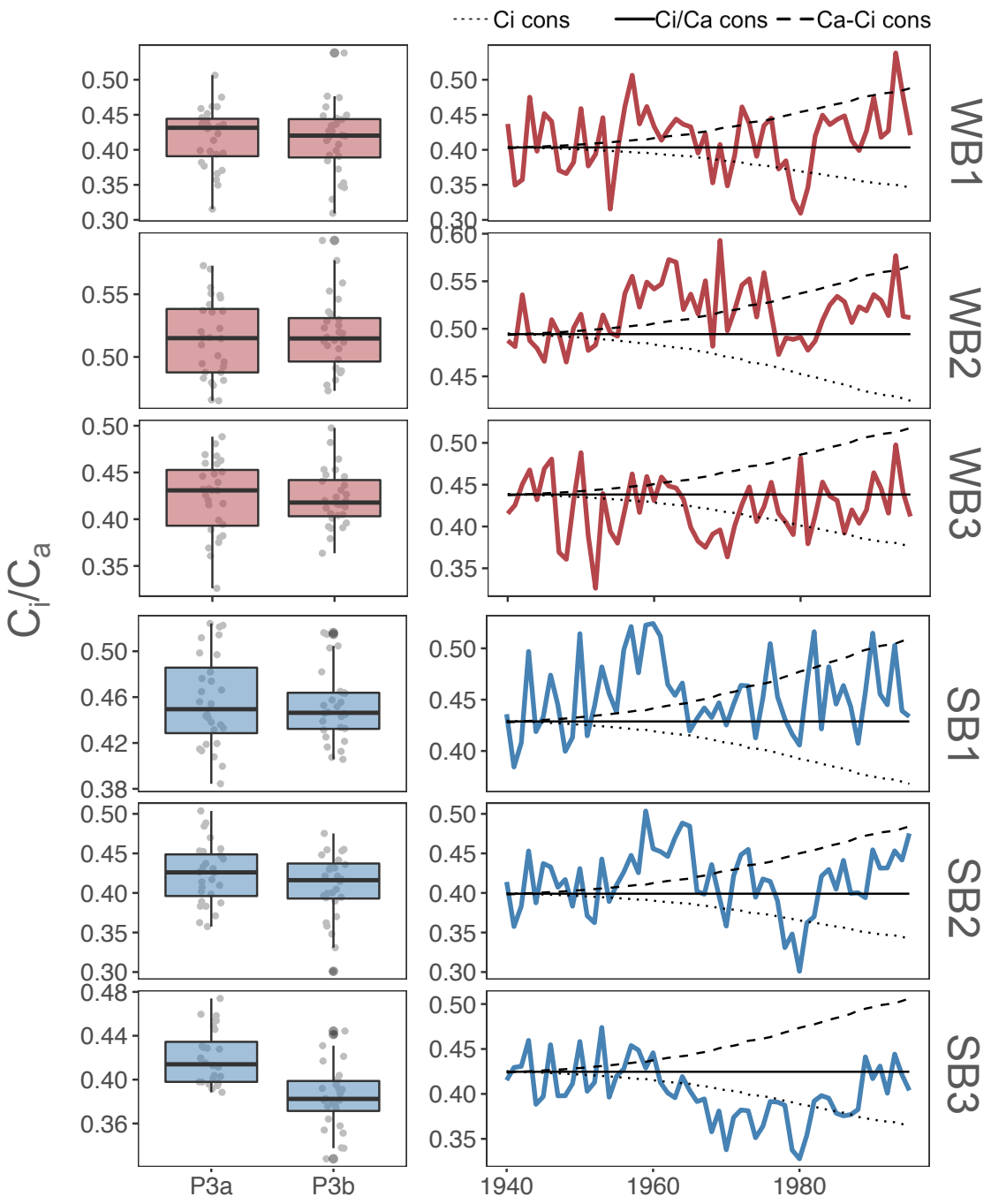

Fig. 2.6. *Left column:* Comparison of the ratio between leaf intercellular and ambient CO_2 concentration (c_i/c_a) during P3a (1940-1967), and P3b (1968-1995) from each WB (red) and SB (blue) tree. These two periods of time have relatively stable moisture and temperature conditions, but rapidly increasing atmospheric CO_2 concentrations (Fig. 2.2). *Right column:* measurements of c_i/c_a for each tree during P3 (1940-1995). Measurements are compared against three scenarios of tree response to increasing atmospheric CO_2: a constant c_i (dotted), a constant c_i/c_a (solid), and a constant c_a-c_i (dashed; Saurer et al. 2004). For each scenario, an initial c_i/c_a value was calculated from the average of the first 5 years (1940-1944) from each tree, and then simulated forward in time.

statistically higher correspondence with Scenario 2 (c_i/c_a constant; Fig. 2.6, Supplemental Table B.3). SB3 had the strongest similarity with Scenario 1 (constant c_i; RMSE = 0.032); and WB2 had a marginally closer association with Scenario 3 (constant c_a-c_i) followed closely by Scenario 2 (RMSE=0.035 and 0.037, respectively).

2.3.6 Tree responses to partial cambial dieback

At a group level, SB trees showed a statistically significant increase in RW_{dt} and $\delta^{13}C_{corr}$ from P1 (1830-1884), a period of frequent stand-wide dieback, to P2, a period with fewer stand-wide dieback events (Fig. 2.4). Conversely, WB trees exhibited stable RW_{dt} and $\delta^{13}C_{corr}$, and a significant decrease in $\delta^{18}O$ from P1 to P2 (Fig. 2.4). While only SB3 had a documented dieback event during P1, it is possible that SB1 and SB2 also experienced dieback during this period of extensive, stand-wide dieback given that strip-bark trees likely experience multiple events as cambial mortality spreads across the stem through time. When excluding SB3 from the SB group-level analysis, SB1 and SB2 retain a significant increase in RW_{dt} and $\delta^{13}C_{corr}$ from P1 to P2 (results not shown).

Next, we assessed physiological changes specifically for tree SB3, with a known dieback event in 1853, by comparing changes in all tree-ring parameters 10-years before and after the dieback event (1843-1852, and 1854-1863, respectively) in all six trees (Fig. 2.7). SB3 mean RW_{dt} increased between these two periods while the other trees, regardless of stem morphology, showed a decrease (Fig. 2.7a). Further, SB3 mean $\delta^{13}C_{corr}$ and $\delta^{18}O$ increased the most among all other trees between the two periods (Fig. 2.7a,b).

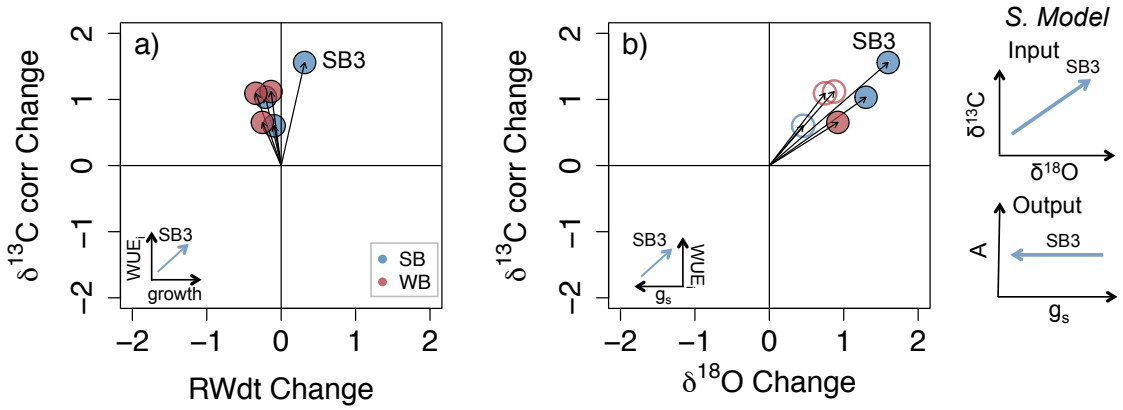

Fig. 2.7. Changes in mean RW_{dt}, $\delta^{13}C_{corr}$, and $\delta^{18}O$ after a dieback event recorded in tree SB3 in the year 1853. Means are calculated from 10-years pre-dieback (1843-1852) set to the origin (0,0), and the arrows/circles show the direction of change to the mean of 10 years post-dieback (1854-1863). We compare concurrent changes in RW_{dt}, $\delta^{13}C_{corr}$ (a) and $\delta^{13}C_{corr}$ and $\delta^{18}O$ (b) of all trees, and SB3 is labeled to highlight its different physiological behavior. The hollow circles in panel (b) represent trees with an insignificant correlation between $\delta^{18}O$ and June-July SPEI. Physiological interpretations of how SB3 changed intrinsic water-use efficiency (WUEi), ring-width (growth), stomatal conductance (g_s), and assimilation (A) relative to all other trees are shown in the insets and in the far right panel using the Scheidegger et al. (2000) model.

2.4 Discussion

Our results reveal that SB and WB *P. sibirica* trees only exhibited distinct growth and leaf-level physiological changes during the mid-1800s. While climate sensitivity during the instrumental period, and response to increasing atmospheric CO_2 during the mid-to-late 20th century were similar regardless of stem morphology, there was evidence of increasing RW_{dt}, $\delta^{13}C_{corr}$, and $\delta^{18}O$ in SB trees following partial cambial dieback. These findings suggest that changes in stem morphology have a direct impact on ring width and leaf-level gas exchange. We hypothesize that partial cambial dieback occurring in SB trees leads to an increase in the ratio of leaf area to sapwood area (A_L:A_S), resulting in stomatal closure to improve water status, and an increase in ring widths due to a sudden decrease in the area of stem growth relative to canopy size.

2.4.1 Climatic and physiological controls on ring-width and stable isotope records

We found strong correlations between RW_{dt} and summer hydroclimate in accordance with previous studies reporting that radial tree growth at Khorgo is strongly limited by moisture availability during the growing season (Davi et al. 2006, Pederson et al. 2014, Hessl et al. 2018). In addition, we found that $\delta^{13}C_{corr}$ and $\delta^{18}O$ are strongly linked to summer hydroclimate and temperature, with enriched (depleted) values during dry/hot (wet/cool) years. Generally high $\delta^{13}C_{corr}$ and $\delta^{18}O$ values, and low RW_{dt} during recent drought conditions (P4) illustrate the importance of hydroclimate on all proxies. The pronounced drought sensitivity of $\delta^{13}C_{corr}$ and $\delta^{18}O$ indicate that stomatal conductance (g_s) plays an important role in regulating their variability during the period of instrumental records (P3-P4). This is especially true for the $\delta^{13}C_{corr}$ chronology, which correlated with summer drought as strongly as RW_{dt}. The $\delta^{18}O$ chronology had a weaker response to summer hydroclimate, but also showed significant, positive correlations with spring temperatures. The $\delta^{18}O$ record has a more complex signal relative to $\delta^{13}C_{corr}$, linked to both summer moisture conditions and growing season temperatures. There is a strong, positive relationship between $\delta^{18}O$ of precipitation and air temperature (Dansgaard 1964), especially in portions of northern Asia (Araguás-Araguás et al. 1998), so this temperature effect may partially leave an imprint on cellulose $\delta^{18}O$ (Saurer et al. 2002). Additional factors influencing $\delta^{18}O$ of precipitation in Mongolia and ultimately cellulose includes the proportion of local moisture recycling, a significant contributor to precipitation in arid central Asia (Wang et al. 2016), or water source changes through time, which are not directly accounted for here.

Our results show that SB and WB trees did not have different climate sensitivities. RW_{dt} and $\delta^{13}C_{corr}$ correlations with SPEI were similar for SB and WB trees, though correlations between SPEI and $\delta^{18}O$ exhibited higher tree-to-tree variability in both types of trees. Some $\delta^{18}O$

series reflected June-July hydroclimate less than others, irrespective of morphology type, suggesting that individual trees might have a weaker evaporative enrichment or stomatal conductance signal in cellulose $\delta^{18}O$ during the modern instrumental period. For those trees, it is possible that a higher proportion of oxygen atoms from stem xylem water exchanges with carbohydrates, diminishing evaporative enrichment signals in cellulose $\delta^{18}O$ relative to source water signals (Roden et al. 2000). Or, some trees might have differing or changing source water signals through their access of deeper ground water than others. Evaluating source water of these trees would be challenging given the complicated hydrology and micro-topography of lava fields. It is apparent that half of the studied trees might not have a strong stomatal conductance signal in their $\delta^{18}O$ records during the growing season, indicating that interpretations from the Scheidegger et al. (2000) dual isotope approach could be limited in this particular case (Roden and Siegwolf 2012). Regardless, we did not find evidence that any particular climate signal is different or stronger for trees with or without partial stem dieback during the instrumental period.

Perhaps contributing to our finding that SB and WB trees do not show consistently different climate sensitivity, there is no evidence that SB or WB trees responded differently to the recent 21st century drought (P4). At the group level, SB and WB trees shared a decrease in RW_{dt} and an increase in $\delta^{13}C_{corr}$ from P3 to P4 (Fig. 2.4), though two individual trees showed no response in $\delta^{13}C_{corr}$ (Supplemental Fig. B.3). Given that $\delta^{13}C_{corr}$ likely reflects variation in g_s based on our climate analysis, and $\delta^{18}O$ series partly reflect stomatal conductance and evaporative enrichment (filled circles Supplemental Fig. B.3b), our results suggest that the 21st century drought resulted in a decrease in radial growth (Pederson et al. 2014) and g_s, an increase in WUE_i, and a stable assimilation rate for both SB and WB trees (Supplemental Fig. B.3).

Overall, we conclude that SB and WB respond similarly to climate variability and extreme drought events.

2.4.2 Tree response to changes in atmospheric CO_2 concentration

The rate of WUE_i increase in Siberian pine during the late 19th and 20th centuries at our study site (Supplemental Fig. B.4) was similar to increases in WUE_i reported in multiple studies (Supplemental Table B.4). The WUE_i across all trees increased by 16.92% from the 1861-1890 mean to 1961-1990 mean, compared to a WUE_i increase of 19.2 +/- 0.9% in other conifers from Eurasia when assessing the same time period (Saurer et al. 2004). A more recent study found that conifers in Europe showed a 25.7 +/- 11.6% WUE_i increase when comparing the 1901-1910 mean to the 1991-2000 mean (Saurer et al. 2014), compared to an 18.85% WUE_i increase at Khorgo during that period. Recent eddy covariance flux observations indicate broad increases in inherent water-use efficiency (IWUE) across forests in the Northern Hemisphere by ~2.3% yr^{-1} over the last two decades (Keenan et al. 2013) or ~1.3% yr^{-1} when adding recent years (Mastrotheodoros et al. 2017). Our WUE_i calculations based on tree-ring records show a 0.94% yr^{-1} increase from 1992-2011. Though increasing WUE_i has been reported on large spatial and temporal scales, a 'fertilization' effect on tree radial growth has not been supported (Andreu-Hayles et al. 2011, Peñuelas et al. 2011, Lévesque et al. 2014, Giguère-Croteau et al. 2019).

It is important to note that our reported trends in WUE_i and intercellular CO_2 derived from tree-ring $\delta^{13}C$ are also affected by variations in climate. Climate influences on WUE_i and c_i are sometimes removed in order to assess trends associated with increasing atmospheric CO_2 alone (e.g., Frank et al. 2015). In addition to potential impacts from climate, stem dieback could also influence c_i and WUE_i and might have contributed to long-term c_i/c_a trends or step-changes identified in strip-bark trees (see *Partial cambial dieback effects on ring-width and stable isotope*

records). In order to isolate and evaluate the impact of increasing c_a on leaf-level physiology, we focused our analyses on P3, a period of stable climate and relatively low reported dieback activity (Fig. 2.2). In general, we found that SB and WB trees had a similar physiological response to rapid increases in atmospheric CO_2 from P3a (1940-1967) to P3b (1968-1995), maintaining a constant ratio between intercellular and atmospheric CO_2. A constant c_i/c_a is the most common physiological response found among trees studied across northern Eurasia (Saurer et al. 2004), and suggests an 'active response' to elevated CO_2 through stomatal closure, resulting in a moderate increase in WUE_i.

SB3 was the only tree with a significant decline in c_i/c_a across the two analyzed periods. The physiological behavior of this tree was more representative of a constant c_i, or Scenario 1 from Saurer et al. (2004), yielding a higher increase in WUE_i compared to other trees. Although it is possible that SB3 is responding differently to increasing atmospheric CO_2, it is plausible that other factors, such as unknown morphological changes, could have contributed to the recent, negative c_i/c_a trend found individually in this tree (see *Partial cambial dieback effects on ring-width and stable isotope records* below). As we do not detect a consistent difference in the physiological response of SB versus WB trees from P3a to P3b, we find it less likely that an atmospheric CO_2 response is driving a difference in stable isotope or ring-width trends of SB and WB trees throughout the entire record. These results support the lack of significant differences in WUE_i trends of SB and WB bristlecone pine in the White Mountains of California over the last 200 years (Tang et al. 1999). Despite similar increases in WUE_i, SB and WB trees could be partitioning biomass differently across various structures of the tree (e.g., stems versus roots), also contributing to different radial growth trends (Graybill and Idso 1993, Tang et al. 1999) though this has not been tested here.

2.4.3 Partial cambial dieback effects on ring-width and stable isotope records

We identified compelling changes in SB RW_{dt} and stable isotopes records following periods of stem dieback in the 19th century. There was an immediate increase in RW_{dt}, $\delta^{13}C_{corr}$, and $\delta^{18}O$ of SB3 after 1853, a known dieback date for this tree, compared to all other trees. The dual-isotope interpretation of these distinct changes in SB3 indicates that stem dieback resulted in a large increase in growth (relative to stem area) and WUE_i (Fig. 2.7a inset), which was linked to a reduction in stomatal conductance but relatively constant assimilation (Fig. 2.7b inset). The rapid nature of changes in RW_{dt}, $\delta^{13}C_{corr}$, and $\delta^{18}O$ after dieback events in tree SB3 supports the idea that stem dieback might directly lead to increased stomatal regulation. The dieback event in 1853 also led to a step-change decline in c_i/c_a of SB3 that persisted until the end of the series, suggesting that morphological changes might also contribute to trends in c_i/c_a and WUE_i (Supplemental Fig. B.5). These results support the group level finding, in which SB and WB trees showed the most notable differences in trends following P1, a period of stand-wide dieback, where SB trees exhibited increasing RW_{dt}, $\delta^{13}C_{corr}$, and relatively stable $\delta^{18}O$ compared to WB trees (Fig. 2.4).

The dual isotope approach for interpreting changes in $\delta^{13}C$ from P1 to P2 might be especially challenging given that the $\delta^{18}O$ of precipitation, or the source water reached by individual trees, can vary over time (Roden and Siegwolf 2012). However, on average, we see that SB trees maintain a stable $\delta^{18}O$ from P1 to P2 compared to WB trees, which experienced a decline from P1 to P2 (Fig. 2.4). The large average increase in $\delta^{13}C_{corr}$, and relative stability in $\delta^{18}O$ from P1 to P2 in all SB trees compared to WB trees could suggest a reduction in stomatal conductance in SB trees after the dieback period.

We find it less likely that differences between SB and WB trees in the 19th century are related to distinct responses to long-term changes in climate or atmospheric CO_2. First, changes in climate and atmospheric CO_2 are gradual from P1 and P2 (Fig. 2.2c,e), and we observed dramatic step changes in RW_{dt}, $\delta^{13}C_{corr}$, and $\delta^{18}O$ in SB3 after partial cambial dieback during P1. Secondly, changes in atmospheric CO_2 are relatively minor in the 19th century, when we see the most significant differences in RW_{dt}, $\delta^{13}C_{corr}$, and $\delta^{18}O$ between SB and WB trees. These results reveal that physical changes to the stem through partial cambial dieback might play a direct role in the distinct radial growth and stable isotopic variation in SB trees.

We hypothesize that the changes we observe in radial growth and leaf-level physiology over the last two centuries in SB trees are most directly related to changes in the ratio of canopy to water-conducting stem area (i.e., ratio of leaf area to sapwood area, A_L:A_S) after stem dieback events. Bunn et al. (2003) similarly hypothesized that increasing ring widths could be associated with an increase in the proportion of crown/root to cambial area in strip-bark whitebark pine. A high leaf area (large crown) can result in fast growth rates in combination with a decrease in stomatal conductance to reduce water loss (Voltas et al. 2013, Gessler et al. 2018). After stem dieback occurs, it is possible that A_L:A_S increases in SB trees, yielding a larger canopy relative to active stem area, thereby increasing ring width, or 'radial growth', on the active area of stem. The higher A_L:A_S after dieback might result in decreased g_s so as to prevent dangerously low xylem water potentials in SB trees. Note that increasing ring width in SB trees might not necessarily indicate more absolute growth than WB trees, but rather, that a higher relative amount of growth is applied to a smaller portion of stem. Comparing absolute growth of SB and WB trees would require detailed allometric measurements of growth increment and active stem

area, and would be a challenge to quantify as the area of active stem in SB trees changes through time.

2.4.4 A hypothetical model of stem dieback

Trees experiencing partial cambial dieback are highly stressed and vulnerable to a sudden loss of resources, either through mechanical damage (e.g., rockfall, wind abrasion) or exposure to adverse climatic conditions (e.g., drought, freezing temperatures, or intense radiation). In many sites with strip-bark trees, the oldest trees have extensive cambial dieback (Wright and Mooney 1965, Kelly et al. 1992, Matthes et al. 2008), reflecting exposure to environmental hazards for long periods of time. While aging trees experience partial dieback as a consequence of adverse environmental conditions, stripping might also relieve stressed Siberian pine trees of a low A_L:A_S (i.e., carbon imbalance), allowing them to maintain stem growth under resource-limited conditions for centuries or millennia. Indeed, LaMarche (1969) posited that many of the oldest bristlecone pine trees have relatively constant annual growth increments due to partial cambial dieback; a continually decreasing area of active stem allows trees to circumvent the need for ever-increasing wood production through time as they grow larger.

Based on results from this study, we developed a hypothetical model on the physiology of partial cambial dieback over the last two centuries at the Khorgo Lava site (Fig. 2.8). The first few decades of the 1800s were particularly cold and dry in Mongolia (Pederson et al. 2014, Davi et al. 2015, Leland et al. 2018), which might have been especially difficult for SB trees growing on poor microsites. The roots on SB trees are often exposed and growing directly over rocks (Fig. 2.1 and field observations), and such exposed conditions might make SB trees especially vulnerable to frost events, inducing root damage and/or crown defoliation (i.e., potentially reducing A_L:A_S), especially when coupled with dry or snow-free conditions (Kullman 1991,

Tuovinen et al. 2005, Schaberg et al. 2011, Voltas et al. 2013). Under particularly severe climatic conditions, we hypothesize that a single partial cambial dieback event (Fig. 2.8a) or several successive dieback events (Fig. 2.8b) occurred on stressed SB trees, effectively increasing their A_L:A_S. Stem dieback was most common in the mid-1800s in Khorgo (Leland et al. 2018), and is possibly linked with premature dehardening, desiccation, or freeze-thaw activity on the southern side of stems in the late winter/early spring from localized solar radiation (Kozlowski et al. 1991, and references in Leland et al. 2018). Even though SB trees lose some of their water conducting area after episodic dieback events, partial dieback could also reduce stressed SB trees to a more sustainable size for continued radial growth. A higher A_L:A_S might be particularly advantageous during climatically favorable conditions when a larger canopy relative to stem area can be supported, such as the warm and wet climate of the 20th century in central Mongolia (Fig. 2.2; Pederson et al. 2014, Davi et al. 2015). In turn, this could contribute to the persistently larger ring widths identified in SB trees at Khorgo compared to WB trees after P1 (Fig. 2.3, Supplemental Fig. B.6).

Compared to SB trees, we hypothesize that WB trees are growing on more favorable microsites, and therefore had a reduced vulnerability to climate-mediated canopy or stem damage during the early 1800s. WB trees often grow on sites with comparably more soil development and less root exposure, which might explain why WB trees experience higher growth rates during young cambial ages relative to SB trees (Leland et al. 2018). As WB trees do not experience dramatic changes in their stem morphology through dieback, we hypothesize that these trees retain a relatively stable A_L:A_S through time compared to SB trees (Fig. 2.8). However, it is possible that A_L:A_S naturally declines over time with increasing height or

hydraulic complexity in all trees in order to alleviate natural reductions in g_s with height, as noted in other *Pinus* species (Schafer et al. 2000, McDowell et al. 2002).

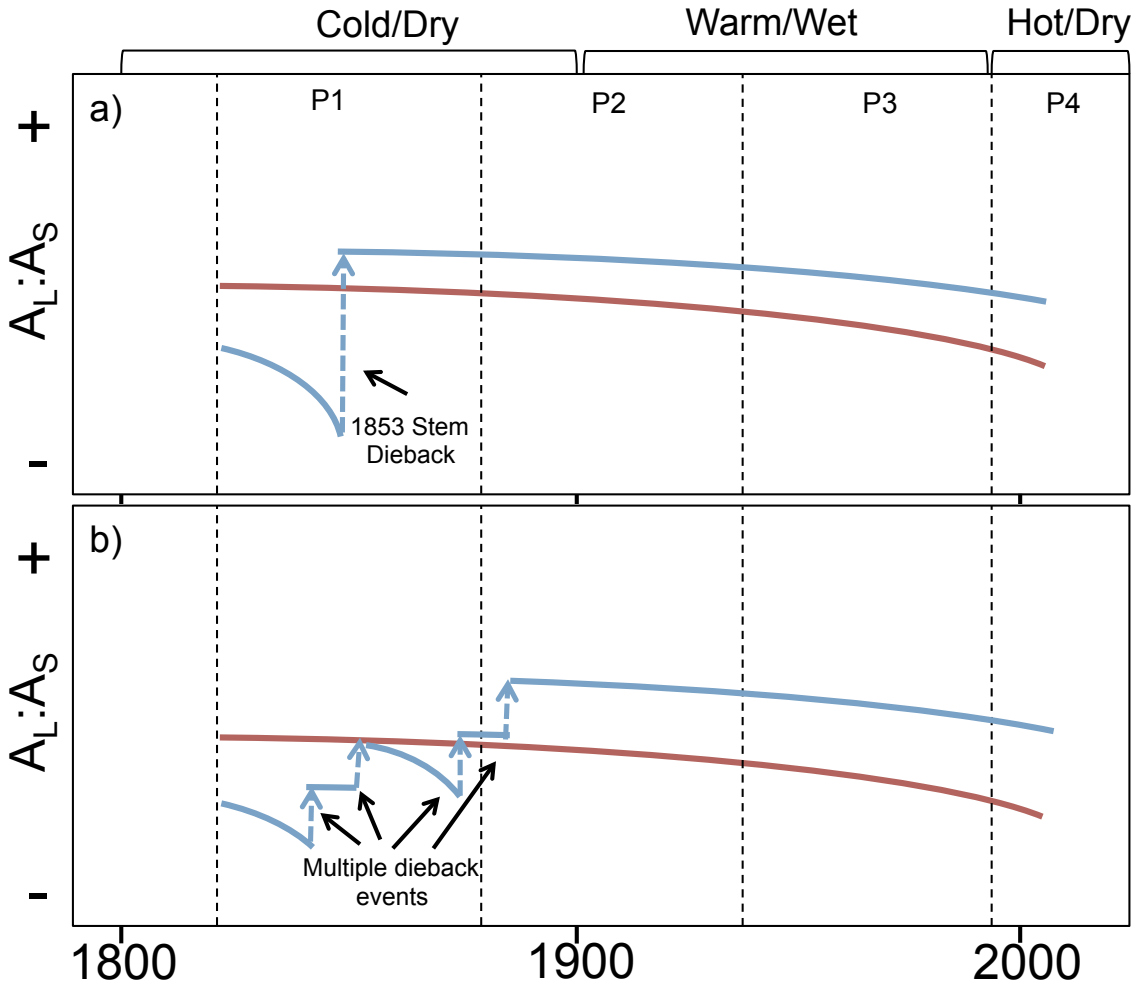

Fig. 2.8. A hypothetical model of partial cambial dieback over the last two centuries in terms of changes in leaf area to sapwood area ratio (A_L:A_S). In both panels, the red line represents a hypothetical WB tree with a relatively stable A_L:A_S. All trees could have a slowly declining A_L:A_S as they age and become larger (see discussion). In panel (a), the blue line indicates hypothetical changes in A_L:A_S for SB3 with a dieback event in 1853. In panel (b), the blue line represents changes in A_L:A_S for a theoretical tree with multiple dieback events, primarily in the 19th century.

This model puts forth a hypothesis on the physiological response of Siberian pine to partial cambial dieback, and could be applied to other tree species in environments with differing environmental hazards causing dieback. Regardless of the cause, partial cambial dieback might

result in an increase in A_L:A_S through decreasing active cambial area. Therefore, episodic cambial dieback might help stressed trees regain a sustainable stem size for continued growth in severely water- or resource-limited sites over long periods of time. This generally follows the conceptual model proposed by Matthes et al. (2002), where partial cambial mortality is the mechanism by which trees reduce their biomass to a sustainable level when the resource pool becomes too small to support the plant. While the model of strip-bark development proposed here is hypothetical and based on limited and inferred measurements of gas-exchange, substantial differences between SB and WB trends in ring width and stable isotopes warrant future physiological work to continue studying this phenomenon. Better understanding the physiology of partial cambial dieback will provide insights on tree longevity and the sensitivity of ancient trees to climatic extremes.

2.5 Conclusion

Siberian pine trees with partial cambial dieback exhibited similar physiological responses to changes in climatic and environmental conditions as those with a fully living stem circumference. However, strip-bark trees had unique radial growth and stable isotopes signatures associated with stem dieback events or periods. Strip-bark trees showed increasing ring widths, increasing WUE_i, and decreasing stomatal conductance following stem dieback, which might be a physiological response to a sudden increase in the ratio of canopy to stem area. Following suggestions from other studies on strip-bark trees, climate-mediated partial cambial dieback might help Siberian pine trees recover a sustainable size for continued radial growth and maintenance. Our results provide key evidence for the notion that partial stem dieback influences gas-exchange processes, and we hypothesize that these physiological responses to cambial dieback can contribute to the longevity of trees growing in resource-limited environments.

Through understanding how long-lived trees growing under extreme environmental conditions responded to past environmental conditions in terms of their leaf-level physiology and morphology, we can assess how trees might respond to future climatic extremes.

Chapter 3: Reducing radial growth bias in tree-ring chronologies of ancient strip-bark conifers

Abstract

In order to estimate past climate using tree-ring data, some form of standardization is typically performed to remove non-climatic variance from tree-ring series. Most standardization methods target non-climatic variance associated with changes in allometry as trees grow (age or size-related trends) and/or stand dynamics, however, the effects of partial cambial dieback on ring-width trends are rarely considered. Across several species and sites, increasing ring-width trends of trees with partial cambial dieback, so-called 'strip-bark' trees, are observed compared to trees with a full cambium ('whole-bark' trees), suggesting that partial cambial dieback can impact ring-width variance. Therefore, this non-climatic, dieback-related variance should be removed from strip-bark trees in order to avoid potential biases in climate reconstructions. Here, we propose two methods of testing for and reducing strip-bark biases in tree-ring data. These methods are evaluated on Siberian pine (*Pinus sibirica* Du Tour) from central Mongolia and Great Basin bristlecone pine (*Pinus longaeva* Bailey) from the western United States. To implement and assess both methods, we use the whole-bark chronology as a target, with the assumption that it has the same climate sensitivities as strip-bark trees, but without a bias associated with cambial dieback. The first "strip-bark correction" method directly corrects decadal and longer-term variance in strip-bark series using the whole-bark chronology as a target. The second "percentile" method tests whether a low-percentile chronology (33rd percentile) can be used to reduce a strip-bark bias relative to the traditional robust mean chronology. The percentile method provides an advantage over the strip-bark correction method because it can be applied even if whole-bark trees are not available, or with sub-fossil material where the cambial status of each tree is unknown. Our results illustrate that both methods work

well for reducing an inflationary strip-bark bias, while retaining medium-to-low frequency variance found in the target whole-bark chronology. Thus, our proposed methods can improve the reliability of climate reconstructions developed from ancient and climatically sensitive strip-bark trees. In the field, we recommend that researchers collect samples from both strip-bark and whole-bark trees with identifying metadata to evaluate potential biasing effects, and to optimize the correction procedure if a strip-bark bias is detected.

3.1 Introduction

Our understanding of climate variability over the Common Era is in large part due to the annual growth rings of long-lived trees. Tree-ring records are used to reconstruct climate spanning centuries or millennia and over local to continental spatial scales. To develop reliable climate reconstructions, the climate signal in tree-ring data must first be isolated while removing or reducing variance related to other non-climatic signals (Fritts 1976, Cook 1985, Cook and Kairiukstis 1990). Non-climatic signals embedded in tree-ring width series include variance associated with changing age/size or allometric effects, endogenous or exogenous disturbances, and other unexplained factors (Cook 1985, Cook and Kairiukstis 1990). Numerous standardization methods have been developed to diminish the effects of non-climatic processes on the radial growth of trees while retaining climate-related variance (Fritts 1976, Cook and Peters 1981, Briffa et al. 1992, Esper et al. 2002). However, each method has inherent advantages and limitations that must be considered in the context of the analyzed trees and study site (Cook and Peters 1997, Briffa and Melvin 2011).

The extent to which non-climatic signals in tree-ring data are minimized is highly dependent on the applied standardization method. Using traditional methods of standardization, allometric (‘age-related’) growth curves are fitted to individual tree-ring measurements series,

and the ratio between the measured and expected value of each year yields a series of dimensionless indices, which ideally represent variation in the external climate forcing on growth (Fritts 1976). In some cases, such as when fitted curves approach zero, the ratios method can lead to a significant inflationary bias in the final indices, which led to the development of the power-transformed residuals method of standardization (Cook and Peters 1997). These methods of curve-fitting standardization are subject to the so-called 'segment length curse', in which the length of individual tree-ring series and the type of fitted standardization curves ultimately limit the preservation of low-frequency climate information in final tree-ring chronologies and subsequent climate reconstructions (Cook et al. 1995). Deterministic curve-fitting methods, such as the commonly used modified negative exponential curve (Fritts et al. 1969), aim to 'conservatively' remove expected allometric growth trends while preserving longer-term climate variability. However, possible variance associated with unwanted signals, such as canopy disturbances, are retained or in some cases, amplified as a consequence. More flexible forms of detrending curves, such as the cubic smoothing spline (Cook and Peters 1981), can be applied broadly to all trees from a site, effectively reducing the influence of closed-canopy gap dynamics on tree-ring series but necessitating the loss of some additional lower-frequency variability in the process. Given the complexity of embedded signals in tree-ring series, finding the most appropriate method of standardization for isolating a particular signal requires a thorough understanding of site and tree characteristics, including the ecological history of a forest stand, which is rarely if ever known in practice.

The presence of allometric and ecological (i.e., forest disturbance) signals in tree-ring series have been recognized for decades, but so far, variance associated with partial cambial dieback in trees has received less attention. Many of the oldest documented conifers, such as

bristlecone pine (*Pinus longaeva* Bailey), Northern white cedar (*Thuja occidentals* L.), and Qilian juniper (*Juniperus przewalskii* Kom), exhibit partial cambial dieback or 'strip-bark morphology'. Partial cambial dieback can spread across the stem in response to harsh environmental conditions, such as rock fall along cliffs (Larson et al. 1993, Matthes et al. 2002), stem exfoliation from wind-blown particles (Schauer et al. 2001, Boyce and Lubbers 2011), or damage related to extreme cold and/or dry conditions (Leland et al. 2018). Studies document that strip-bark Siberian pine (*Pinus sibirica* Du Tour) trees have increasing ring-width trends through time relative to whole-bark trees with a fully-living circular morphology (Pederson et al. 2014, Leland et al. 2018). Increasing ring widths in Siberian pine trees might reflect an increase in the leaf-to-stem cambial area ratio after stem dieback occurs, resulting in a higher photosynthetic area relative to stem area (Leland et al, in prep). Bristlecone pine chronologies from strip-bark trees are also noted to have increasing long-term trends relative to whole-bark trees (Graybill and Idso 1993, Ababneh 2006), though trend differences during the 20th and 21st centuries may have been a consequence of the 'conservative' standardization methods applied (Salzer et al. 2009). Although the drivers and timing of cambial dieback in strip-bark trees are unknown in many sites and across various species, several studies indicate that strip-bark trees have long-term increasing radial growth trends that are not present in whole-bark trees from the same site (Bunn et al. 2003, Ababneh 2006, Yang et al. 2014, Pederson et al. 2014).

Strip-bark trees are valuable for climate reconstructions due to their long annual growth records and, in many cases, strong sensitivity to climate on various time scales. However, to develop reliable climate reconstructions from sites with strip-bark trees, potential trends associated with partial cambial dieback should first be accounted for and reduced while retaining as much climate-related variance as possible. In this study, we assess two methods for reducing a

strip-bark bias in tree-ring chronologies. The first "strip-bark correction" method requires that strip-bark and whole-bark (i.e., full cambium) trees from the same site are available. The "percentile" method does not explicitly require both strip-bark and whole-bark trees, but can be optimized when both types of trees are available for comparison. All methods are based on the assumption that all trees, regardless of morphology, respond similarly to the same climate forcing, and that any difference between long-term ring-width trends of strip-bark and whole-bark trees is related to the effect of cambial dieback on strip-bark trees alone. In this study, we use the whole-bark chronology as a target for correction, based on the assumption that whole-bark trees have a reliable climate signal, not contaminated by cambial dieback processes.

Our chronology development methods are first tested on strip-bark (SB) and whole-bark (WB) Siberian pine from central Mongolia (Pederson et al. 2014, Hessl et al. 2018). In this site, the timing and potential drivers of partial cambial dieback and effects of dieback on ring widths of strip-bark trees are well-documented (Leland et al. 2018). We also test these methods on strip-bark (SB) and whole-bark (WB) radial growth trends in a Great Basin bristlecone pine collection from Mount Washington, Nevada. For this site, a history of dieback events and the direct effect of dieback on radial growth trends are unknown. Challenges and considerations associated with assessing and correcting strip-bark ring-width trends are discussed in the context of these two sites and tree species.

3.2 Materials and Methods

3.2.1 Tree-ring data

We analyzed existing SB and WB tree-ring records from two sites: (i) Siberian pine growing on an ancient lava flow in Central Mongolia ('Khorgo', KLP, 48.16°N, 99.84°E, elevation: ~2060 m a.s.l.), and (ii) Great Basin bristlecone pine from a high-elevation site on Mt.

Washington, Nevada (MWA, 38.91°N, 114.30°W, elevation: ~3300 m a.s.l.; data provided by M. Salzer and A. Bunn). Both sites are xeric and exposed, yet many individual trees can exceed 1000 years in age, supporting the observation of 'longevity under adversity' (Schulman 1954). These long-lived individuals typically have a weathered appearance, with stunted growth forms, a spiral grain (twisting) bole, and strip-bark morphology (Swetnam and Brown 1992). In both tree species, the oldest individuals typically have a high proportion of strip bark with only a small portion of living cambium remaining (Wright and Mooney 1965).

The KLP site is located at the lower tree line in central Mongolia. The terrain has little to no soil development, and many Siberian pine trees grow directly on the lava rock. These trees are highly drought-sensitive and have been used for reconstructions of past moisture variability (Pederson et al. 2014, Hessl et al. 2018). In this study, we used the same KLP dataset as Leland et al. (2018), which consists of 45 SB trees (78 series) and 35 WB trees (60 series). KLP SB trees have a strong signal strength from 1215-2014 (Expressed Population Signal, EPS >0.85; Wigley et al. 1984), and WB trees have an EPS>0.85 from 1315-2014, though the WB sample depth begins to drop rapidly below n=15 prior to 1500.

From the MWA site, we analyzed 26 SB trees (26 series) and 16 WB trees (16 series). SB MWA trees retain a high EPS (>0.85) from ~1380-2007, and WB MWA trees from ~1650-2007 (>0.85). Bristlecone pine can survive on xeric and exposed sites, across a range of elevations from the lower forest border to tree-line in the Great Basin of the western United States. Although the MWA trees range in elevation from 3213-3334 m a.s.l., more than 75% of the trees analyzed for this study are growing below the 3320 m a.s.l. threshold for a consistently positive temperature signal (Salzer et al. 2009). Therefore, the bristlecone pine trees analyzed here are likely more sensitive to moisture variability. However, bristlecone pine climate signals are

exceedingly complex across space and time, and mixed-climate signals (drought and temperature) are common at both high and low frequencies (Kipfmueller and Salzer 2010, Bunn et al. 2011, Salzer et al. 2014, Tran et al. 2017, Bunn et al. 2018).

3.2.2 Initial chronology development

We developed initial SB and WB tree-ring chronologies for both KLP and MWA using a relatively conservative standardization method. We detrended individual trees using a time-varying ('age-dependent') spline (ADS), which is a modified cubic smoothing spline that allows for decreasing flexibility (increasing stiffness) through time (Melvin et al. 2007). The spline has high flexibility during an early cambial age when more rapidly changing allometric trends are possible, and lower flexibility at the end of tree-ring series as the slope of the allometric growth trend declines and reaches its asymptotic lower limit (Fritts et al. 1969). The ADS was set to have an initial stiffness of 50 years, and was constrained to not increase at the end of each series. This conservative version of the ADS ensures that positive ring-width trends at the ends of time-series are not removed. In this sense, the non-increasing ADS is similar to the modified negative exponential curve developed by Fritts et al. (1969) to standardize the ring-width series of over-age conifers. Indices for individual series were computed as the ratio between the raw ring-widths of each series and its fitted ADS growth curve. The indices were averaged together using a robust biweight mean to develop final chronologies. We developed a total of four chronologies that include two morphological types (SB and WB) at each site (KLP and MWA). All chronologies were computed in program ARSTAN (Cook and Krusic 2014).

The slopes of SB and WB mean raw ring-width and standardized chronologies were calculated using the highly robust Siegel repeated medians regression method (Siegel 1982) using package 'mblm' in program R (Komsta 2013, R Core Team 2016). Considering biases

potentially introduced by the conservative standardization method used here (Salzer et al. 2009), we also evaluated trends in mean raw ring-width chronologies from both sites. Then, the robust slopes of individual SB and WB raw ring-width data and detrended indices were compared from 1850-2014 and 1850-2006 for KLP and MWA, respectively. We selected the last ~150 years in order to include the majority of tree-ring series in both sites, and to reduce the impact of allometric growth trends, most apparent in raw ring-width data in early years. The non-parametric Mann-Whitney U test was used to determine whether the robust regression coefficients were significantly different between the two growth forms ($\alpha \leq 0.05$).

3.2.3 Climate sensitivity comparison

Our proposed methods operate on the assumption that any difference between SB and WB chronology variation is 'noise' associated with stem dieback in SB trees, and not related to a difference in climate sensitivity. To compare the climate response of SB and WB trees from KLP and MWA, we calculated monthly correlations between the standardized chronologies and various climate datasets during the instrumental period. In Mongolia, we compared KLP and monthly precipitation and average temperature datasets from the Climatic Research Unit (CRU version 4.01) (Harris et al. 2014) and a 1-month Standardized Precipitation-Evapotranspiration Index (SPEI-1; Vicente-Serrano et al. 2010) based on the grid point nearest to the study site. Meteorological records and gridded climate products are less reliable prior to ~1940 in Mongolia, so climate correlations for KLP were calculated for the period 1940-2014. In Nevada, MWA chronologies were compared with monthly precipitation and average temperature from PRISM (PRISM Climate Group, 2004), and SPEI-1. We used the full common period of all datasets for MWA climate correlations (1901-2007), however, we also tested 1950-2007, and the results were similar.

3.2.4 Chronology method 1: Strip-bark correction

Our first method involves the direct correction of individual SB ring-width series by removal of decadal and longer-term variance not present in the target WB chronology. We implemented a method inspired by the 'signal-free' standardization method (Melvin and Briffa 2008), which seeks to reduce so-called trend distortion bias caused by common medium-frequency signals in the tree-ring series being detrended. A brief description of the signal free standardization method is provided here to enable the reader to understand the link between the signal-free method and the strip-bark correction method developed and tested here.

The signal-free standardization method is based on the observation that the common medium-frequency signal in tree-ring measurements can bias the fitted detrending curves in a common way, especially at the ends of the series, and consequently distort the pattern of variability in the resulting mean chronology. This trend distortion can lead to erroneous interpretations because the final tree-ring chronology may artificially fail to track the climate signal being modeled (Melvin and Briffa, 2008). The removal of this trend distortion artifact is accomplished by using the mean chronology, as the best estimate of the common medium-frequency signal among all series, for removing the trend-distorting common signal from the individual ring-width measurements before their growth curves are estimated. The growth curves fitted to these signal-free series are then applied to their respective original measurements to create a less biased mean chronology that can be further refined. The signal-free method is thus performed iteratively to continually improve the mean chronology used to produce the 'signal free' measurements for better growth trend estimation until convergence is achieved. At this point, the signal-free chronology has been produced. See Melvin and Briffa (2008) for details.

The inspiration here is to use the WB chronology, as if it were the final 'signal free' chronology, for extracting the common medium-frequency signal from the SB ring-width series prior to curve fitting. The growth curves fitted to the signal-free SB series are then used to detrend the original SB ring-width measurements. This does not require iterations because the target WB chronology is fixed. The excess variance associated with allometric changes and cambial dieback in the SB trees is removed here through fitting a highly flexible 10-year spline to the SF series and then applying this spline to the original ring-width measurements. This spline is designed to remove unwanted variance associated with the climate signal inferred from the WB target chronology. The procedure is outlined below and an example is illustrated in Figure 3.1:

1) A WB mean chronology is generated as described in "*3.2.2: Initial chronology development*" (red line; Fig. 3.1a)

2) A SB raw ring-width series for an individual tree (black line; Fig. 3.1a) is divided by the WB mean chronology (red line; Fig. 3.1a) to produce a SF series for the corresponding tree (gray line; Fig. 3.1b). Note that the SF series was re-scaled to match the mean of the original SB raw ring-width series.

3) A flexible 10-year spline (green line; Fig. 3.1b) is fitted to the SF series for the corresponding SB tree (gray line; Fig. 3.1b).

4) The spline fitted to the SF series (green line; Fig. 3.1b) is fitted to the original, respective SB raw ring-width series (black line; Fig. 3.1c with spline shown on top)

5) The SB raw ring-width series (black line; Fig. 3.1c) is divided by the spline fitted to the SF series (green line; Fig. 3.1c) to produce a corrected SB index (Fig. 3.1d, orange line; blue line is the original index for the example tree for comparison).

6) This procedure (#1-5) is repeated for raw ring-widths of every SB tree, so that each SB tree has a respective corrected index series.

7) The SB corrected indices are averaged with a robust mean to produce a corrected SB chronology.

The strip-bark correction procedure was applied to all SB series from KLP and MWA. From each site, we compared the target WB mean chronology, the original SB chronology (i.e., no correction), and SB-corrected chronology over time to determine how well the SB-corrected chronology corresponded to the WB target. We additionally compared the spectrum of all chronologies using 'redfit' in package dplR (Bunn 2008), based on the Lomb-Scargle Fourier Transform from program REDFIT (Schulz and Mudelsee 2002).

3.2.5 Chronology method 2: Percentile

A tree-ring chronology is traditionally calculated by averaging detrended tree-ring indices from a site, with the expectation that the mean will best reflect the common growth forcing, typically climate, across all trees (Fritts 1976). An alternative and less-common approach is to produce a site chronology from a particular percentile of detrended indices across trees for each year (e.g., Stine and Huybers 2017). For example, the median chronology would be based on the 50^{th} percentile index value for each year. This 50^{th} percentile chronology would be essentially the same as the mean if the data are symmetrically distributed, but more robust and closer to the mode of the distribution if significant asymmetry exists. Given that SB trees have increasing

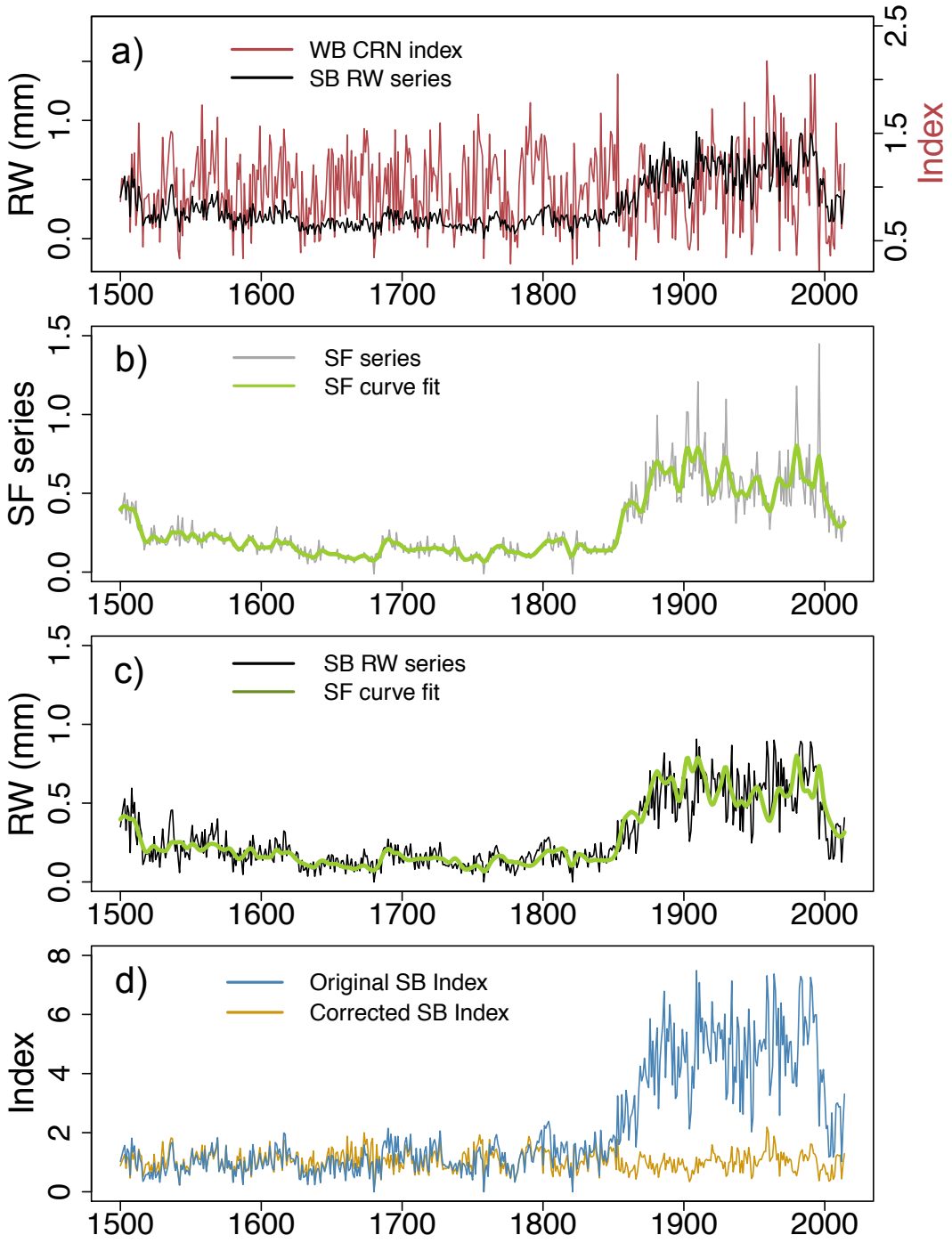

Fig. 3.1. An example of *Chronology method 1* (strip-bark correction) using a SB raw ring-width series from KLP. In panel a), the SB raw ring-width series (black) is divided by the WB mean chronology from the site (red) to produce a SF series (gray) shown in panel b). A 10-year spline (green) is fitted to the signal free series (gray), and then applied to the original ring-width series (black) in panel c). The original raw ring-width series (black) is divided by the signal-free curve fit (green) to produce a corrected SB index (orange) shown in panel d). The original index for the example tree, without correction, is shown in blue. Full details of the procedure are in the Methods section: "*Chronology method 1: Strip-bark correction"*.

trends relative to WB trees, we evaluate whether there is an 'optimal' percentile that can reduce SB inflationary bias relative to the mean chronology. One advantage of using a percentile chronology versus the direct SB correction (*Chronology method 1*) is that the percentile chronology method does not require a WB chronology if a reasonable estimate of the optimal percentile can be determined *a priori*. Thus, SB trees older than the oldest WB trees, or subfossil material with unknown morphology, can be corrected for a SB bias. This is not the case for the SB correction method (*Chronology method 1*) in which the time-span of correction is limited by the length of the WB chronology.

For both KLP and MWA sites, we computed percentiles based on all individually detrended indices from each tree (SB and WB trees combined), a subset of only SB series and a subset of only WB series. In all cases, percentiles were calculated across all indices for every year; the lowest index value for a particular year is equal to 0%, the highest index value corresponds to 100%, and intermediate values are typically interpolated between series, though this does not always occur. An example of percentile series based on indices of all trees (SB and WB) from each site in shown in Supplemental Figure C.1, and the mean and 95% confidence intervals of the bootstrapped upper tercile percentiles (33rd, 67th, and 100th) are shown in Figure 3.2, relative to the WB mean target chronology.

We performed sensitivity analyses for both sites to assess how each percentile chronology compared with the target WB mean chronology, especially in relation to the relative proportion of strip-bark and whole-bark trees. Percentile chronologies were generated with bootstrapped resampling (n=200) for three subsets of data (WB+SB, Only SB, Only WB), and each bootstrapped percentile chronology was correlated with the WB mean chronology over the common period (1500-2014 for KLP and 1650-2007 for MWA). The percentile chronology with

the highest correlation with the WB mean chronology was considered best for capturing the target WB signal. However, we also evaluated the use of the lower tercile of indices (33rd percentile), based on all trees, as a near-optimal percentile across both sites, and we compared this percentile calculated from all trees with the WB mean chronology in terms of their variance over time and spectral properties.

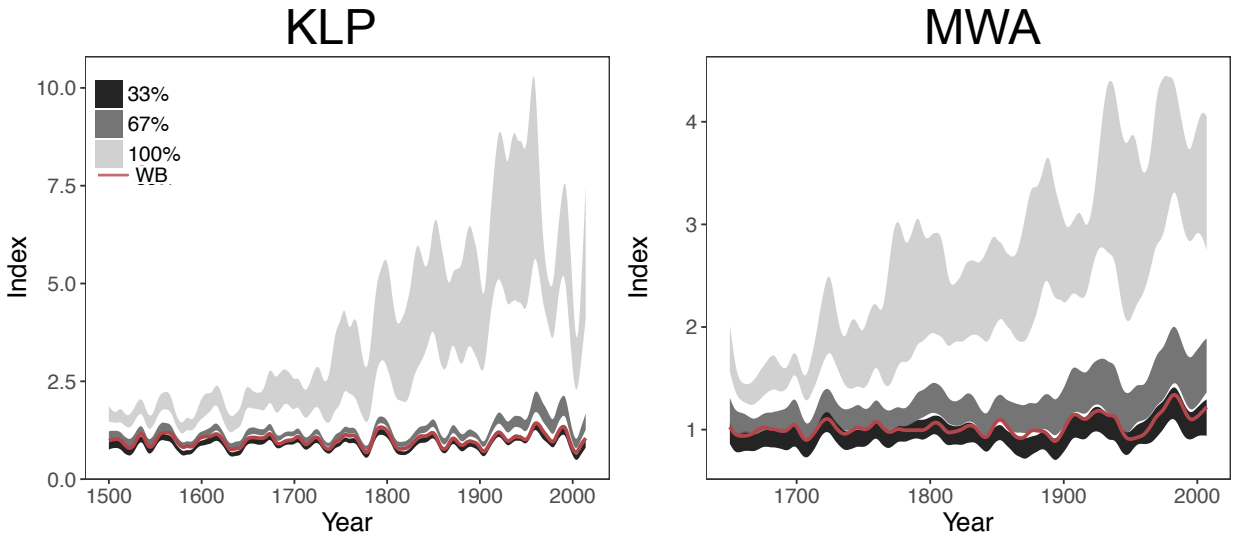

Fig. 3.2. An example of *Chronology method 2* (Percentile method). Upper terciles of bootstrapped percentile chronologies (33%, 67%, and 100%) calculated from indices of all trees (SB+WB) for KLP (left) and MWA (right). The color shading illustrates the range of the mean and 95% BCa bootstrap confidence intervals for each percentile chronology. The WB mean chronology from each site is shown in red. All chronologies have been smoothed with a 20-year spline for illustrative purposes.

As SB trees tend to be older than WB trees, we also explored whether the 33rd percentile chronology could be used for reducing a potential SB bias relative to standardized mean chronologies further back in time, prior to the establishment of most WB trees. In addition to KLP and MWA, we also compared this optimal percentile chronology with the mean standardized chronology from a previously-published bristlecone pine site at Sheep Mountain, California (Graybill and Idso 1993; here, referred to as SM G&I), where there is a documented difference in trends of SB and WB standardized chronologies over the last several centuries

(Supplemental Fig. C.2) and some controversy regarding its presence and interpretation (Graumlich 1991, Salzer et al. 2009). Sample replication of the original Sheep Mountain collection is comparatively low (17 WB trees/series, 13 SB trees/series), however, it provides an additional, independent test of the percentile method. In these three sites, we truncate the percentile chronology when sample depth declines below 10 series (KLP: 1300-2014; MWA: 1450-2007; SM G&I Sheep Mountain: 1150-1990).

3.3 Results and Discussion

3.3.1 Tree-ring chronologies

Mean ring-width chronologies of SB and WB trees show differing long-term trends in the KLP and MWA collections (Fig. 3.3a,b), though differences are particularly notable in KLP. KLP WB trees have a clear declining allometric trend ($\beta_{1500\text{-}2014} = -6.7\text{x}10^{4}$, $p<0.01$), whereas SB trees maintain relatively narrow ring widths with little trend until the 20th century, when ring widths rapidly increase ($\beta_{1500\text{-}2014} = 1.2\text{x}10^{4}$, $p<0.01$, Fig. 3.3a). Conversely, both SB and WB mean ring-width chronologies in the MWA collection show a similar increasing trend through time ($\beta_{1650\text{-}2007} = 4.1\text{x}10^{4}$ and $4.6\text{x}10^{4}$, both $p<0.01$, respectively, Fig. 3.3b). In both sites, SB series exhibit a higher ring-width trend during the last ~150 years compared to WB series, though these differences are insignificant in MWA (Fig. 3.4a,b; W=1836, $p_{wilcox} <0.001$ for KLP; W=219, $p_{wilcox}=0.206$ for MWA). Regarding standardized chronologies, both the KLP and MWA SB chronologies have a steeper increasing long-term trend than the WB chronologies, but differences are larger in KLP (Fig. 3.3c,d). SB robust regression coefficients of detrended series are significantly higher than WB at KLP from 1850-2014 (Fig. 3.4c; W=2423, $p_{wilcox} =0.025$), and MWA SB coefficients are higher than WB from 1850-2006, but the differences are statistically insignificant (Fig. 3.4d; W=238, $p_{wilcox} = 0.067$).

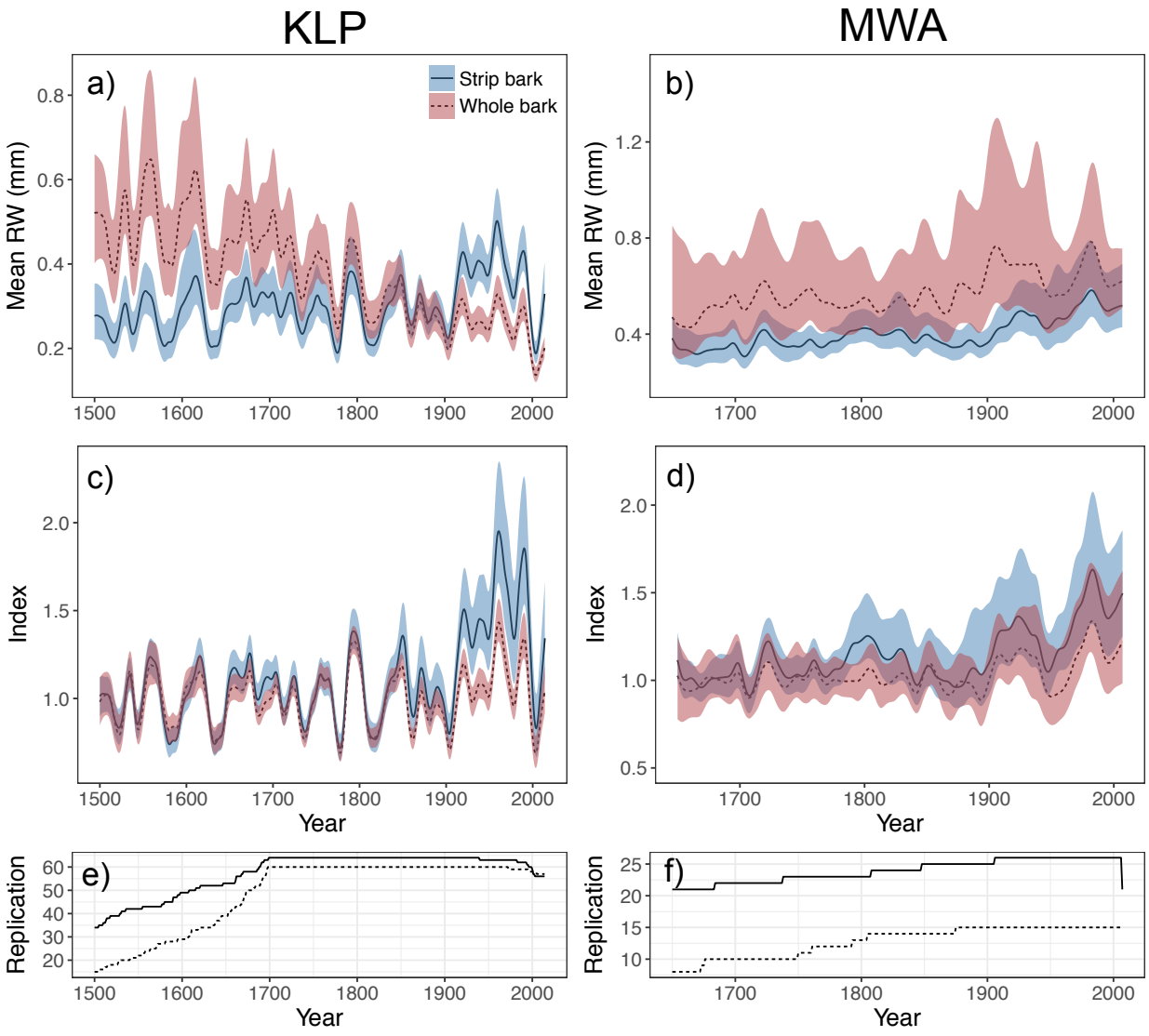

Fig. 3.3. Mean ring-width KLP (panel a) and MWA (panel b) chronologies. Standardized KLP and MWA chronologies are shown in panels c) and d), respectively. The mean and 95% BCa bootstrap confidence intervals are shown for both SB (solid line, blue envelope) and WB (dashed line, pink envelope) trees. All chronologies were smoothed with a 20-year spline. Panels e) and f) show the number of cores for SB (solid) and WB (dashed) trees incorporated into the KLP and MWA chronologies, respectively.

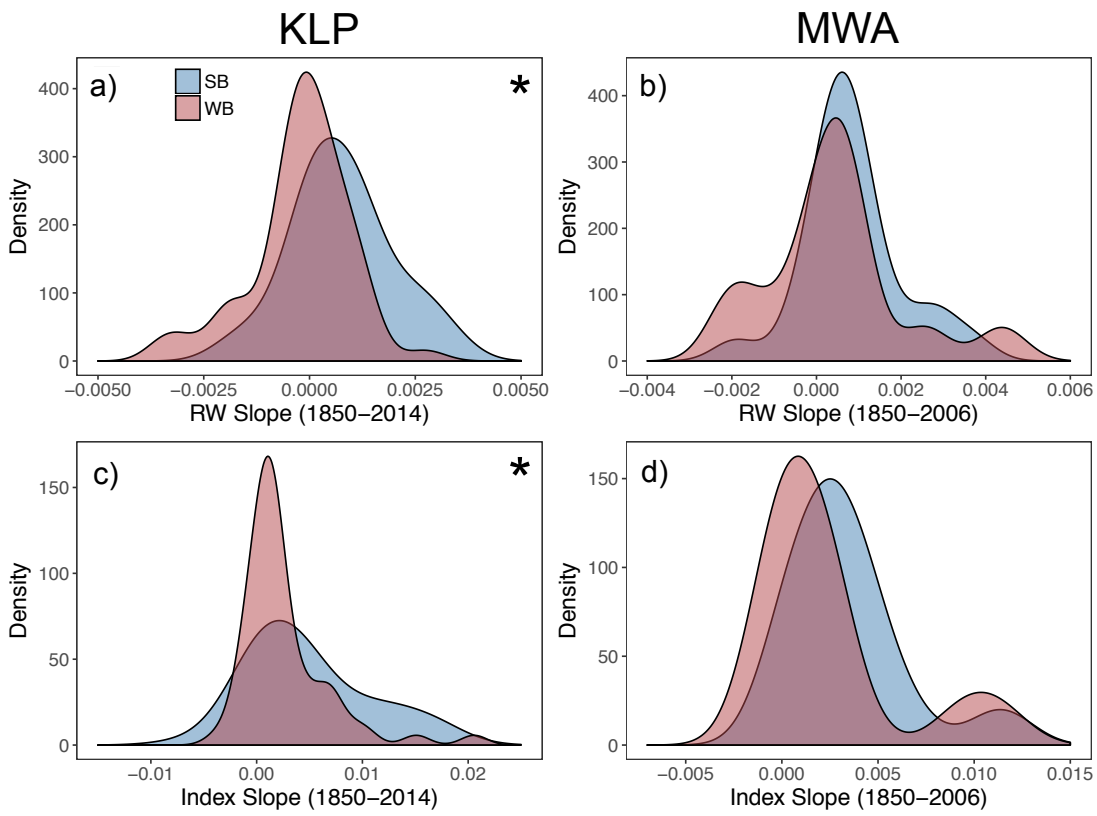

Fig. 3.4. Robust regression coefficients based on the Siegel repeated median method of linear model fitting for ring-widths (a,b) and indices (c,d) of individual SB (blue) and WB (red) trees. The regression coefficients were calculated over the 1850-2014 for KLP, and 1850-2006 for MWA. The * indicates a statistically significant difference between the regression coefficients of SB and WB trees ($p<0.05$).

3.3.2 Considerations of standardization method

Positive trends in SB trees relative to WB trees were observed in mean ring-width and standardized chronologies in other bristlecone pine sites (Graybill and Idso 1993, Ababneh 2006), and in other species, such as whitebark pine (Ababneh 2006, Graybill and Idso 1993) and Qilian juniper (Yang et al. 2014). However, trend differences between SB and WB standardized chronologies can be introduced or amplified at the ends of chronologies as an artifact of the chosen detrending method. Salzer et al. (2009) illustrated that a significant divergence between

SB and WB bristlecone pine chronologies in the 20th century reported by Graybill and Idso (1993) was due to the conservative methods they used for detrending their series (i.e. negative exponential/linear detrending). While raw ring-width measurements of SB and WB trees showed a similar trend during the 20th century, the slower-growing nature of SB trees prior to recent increases in growth caused an apparent 'inflation' relative to WB trees during the 20th century after standardization (Salzer et al. 2009). Thus, the timing and extent of divergence between SB and WB trees can be altered due to the standardization process. As a consequence, raw ring-width measurements of mature trees without allometric growth trends are sometimes preferred for analysis of bristlecone pine (Salzer et al. 2009, Bunn et al. 2018). However, when including trees with clear allometric trends, such as in many of the KLP trees (Fig. 3.3a), and some individual MWA trees analyzed here, standardization is required to minimize or reduce this age-related, non-climatic variance.

In this study, we applied traditional and relatively conservative methods of standardization with the expectation that the WB chronology provides a reasonable target for producing corrected chronologies without compromising increasing trends related to climate at the ends of the series. However, we acknowledge that traditional methods of standardization can lead to biases particularly at the ends of chronologies, such as those associated with using ratios for index calculations when a standardization curve approaches zero (Cook and Peters 1997), or "trend distortion" when climate-related variance impacts removal of non-climatic variance (Melvin and Briffa 2008). The extent of bias from traditional standardization methods varies considerably, and artifacts are complex and difficult to assess based on resulting tree-ring chronologies alone (Anchukaitis et al. 2013). While our results presented here use a traditional standardization approach based on ratios, alternative methods could be further explored for these

and other data, such as using the power-transformed residuals method (Cook and Peters 1997), or the signal-free method for developing the initial chronologies (Melvin and Briffa 2008), which both aim to reduce biases associated with traditional detrending methods.

3.3.3 Climate sensitivity

The methods proposed here are based on the assumption that the same climate forcing influences SB and WB trees equally, and that the primary factor causing a divergence between SB and WB chronologies is an additional source of low-frequency variance associated with morphological changes in SB trees. Accordingly, we find no significant difference between KLP SB and WB climate sensitivities during the instrumental period (Supplemental Fig. C.3). Both SB and WB trees at KLP have significant, positive correlations to precipitation and the 1-month standardized precipitation-evaporation index (SPEI-1) during summer months of the current and previous growing season, and negative correlations to summer temperatures (Supplemental Fig. C.3). It is more difficult to determine whether SB and WB trees could have differing climate sensitivities over lower frequencies (longer time scales) because the available climate records are too short to assess this possibility. However, an earlier study suggests that differences in their trends could be associated directly with stem dieback impacts on the canopy/stem ratio of SB trees, rather than differences in climate sensitivity or CO_2 response over longer time periods (see Chapter 2).

Similar to KLP, SB and WB MWA trees do not have notably different climate responses (Supplemental Fig. C.3), and both show weak, positive correlations with growing season precipitation and SPEI-1 during the current, and in some cases, previous growing season. While we do not find a significant difference in their interannual climate response during the instrumental period, the climate sensitivity of high-elevation bristlecone pine trees is complex,

and can shift over short distances and through time (Kipfmueller and Salzer 2010, Bunn et al. 2011, Salzer et al. 2014, Tran et al. 2017, Bunn et al. 2018). Bristlecone pine were found to have a temperature signal above a transitional elevation in the White Mountains (~3320-3470 m asl), but a consistent drought signal below (Salzer et al. 2009). Further, fine-scale climate variability associated with micro-topographic changes in tree location (topoclimate) can impact the climate signal (temperature or moisture) recorded by individual trees from the same site (Tran et al. 2017, Bunn et al. 2018). These mixed climate responses can lead to discrepancies in both high- and low-frequency climate information. Indeed, many high-elevation bristlecone pine trees are shown to express moisture variability at high frequencies, which is evident in the trees studied here, but a temperature signal at lower frequencies (Hughes and Funkhouser 2003). In this study, it is possible that individual bristlecone pine trees experience different climate sensitivities at lower frequencies, but in combination with potential biasing trends associated with strip-bark morphology (Ababneh 2006, Salzer et al. 2009), it is inherently challenging to disentangle climate versus dieback-related effects on growth. Further research should evaluate the potential compounding influences of cambial dieback and climate on low-frequency trends in bristlecone pine trees.

3.3.4 Assessing chronology method 1: Strip-bark corrected chronologies

After implementing the correction procedure on all SB trees from KLP and MWA (*Chronology method 1*), we found that a mean chronology of the corrected indices ("SB-corr") nearly matches the target WB chronology on interannual (Fig. 3.5a,b) and smoothed (Fig. 3.5c,d) time scales. The SB chronology has much higher power at low frequencies relative to the WB chronology in both sites (Fig. 3.5e,f), reflecting a long-term bias from radial growth inflation. The SF procedure produces SB-corrected series that reduce this low-frequency bias to match the

spectral properties of the WB chronology (Fig. 3.5e,f), all while maintaining high-frequency variability found in the original SB series. When combining the SB-corrected indices and WB indices to produce an overall "Corrected chronology" for KLP and MWA, positive trends found in the original chronologies derived from SB (not corrected) and WB indices are reduced (Fig. 3.6).

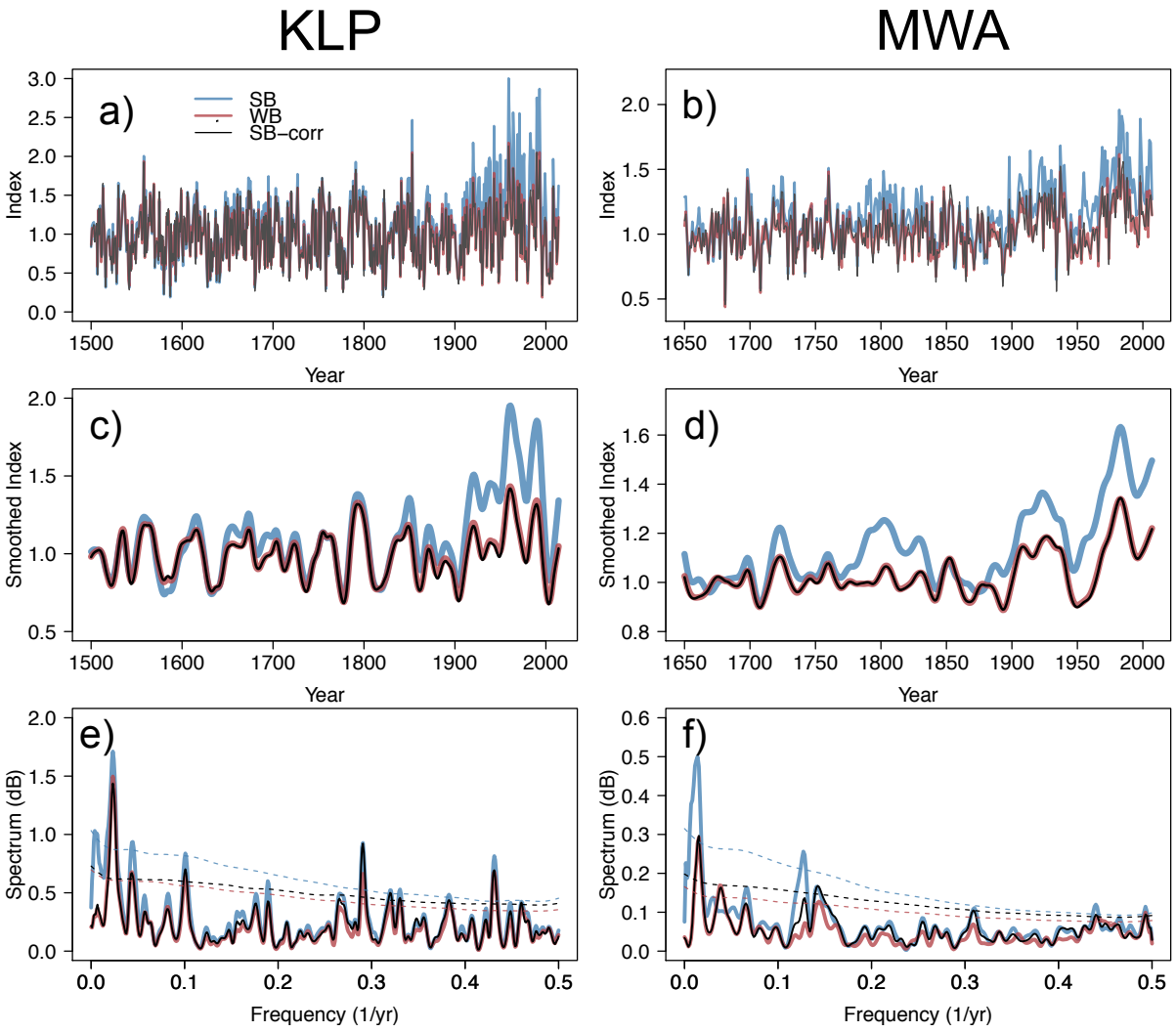

Fig. 3.5. *Chronology method 1*: correction of SB series. SB (blue), WB (red), and corrected SB (black) annual (a,b) and 20-year smoothed (c,d) chronologies for KLP and MWA, respectively. Panels e) and f) show the power spectra for all annual chronologies plotted in a) and b), and the dotted line shows the 95% confidence interval from 1000 simulated red-noise spectra.

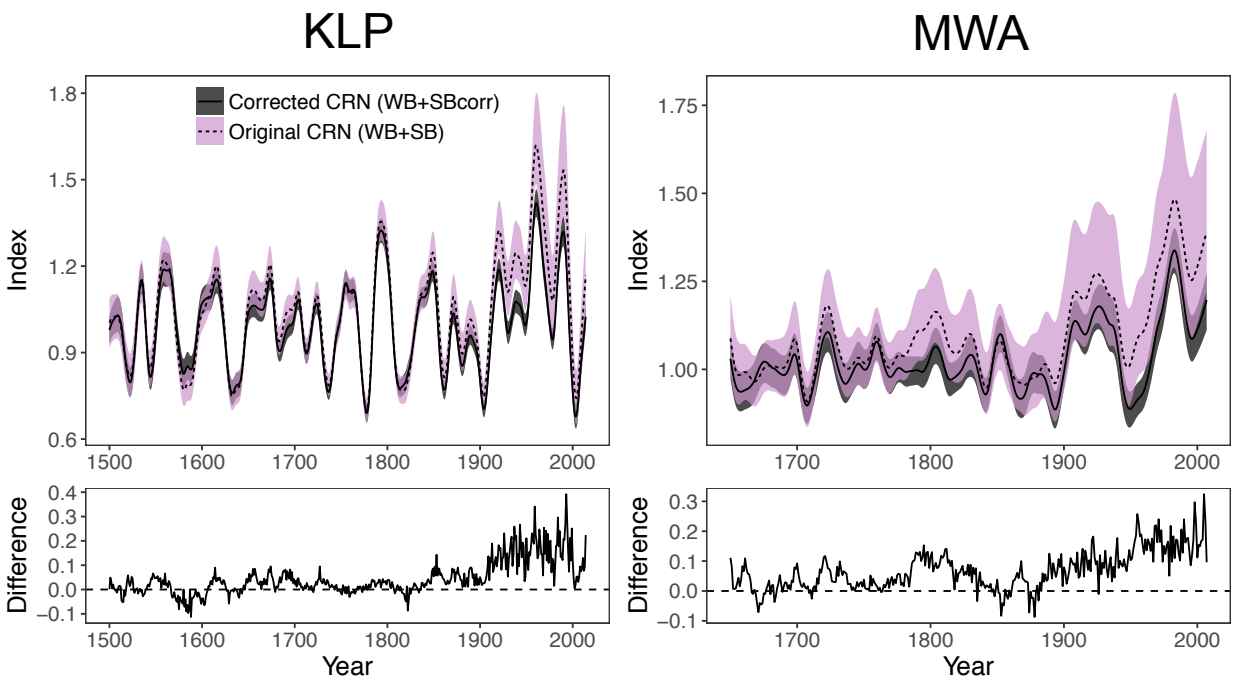

Fig. 3.6. Comparison of a chronology composed of all trees where SB trees have been corrected using *Chronology method 1* ("Corrected CRN", solid, gray), and an original chronology without a SB correction ("Original CRN", dotted, purple) for KLP (left) and MWA (right). Both chronologies were smoothed with a 20-year spline. Shading around the chronologies shows the 95% BCa bootstrap confidence interval. The bottom panel shows the difference between the original and corrected annual chronology through time for both sites.

In the SB correction method proposed here, we used a very flexible (10-year) spline on the SF measurements to liberally remove medium-to-low frequency variance not present in the WB chronology. Spectral comparisons (Fig. 3.5e,f) do not indicate any meaningful loss of medium-to-low frequency signals in the SB-corrected chronologies, relative to the target WB chronologies, due to the use of a highly flexible spline. Therefore, SB-corrected series can be included with WB series to improve sample replication in chronology development, while effectively reducing low-frequency bias associated with dieback. However, there are two potential limitations of this method. First, the morphological form of each tree (i.e., SB or WB) must be known *a priori*, thus identifying field notes are required. Second, this correction

procedure can only be applied during the common period between SB and WB trees. As WB trees tend to be younger than SB trees, this method may be useful for correcting SB variance only in recent centuries.

3.3.5 Assessing chronology method 2: Percentile chronologies

We also investigated whether a percentile method could provide an alternative to the commonly used robust mean chronology for reducing a SB bias, without necessarily requiring a WB target chronology. While inflated SB indices may influence the mean chronology, even after using the robust mean, lower percentiles of growth should theoretically represent trees that do not exhibit excessively large or inflated index values (e.g., WB trees or SB trees with a relatively smaller bias). One challenge is that this method requires finding an optimal percentile to best reduce effects from SB growth inflation, while capturing the climate signal of interest. This depends on the relative percentages of WB and SB trees at a particular site, and the extent to which individual SB trees have inflated indices. Factors such as the proportion of cambial dieback on the stem, or the timing of dieback, might influence relative inflation in individual SB trees (Leland et al. 2018).

To test how the relative proportion of SB and WB trees impacts the optimal percentile chronology, we compared all percentiles from three data subsets: Only WB, Only SB, and all trees (SB+WB) to the target WB mean chronology for both sites (Fig. 3.7). All KLP data subsets under the 50^{th} percentile correlate well with the WB mean chronology until very low percentiles ($< \sim 10^{th}$ percentile; Fig. 3.7a), but the SB subset correlates better with the target across a wide range of lower percentiles, with the maximum correlation at the 29^{th} percentile ($r=0.96$, $p<0.01$). Percentile correlations using the SB subset rapidly decline above the $\sim 50^{th}$ percentile, whereas the correlation for the WB subset peaks at the 50^{th} percentile ($r=0.99$, $p<0.01$), and declines

precipitously only in the extremely high percentiles (> ~90th percentile). As expected, the peak correlation of all trees (SB+WB) falls in between the WB and SB subsets at the 36th percentile (r=0.99, p<0.01). The MWA results are similar to KLP (Fig. 3.7b). The SB subset and SB+WB dataset correlate best with the target WB mean chronology across a range from the highest value of the lower tercile (33rd percentile) to the 50th percentile. The WB subset exhibits the highest correlations around the 50th percentile (max=53rd percentile, r=0.85, p<0.05). The correlations of all data subsets with the target decline rapidly below the lower 25th and above the upper 67th percentiles (Fig. 3.7b).

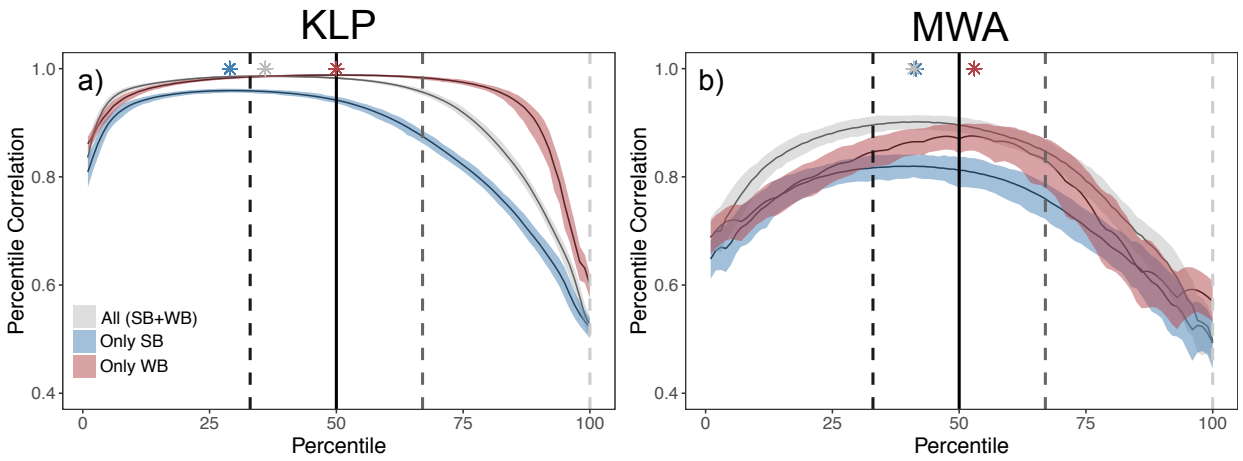

Fig. 3.7. Pearson's correlations between percentile series and the WB mean chronology for KLP (a) and MWA (b). Percentile series and respective correlations are based on all trees (gray), a subset of only SB trees (blue), and a subset of only WB trees (red). Each line and respective envelope represents the mean and 2-sided 95% confidence intervals of the correlations based on bootstrapped percentile series. The vertical lines show the upper tercile percentiles (33%, 67%, and 100%), in addition to the median (50%). Color-coded asterisks indicate the percentile with the highest correlation for each data subset (All SB+WB, Only SB, Only WB).

Given these results, we decided to use the 33rd percentile in lieu of a mean chronology as a more conservative estimate of growth while diminishing or precluding biasing impacts from SB trees. This conservative selection falls between the 29th percentile optimum for the KLP SB subset and the 36th percentile for MWA SB subset. In general, the 33rd percentile of all data

subsets correlates well with the WB mean chronology for both sites. Indeed, the 33rd percentile chronology based on all trees, when scaled to have a mean of one, matches the target WB chronology well for KLP and MWA on both interannual (Fig. 3.8a,b) and smoothed time scales (Fig. 3.8c,d). In both cases, the SB inflation at the end of the each chronology is greatly reduced to closely match the WB chronology (Fig. 3.8c,d), without the need for any additional curve fitting. As a result, the spectral properties of the 33rd percentile chronology are more closely aligned with the WB target chronology, and there is a reduction in high power associated with low-to-medium frequencies identified in the SB chronology (Fig. 3.8e,f).

A primary advantage of the percentile method compared to the SB-correction method is that WB trees are not explicitly required for calculating percentiles if the 33rd percentile is accepted as the 'optimal' choice. While this percentile may not always be the best option, the very flat range of near-optimal SB subset chronologies around the lower tercile (Fig. 3.7a,b) suggests that 33rd percentile can be used as a provisional near-optimal choice. Therefore, we extended the 33rd percentile further back in time for KLP, MWA, and the additional bristlecone pine site, SM (Graybill and Idso 1993), prior to a period with ample WB samples, and compared the percentile chronology with the robust mean chronology from each site (Fig. 3.9). In the KLP collection, there is a general increase in the mean chronology relative to the 33rd percentile chronology, especially in the early (1300-1500) and late (1800-2014) portions of the chronology (Fig. 3.9a, bottom panel). In MWA and SM, the mean chronologies show a notably larger increase than the 33rd percentile chronology in 19th and 20th centuries (Fig. 3.9b,c). These results further illustrate that the most extreme biases occur during recent centuries, perhaps induced by the combined effects of partial cambial dieback on radial growth, no overlap with remnant wood samples, and the conservative and traditional standardization methods used here.

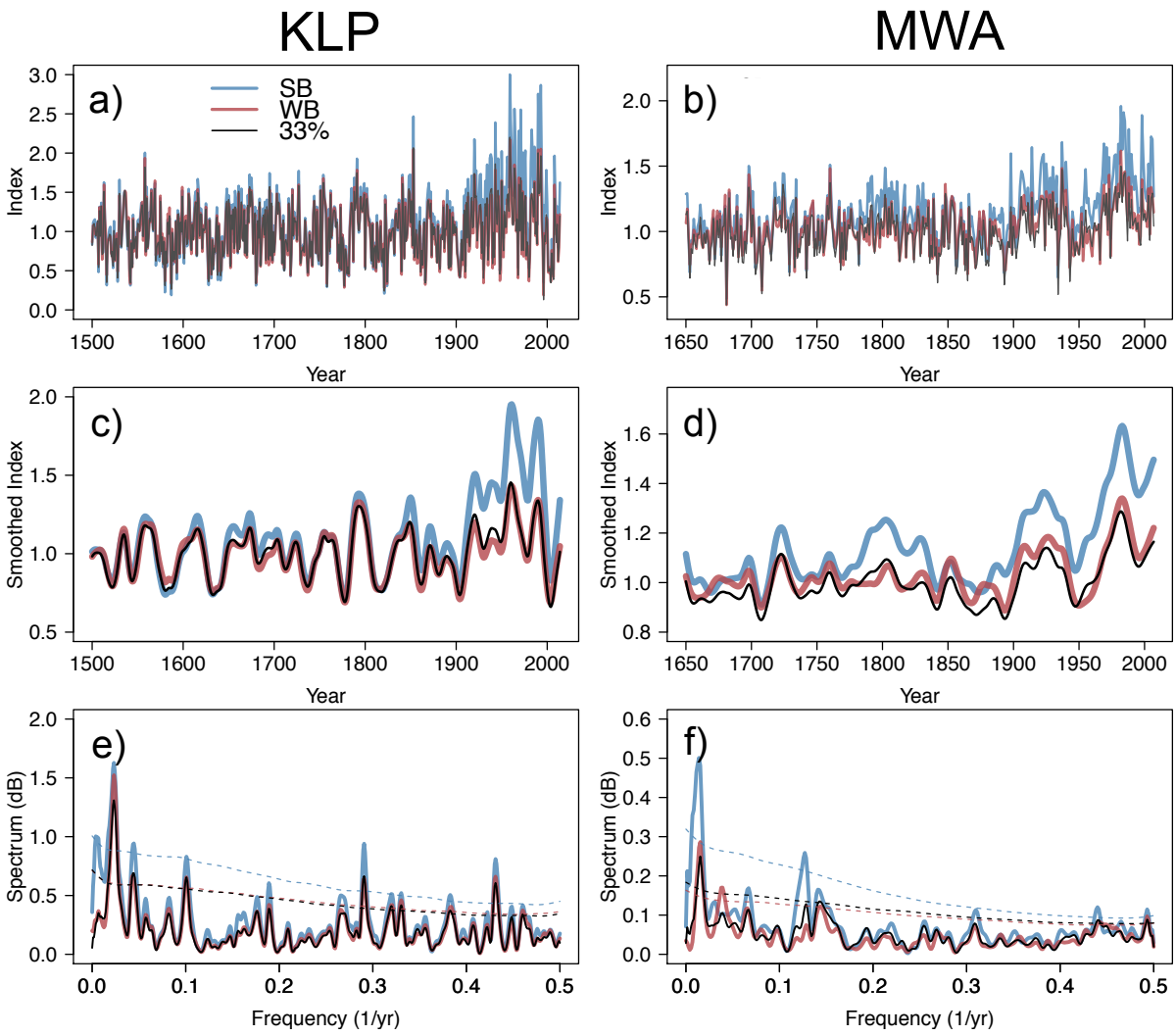

Fig. 3.8. *Chronology method 2*: Percentile method. SB (blue), WB (red), and 33rd percentile (black) annual (a,b) and 20-year smoothed (c,d) chronologies for KLP and MWA, respectively. Panels e) and f) show the power spectra for all annual chronologies plotted in a) and b), and the dotted line shows the 95% confidence interval from 1000 simulated red-noise spectra.

While we believe that the 33rd percentile described here can be broadly used, researchers are encouraged to sample and compare SB and WB trees from new sites, and if needed, establish site-specific optimal percentiles for correcting the effects of radial growth inflation caused by partial cambial dieback. Ideally, the selected percentile would reduce a SB bias without compromising a climate signal. In contrast to our study, Stine and Huybers (2017) concluded that high percentiles (~91%) of growth across the stand are preferable because they more

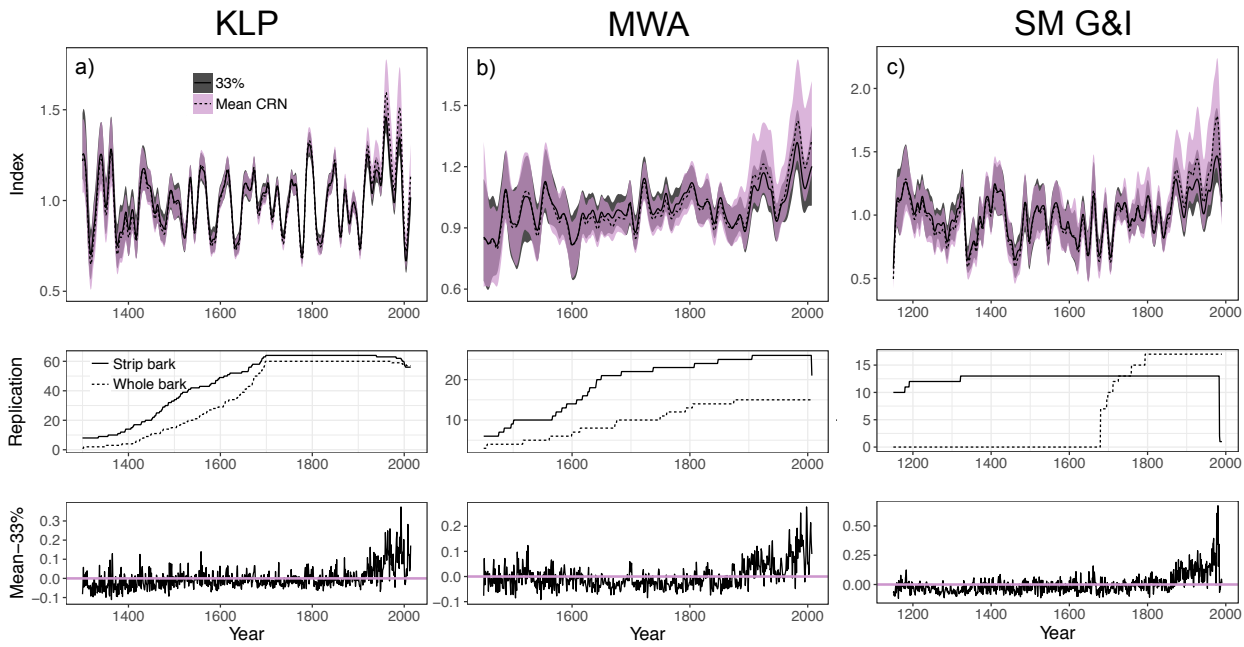

Fig. 3.9. Comparison of the 33rd percentile chronology (solid, gray) based on all trees, and the mean chronology ("Mean CRN", dotted, purple) for KLP (a), MWA (b), and the Graybill and Idso (1993) Sheep Mountain site (c). The mean and 95% BCa bootstrap confidence intervals for each chronology are shown. The middle panel shows replication at each site through time, and the bottom panel shows the difference between the annual original and 33rd percentile chronology for each site.

continuously reflect macro-scale growth-limiting factors (e.g., overall temperature variability) across all trees, rather than local and more variable microscale factors. It is possible that our low percentile method selects for series experiencing suppression and reduced climate sensitivity during some years, especially in temperature-sensitive sites. However, we argue that this is a minor concern relative to the need to correct for the demonstrated ring-width inflation bias associated with SB trees, particularly evident in KLP. At these drought-sensitive sites, the upper percentiles would select for trees with a substantial SB bias in recent centuries, and this could create a false impression of highly accelerated radial growth due to climatic change or some hypothesized non-climatic factor, such as CO_2 fertilization (e.g., Graybill and Idso 1993).

3.4 Concluding Comments and Future Recommendations

The chronology methods described here effectively reduce biases associated with radial growth inflation in SB trees. The SB growth phenomenon is particularly common during recent centuries in the trees studied here, and this could potentially bias the reliability of climate reconstructions based partly or fully on SB trees. Little research has been done comparing growth trends of SB and WB trees across different species and sites, even though there is a need to better understand the extent to which morphological changes can impact ring-width and chronology trends. To alleviate concerns regarding bias associated with SB trees, we first recommend that researchers document the morphology of trees that are sampled in the field, even to the extent of recording the percent cambial dieback along the main stem of each SB tree (Leland et al. 2018), so that comparisons between SB and WB ring-width and standardized chronology trends can be established for individual sites. If there are significant differences between the growth forms, and researchers have evidence that there is a non-climatic bias present in SB trees, then these biases can be conservatively corrected using one of the methods proposed in this study.

If WB trees are old enough to develop a sufficiently long chronology, we suggest producing a target WB mean chronology to adjust individual SB series (*Chronology method 1*). However, if WB trees are young relative to SB trees, the percentile method (*Chronology method 2*) may be an appropriate alternative to a mean chronology for developing a longer chronology based on the inclusion of older SB trees. While we used the 33rd percentile broadly for reducing a SB bias, an ideal percentile should be developed for particular sites where a WB mean chronology target is available for comparison with percentile chronologies. In the case where samples are analyzed from a site where SB trees were present, but the cambial status of

individual trees is unknown, we suggest that researchers compare a conservative lower percentile chronology (e.g., 33rd percentile) against the mean chronology to evaluate potential differences. Better understanding the extent to which partial cambial dieback can influence our tree-ring proxies will be essential for reducing potential biases in tree-ring chronologies and improving subsequent climate reconstructions.

Conclusions

Understanding the association between partial cambial dieback and ring-width trends is critical for improving tree-ring climate reconstructions based on ancient strip-bark conifers. This dissertation explores the timing and potential causes of partial cambial dieback, as well as its effect on ring-width trends and stable isotope records of Siberian pine, a long-lived species found in arid Central Asia. Importantly, this dissertation reveals that strip-bark Siberian pine trees have increasing ring-width and stable carbon isotope trends relative to whole-bark trees, perhaps related to an increase in the ratio of leaf area to sapwood area after cambial dieback events. Such distinct impacts of morphological changes on tree-ring parameters can lead to significant biases in climate reconstructions if cambial dieback effects are not considered as non-climatic signals during the standardization process.

Few studies have investigated the causes of partial cambial dieback and its direct effect on radial growth, particularly in species other than bristlecone pine and northern white cedar. In Chapter 1, I conducted the first detailed study on cambial dieback processes in Siberian pine. Using a combination of field notes and tree-ring methods, I found that cambial dieback was dominant on the southern side of tree stems, and occurred more frequently during the cold and dry mid-19th century. These results suggest that extreme temperature fluctuations from solar radiation might damage cambial tissue on trees at this particular site. This driver of stem dieback had not been previously reported in other studies, supporting the idea that different environmental hazards can lead to dieback, and that these hazards can be site-specific. Secondly, dramatic increases in ring widths of strip-bark trees, compared to whole-bark trees from the same site, were identified soon after the stand-wide dieback period. These results have considerable implications for paleoclimate studies. Compared to a hypothetical climate reconstruction derived

from the whole-bark chronology, a reconstruction computed from the strip-bark chronology would suggest that central Mongolia during the 20th century was drastically wetter than previous centuries. Chapter 1 confirmed that Siberian pine strip-bark trees do indeed have differing ring-width trends compared to whole-bark trees, and laid the necessary foundation for the following two chapters.

In Chapter 2, I assessed the physiological mechanisms behind increasing radial growth trends in strip-bark trees during the last two centuries. Currently, there is no clear consensus on what causes increasing ring-width trends in strip-bark trees. Graybill and Idso (1993) first speculated that bristlecone pine strip-bark trees have a more prominent CO_2 fertilization signal than whole-bark trees, but this has been highly debated (Graumlich 1991, Jacoby and D'Arrigo 1997, Bunn et al. 2003). Results from Chapter 2 suggest that strip-bark Siberian pine trees did not respond differently to increasing atmospheric CO_2 (supporting Tang et al. 1999) or climate during the 20th century. However, dieback events imprinted a unique stable isotope and ring-width signature on strip-bark series. Based on a sudden increase in ring width and an enrichment in $\delta^{13}C$ and $\delta^{18}O$ values following a known dieback event, I hypothesized that the ratio of leaf-to-sapwood area increases in strip-bark trees after cambial dieback. These results support the notion that dieback might contribute to the impressive longevity of conifers growing in adverse environments, as periodic dieback may help trees recover a sustainable stem size over centuries or millennia. Findings from this chapter shed light on ways in which long-lived trees, growing in adverse and climatically extreme sites, can respond to environmental changes over centuries.

From a broader context, results from Chapter 2 show that the Siberian pine trees from Khorgo, averaged across all samples, exhibited increasing intrinsic water-use efficiency (WUE_i) at rates similar to that reported in many other studies of conifers during the 20th century (Saurer

et al. 2004, 2014, Frank et al. 2015). Estimates of WUE_i trends can be affected not only by increasing atmospheric CO_2 concentrations, but also climate variability, which was not accounted for here. Moreover, results from Chapter 2 indicate that strip-bark trees can exhibit increasing $\delta^{13}C$ following cambial dieback events, suggesting that morphological changes in strip-bark trees over time could also have an impact on long-term estimates of WUE_i. In this study, dieback-related effects on $\delta^{13}C$ were most prevalent during the mid-19th century, prior to the period in which many studies evaluate changes in stable carbon isotopes as related to increasing atmospheric CO_2 concentrations. However, it is possible that in other sites, potential dieback-related effects on stable isotope ratios during recent decades could affect recent trend estimates of WUE_i. Assessing whether, and the extent to which, cambial dieback can influence stable isotope records in other tree species with strip-bark morphology will be important for improving estimates of the physiological response of ancient trees to increasing atmospheric CO_2.

After identifying a significant radial growth bias associated with partial cambial dieback in the first two chapters, I proposed methods for reducing strip-bark biases in Chapter 3. These methods were tested on both bristlecone pine and Siberian pine. While the first method directly corrects individual strip-bark trees to match low and medium-frequency variance of a 'target' whole-bark chronology, the second method is based on developing a low percentile (33rd percentile) chronology in lieu of a mean chronology. Both methods performed well to remove or reduce low-frequency variance associated with dieback, without removing climate-related variance that was inferred from the whole-bark chronology. These newly-developed methods are an important outcome of this dissertation because they can be applied across any site with strip-bark trees, assuming that there is a significant radial growth bias associated with cambial

dieback. Therefore, I strongly recommended that researchers collect samples from both strip-bark and whole-bark trees from their sites of interest to confirm whether such a bias exists. In the case of tree species with complex climate sensitivities, such as bristlecone pine, it will be very important to have a complete dataset to disentangle low-frequency signals associated with both climate and cambial dieback. While it is strongly encouraged that researchers record the morphological type of each tree prior to performing these methods, in some cases, this information might not be available (e.g., a previously sampled site without metadata for each tree). Under the scenario where the morphological type of each tree is unknown, the low percentiles method (~33rd percentile) could be used as conservative estimate of growth in case of strip-bark bias.

Future directions

I recommend three avenues of future research for advancing our knowledge on strip-bark morphology and its effect on radial growth. First and foremost, comparisons between strip-bark and whole-bark trees should be made across a variety of tree species, sites, and environments. The majority of research on partial cambial dieback has focused on bristlecone pine, northern white cedar, and most recently, Siberian pine; however, cambial dieback is a common morphological feature found on many other long-lived conifer species. It will be important to establish the causes of cambial dieback, and perhaps even more critical, to evaluate the extent to which dieback might cause ring-width inflation in strip-bark trees across different species and environments. The relationship between cambial dieback and ring-width trends has not been unequivocally established even for well-studied species. For bristlecone pine, in particular, more research should go towards disentangling low-frequency climatic and morphological signals.

Secondly, *in situ* and direct physiological measurements (e.g., estimates of the leaf area to sapwood area ratio, stomatal conductance, water potential, or embolism) should be taken from strip-bark and whole-bark trees. This information could be used to test some of the hypotheses in this dissertation, and would contribute to our understanding of how these trees are interacting with their environment. Measures of embolism (percentage loss of hydraulic conductivity) or water potential, for example, could indicate the degree of stress along particular sides of strip-bark trees, which might help point to environmental drivers of dieback (Sperry et al. 1988). More direct, experimental studies, such as those using dye to track hydraulic pathways (Larson et al. 1994), can also be performed to evaluate the degree of sectoriality in different species prone to strip-bark morphology. Studies of wood anatomy, an emerging topic of interest in dendrochronology, could also be informative on the physiological response of strip-bark and whole-bark trees to environmental changes, or their general hydraulic safety levels (Fonti et al. 2010). Wood anatomical metrics, especially measures of tracheid pits, cell lumen size, or cell wall thickness (e.g., Camarero et al. 2016, Martin-Benito et al. 2017), or measurements of needle traits, such as stomatal density or diameter (e.g., Guérin et al. 2018), could indicate whether strip-bark and whole-bark trees respond differently to extremes in their environment, or importantly, have different vulnerabilities to cavitation. For example, a study on Northern white cedar trees found that tracheids in older strip-bark trees had the largest pits, suggesting that older trees may be more susceptible to cavitation and thus, stem stripping (Matthes et al. 2002).

Lastly, it will be important to further quantify how various methods of tree-ring standardization either reduce, retain, or enhance strip-bark biases in tree-ring records, so that researchers can make informed decisions on how to statistically treat strip-bark ring-width series prior to developing climate reconstructions. This dissertation demonstrates that conservative

methods of standardization (i.e., the application of detrending curves that do not increase at the ends of tree-ring series; e.g., Fritts et al. 1969) retain a strip-bark bias when applied blindly to all trees. Further, Chapter 1 reveals that the signal-free method of standardization (Melvin and Briffa 2008) might emphasize these morphological signals in the tree-ring data even more strongly, thereby exacerbating differences in radial growth trends between strip-bark and whole-bark trees. The implications of using various standardization methods on strip-bark trees, and the chronology development methods proposed in Chapter 3, should be further explored. Recognizing and addressing potential strip-bark biases in tree-ring data will be essential for the paleoclimate community, especially as these data are critically important for understanding the range of climatic variability over the Common Era.

Bibliography

Ababneh LN. 2006. Analysis of radial growth patterns of strip-bark and whole-bark bristlecone pine trees in the White Mountains of California: implications in paleoclimatology and archaeology of the Great Basin. (Doctoral dissertation, University of Arizona)

Ainsworth EA, Rogers A. 2007. The response of photosynthesis and stomatal conductance to rising [CO_2]: mechanisms and environmental interactions: Photosynthesis and stomatal conductance responses to rising [CO_2]. *Plant, Cell & Environment* 30(3): 258–270.

Akaike H. 1974. A new look at the statistical model identification. *IEEE transactions on automatic control* 19: 716–723.

Allen CD, Macalady AK, Chenchouni H, Bachelet D, McDowell N, Vennetier M, Kitzberger T, Rigling A, Breshears DD, Hogg EH (Ted), *et al.* 2010. A global overview of drought and heat-induced tree mortality reveals emerging climate change risks for forests. *Forest Ecology and Management* 259(4): 660–684.

Allen CD, Breshears DD, McDowell NG. 2015. On underestimation of global vulnerability to tree mortality and forest die-off from hotter drought in the Anthropocene. *Ecosphere* 6(8): art129.

Anchukaitis KJ, D'Arrigo RD, Andreu-Hayles L, Frank D, Verstege A, Curtis A, Buckley BM, Jacoby GC, Cook ER. 2013. Tree-Ring-Reconstructed Summer Temperatures from Northwestern North America during the Last Nine Centuries. *Journal of Climate* 26(10): 3001–3012.

Andreu-Hayles L, Planells O, GutiéRrez E, Muntan E, Helle G, Anchukaitis KJ, Schleser GH. 2011. Long tree-ring chronologies reveal 20th century increases in water-use efficiency but no enhancement of tree growth at five Iberian pine forests. *Global Change Biology* 17(6): 2095–2112.

Andreu-Hayles L, Levesque M, Martin-Benito D, Huang W, Harris R, Oelkers R, Leland C, Martin-Fernández J, Anchukaitis KJ, Helle G. 2019. A high yield cellulose extraction system for small whole wood samples and dual measurement of carbon and oxygen stable isotopes. *Chemical Geology* 504: 53–65.

Araguás-Araguás L, Froehlich K, Rozanski K. 1998. Stable isotope composition of precipitation over southeast Asia. *Journal of Geophysical Research: Atmospheres* 103: 28721–28742.

Bailey DK. 1970. Phytogeography and Taxonomy of Pinus Subsection Balfourianae. *Annals of the Missouri Botanical Garden* 57: 210–249.

Barbour MM. 2007. Stable oxygen isotope composition of plant tissue: a review. *Functional Plant Biology* 34(2): 83–94.

Beasley RS, Klemmedson JO. 1973. Recognizing site adversity and drought-sensitive trees in stands of bristlecone pine (*Pinus longaeva*). *Economic Botany* 27(1): 141–146.

Begum S, Nakaba S, Bayramzadeh V, Yuichiro Oribe, Kubo T, Funada R. 2008. Temperature responses of cambial reactivation and xylem differentiation in hybrid poplar (*Populus sieboldii* × *P. grandidentata*) under natural conditions. *Tree Physiology* 28: 1813–1819.

Beier CM, Sink SE, Hennon PE, D'Amore DV, Juday GP. 2008. Twentieth-century warming and the dendroclimatology of declining yellow-cedar forests in southeastern Alaska. *Canadian Journal of Forest Research* 38(6): 1319–1334.

Boyce RL, Lubbers B. 2011. Bark-stripping patterns in bristlecone pine (Pinus aristata) stands in Colorado, USA. *The Journal of the Torrey Botanical Society* 138(3): 308–321.

Brienen RJW, Gloor E, Clerici S, Newton R, Arppe L, Boom A, Bottrell S, Callaghan M, Heaton T, Helama S, *et al.* 2017. Tree height strongly affects estimates of water-use efficiency responses to climate and CO2 using isotopes. *Nature Communications* 8(1): 288.

Briffa KR, Jones PD, Bartholin TS, Eckstein D, Schweingruber FH, Karlén W, Zetterberg P, Eronen M. 1992. Fennoscandian summers from ad 500: temperature changes on short and long timescales. *Climate Dynamics* 7(3): 111–119.

Briffa KR, Jones PD, Schweingruber FH, Karlén W, Shiyatov SG. 1996. Tree-ring variables as proxy-climate indicators: problems with low-frequency signals. In: Climatic variations and forcing mechanisms of the last 2000 years. Springer, 9–41.

Briffa KR, Melvin TM. 2011. A Closer Look at Regional Curve Standardization of Tree-Ring Records: Justification of the Need, a Warning of Some Pitfalls, and Suggested Improvements in Its Application. In: Hughes MK, Swetnam TW, Diaz HF, eds. Developments in Paleoenvironmental Research. Dendroclimatology. Springer Netherlands, 113–145.

Buchmann N, Kao W-Y, Ehleringer J. 1997. Influence of stand structure on carbon-13 of vegetation, soils, and canopy air within deciduous and evergreen forests in Utah, United States. *Oecologia* 110(1): 109–119.

Bunn A, Lawrence R, Bellante G, Waggoner L, Graumlich L. 2003. Spatial Variation in Distribution and Growth Patterns of Old Growth Strip-Bark Pines. *Arctic, Antarctic, and Alpine Research* 35(3): 323–330.

Bunn AG. 2008. A dendrochronology program library in R (dplR). *Dendrochronologia* 26(2): 115–124.

Bunn AG, Salzer MW, Anchukaitis KJ, Bruening JM, Hughes MK. 2018. Spatiotemporal Variability in the Climate Growth Response of High Elevation Bristlecone Pine in the White Mountains of California. *Geophysical Research Letters* 45(24): 13,312-13,321.

Camarero JJ, Guada G, Sánchez-Salguero R, Cervantes E. 2016. Winter drought impairs xylem phenology, anatomy and growth in Mediterranean Scots pine forests (A Mäkelä, Ed.). *Tree Physiology* 36(12): 1536–1549.

Connor KF, Lanner RM. 1990. Effects of tree age on secondary xylem and phloem anatomy in stems of Great Basin bristlecone pine (Pinus longaeva). *American Journal of Botany* 77(8): 1070–1077.

Cook ER, Peters K. 1981. The Smoothing Spline: A New Approach to Standardizing Forest Interior Tree-Ring Width Series for Dendroclimatic Studies. *Tree-Ring Bulletin* 41: 45–53.

Cook ER. 1985. A Time Series Analysis Approach to Tree Ring Standardization. (Doctoral dissertation, University of Arizona)

Cook ER, Kairiukstis LA. 1990. *Methods of dendrochronology: applications in the environmental sciences*. Springer Science & Business Media.

Cook ER, Briffa KR, Meko DM, Graybill DA, Funkhouser G. 1995. The 'segment length curse' in long tree-ring chronology development for palaeoclimatic studies. *The Holocene* 5(2): 229–237.

Cook ER, Peters K. 1997. Calculating unbiased tree-ring indices for the study of climatic and environmental change. *The Holocene* 7(3): 361–370.

Cook ER, Krusic PJ. 2014. Program *ARSTAN*. Accessed from: https://www.ldeo.columbia.edu/tree-ring-laboratory/resources/software

Cook BI, Anchukaitis KJ, Touchan R, Meko DM, Cook ER. 2016. Spatiotemporal drought variability in the Mediterranean over the last 900 years. *Journal of Geophysical Research: Atmospheres* 121(5): 2060-2074.

Dansgaard W. 1964. Stable isotopes in precipitation. *Tellus* 16(4): 436–468.

D'Arrigo R, Davi N, Jacoby G, Wilson R, Wiles G. 2014. *Dendroclimatic Studies: Tree Growth and Climate Change in Northern Forests*. John Wiley & Sons.

Davi NK, Jacoby GC, Curtis AE, Baatarbileg N. 2006. Extension of Drought Records for Central Asia Using Tree Rings: West-Central Mongolia. *Journal of Climate* 19(2): 288–299.

Davi NK, D'Arrigo R, Jacoby GC, Cook ER, Anchukaitis KJ, Nachin B, Rao MP, Leland C. 2015. A long-term context (931–2005 C.E.) for rapid warming over Central Asia. *Quaternary Science Reviews* 121: 89–97.

De Grandpré L, Tardif JC, Hessl A, Pederson N, Conciatori F, Green TR, Oyunsanaa B, Baatarbileg N. 2011. Seasonal shift in the climate responses of Pinus sibirica, Pinus sylvestris, and Larix sibirica trees from semi-arid, north-central Mongolia. *Canadian Journal of Forest Research* 41(6): 1242–1255.

Di Filippo A, Pederson N, Baliva M, Brunetti M, Dinella A, Kitamura K, Knapp HD, Schirone B, Piovesan G. 2015. The longevity of broadleaf deciduous trees in Northern Hemisphere temperate forests: insights from tree-ring series. *Frontiers in Ecology and Evolution* 3.

Dietrich L, Hoch G, Kahmen A, Körner C. 2018. Losing half the conductive area hardly impacts the water status of mature trees. *Scientific Reports* 8(1): 15006.

Druckenbrod DL, Pederson N, Rentch J, Cook ER. 2013. A comparison of times series approaches for dendroecological reconstructions of past canopy disturbance events. *Forest Ecology and Management* 302: 23–33.

Duquesnay A, Bréda N, Stievenard M, Dupouey JL. 1998. Changes of tree-ring δ13C and water-use efficiency of beech (Fagus sylvatica L.) in north-eastern France during the past century. *Plant, Cell & Environment*, *21*(6): 565-572.

Efron B. 1987. Better Bootstrap Confidence Intervals. *Journal of the American Statistical Association* 82(397): 171–185.

Esper J. 2000. Long-term tree-ring variations in Juniperus at the upper timber-line in the Karakorum (Pakistan). *The Holocene* 10(2): 253–260.

Esper J, Cook ER, Schweingruber FH. 2002. Low-Frequency Signals in Long Tree-Ring Chronologies for Reconstructing Past Temperature Variability. *Science* 295: 2250–2253.

Farquhar GD, O'leary MH, Berry JA. 1982. On the relationship between carbon isotope discrimination and the intercellular carbon dioxide concentration in leaves. *Functional Plant Biology* 9(2): 121–137.

Farquhar GD, Ehleringer JR, Hubick KT. 1989. Carbon Isotope Discrimination and Photosynthesis. *Annual Review of Plant Physiology and Plant Molecular Biology* 40(1): 503–537.

Fonti P, von Arx G, García-González I, Eilmann B, Sass-Klaassen U, Gärtner H, Eckstein D. 2010. Studying global change through investigation of the plastic responses of xylem anatomy in tree rings. *New Phytologist* 185(1): 42–53.

Francey RJ, Farquhar GD. 1982. An explanation of 13C/12C variations in tree rings. *Nature* 297(5861): 28.

Frank DC, Poulter B, Saurer M, Esper J, Huntingford C, Helle G, Treydte K, Zimmermann NE, Schleser GH, Ahlström A, *et al.* 2015. Water-use efficiency and transpiration across European forests during the Anthropocene. *Nature Climate Change* 5(6): 579–583.

Fritts HC. 1969. Bristlecone pine in the White Mountains of California. (No. 4). University of Arizona Press.

Fritts H, Mosimann J, Bottorff C. 1969. A revised computer program for standardizing tree-ring series. Tree-Ring Bulletin 29, 15-20.

Fritts HC, Blasing TJ, Hayden BP, Kutzbach JE. 1971. Multivariate techniques for specifying tree-growth and climate relationships and for reconstructing anomalies in paleoclimate. *Journal of Applied Meteorology* 10(5): 845–864.

Fritts HC. 1976. *Tree rings and climate*. London, UK: Academic Press.

Fritts HC, Swetnam TW. 1989. Dendroecology: A Tool for Evaluating. *Advances in ecological research* 19: 111.

Gagen M, McCarroll D, Edouard J-L. 2004. Latewood Width, Maximum Density, and Stable Carbon Isotope Ratios of Pine as Climate Indicators in a Dry Subalpine Environment, French Alps. *Arctic, Antarctic, and Alpine Research* 36(2): 166–171.

Gagen M, McCarroll D, Loader NJ, Robertson I, Jalkanen R, Anchukaitis KJ. 2007. Exorcising the `segment length curse': summer temperature reconstruction since AD 1640 using non-detrended stable carbon isotope ratios from pine trees in northern Finland. *The Holocene* 17(4): 435–446.

Gagen M, McCarroll D, Loader NJ, Robertson I. 2011. Stable Isotopes in Dendroclimatology: Moving Beyond 'Potential'. In: Hughes MK, Swetnam TW, Diaz HF, eds. Dendroclimatology. Dordrecht: Springer Netherlands, 147–172.

Gessler A, Cailleret M, Joseph J, Schönbeck L, Schaub M, Lehmann M, Treydte K, Rigling A, Timofeeva G, Saurer M. 2018. Drought induced tree mortality - a tree-ring isotope based conceptual model to assess mechanisms and predispositions. *New Phytologist* 219: 485–490.

Giguère-Croteau C, Boucher É, Bergeron Y, Girardin MP, Drobyshev I, Silva LCR, Hélie J-F, Garneau M. 2019. North America's oldest boreal trees are more efficient water users due to increased [CO_2], but do not grow faster. *Proceedings of the National Academy of Sciences* 116(7): 2749–2754.

Graumlich LJ. 1991. Subalpine Tree Growth, Climate, and Increasing CO_2: An Assessment of Recent Growth Trends. *Ecology* 72(1): 1–11.

Graybill DA, Idso SB. 1993. Detecting the aerial fertilization effect of atmospheric CO2 enrichment in tree-ring chronologies. *Global Biogeochemical Cycles* 7(1): 81–95.

Guérin M, Martin‐Benito D, von Arx G, Andreu‐Hayles L, Griffin KL, Hamdan R, McDowell NG, Muscarella R, Pockman W, Gentine P. 2018. Interannual variations in needle and sapwood traits of *Pinus edulis* branches under an experimental drought. *Ecology and evolution* 8(3):1655-72.

Harris I, Jones PD, Osborn TJ, Lister DH. 2014. Updated high-resolution grids of monthly climatic observations - the CRU TS3.10 Dataset. *International Journal of Climatology* 34: 623–642.

Harvey RB. 1923. Cambial temperatures of trees in winter and their relation to sun scald. *Ecology* 4(3): 261–265.

Hereş A-M, Voltas J, López BC, Martínez-Vilalta J. 2014. Drought-induced mortality selectively affects Scots pine trees that show limited intrinsic water-use efficiency responsiveness to raising atmospheric CO_2. *Functional Plant Biology* 41(3): 244.

Hessl AE, Anchukaitis KJ, Jelsema C, Cook B, Byambasuren O, Leland C, Nachin B, Pederson N, Tian H, Hayles LA. 2018. Past and future drought in Mongolia. *Science Advances* 4: e1701832.

Holmes RL. 1983. Computer-assisted quality control in tree-ring dating and measurement. *Tree-ring bulletin* 43: 69–78.

Huckaby LS, Kaufmann MR, Fornwalt PJ, Stoker JM, Dennis C. 2003. *Identification and ecology of old ponderosa pine trees in the Colorado Front Range*. Ft. Collins, CO: U.S. Department of Agriculture, Forest Service, Rocky Mountain Research Station.

Hughes MK, Funkhouser G. 2003. Frequency-Dependent Climate Signal in Upper and Lower Forest Border Tree Rings in the Mountains of the Great Basin. In: Diaz HF, ed. Advances in Global Change Research. Climate Variability and Change in High Elevation Regions: Past, Present & Future. Springer Netherlands, 233–244.

Jacoby GC, D'Arrigo RD, Davaajamts T. 1996. Mongolian Tree Rings and 20th-Century Warming. *Science* 273(5276): 771–773.

Jacoby GC, D'Arrigo RD. 1997. Tree rings, carbon dioxide, and climatic change. *Proceedings of the National Academy of Sciences* 94(16): 8350–8353.

Kalman RE. 1960. A New Approach to Linear Filtering and Prediction Problems. *Journal of Fluids Engineering* 82(1): 35–45.

Keenan TF, Hollinger DY, Bohrer G, Dragoni D, Munger JW, Schmid HP, Richardson AD. 2013. Increase in forest water-use efficiency as atmospheric carbon dioxide concentrations rise. *Nature* 499(7458): 324–327.

Kelly PE, Cook ER, Larson DW. 1992. Constrained Growth, Cambial Mortality, and Dendrochronology of Ancient Thuja occidentalis on Cliffs of the Niagara Escarpment: An Eastern Version of Bristlecone Pine? *International Journal of Plant Sciences* 153(1): 117–127.

Kipfmueller KF, Salzer MW. 2010. Linear trend and climate response of five-needle pines in the western United States related to treeline proximity. *Canadian Journal of Forest Research* 40(1), pp.134-142.

Klesse S, Weigt R, Treydte K, Saurer M, Schmid L, Siegwolf RTW, Frank DC. 2018. Oxygen isotopes in tree rings are less sensitive to changes in tree size and relative canopy position than carbon isotopes: Oxygen isotopes in tree-rings are less sensitive. *Plant, Cell & Environment* 41(12): 2899-2914.

Knölller K, Boettger T, Weise SM, Gehre M. 2005. Carbon isotope analyses of cellulose using two different on-line techniques (elemental analysis and high-temperature pyrolysis)-a comparison. *Rapid Communications in Mass Spectrometry* 19(3): 343–348.

Komsta L. 2013. *mblm: Median-Based Linear Models*. R package version.

Kozlowski TT, Kramer PJ, Pallardy SG. 1991. Temperature. In: The Physiological Ecology of Woody Plants. Elsevier, 168–211.

Kramer PJ, Kozlowski, T.T. 1979. *Physiology of Woody Plants*. Academic Press, New York.

Kubler H. 1991. Function of spiral grain in trees. *Trees-Structure and Function* 5: 125–135.

Kullman L. 1991. Cataclysmic response to recent cooling of a natural boreal pine (*Pinus sylvestris* L.) forest in northern Sweden. *New Phytologist* 117(2): 351–360.

LaMarche VC Jr. 1969. Environment in Relation to Age of Bristlecone Pines. *Ecology* 50: 53–59.

Larson DW, Matthes-Sears U, Kelly PE. 1993. Cambial Dieback and Partial Shoot Mortality in Cliff-Face Thuja occidentalis: Evidence for Sectored Radial Architecture. *International Journal of Plant Sciences* 154(4): 496–505.

Larson DW, Doubt J, Matthes-Sears U. 1994. Radially Sectored Hydraulic Pathways in the Xylem of Thuja occidentalis as Revealed by the Use of Dyes. *International Journal of Plant Sciences* 155(5): 569–582.

Larson DW. 2001. The paradox of great longevity in a short-lived tree species. *Experimental Gerontology* 36(4-6): 651–673.

Leland C, Pederson N, Hessl A, Nachin B, Davi N, D'Arrigo R, Jacoby G. 2013. A hydroclimatic regionalization of central Mongolia as inferred from tree rings. *Dendrochronologia*. 31(3): 205-215

Leland C, Cook ER, Andreu-Hayles L, Pederson N, Hessl A, Anchukaitis KJ, Byambasuren O, Nachin B, Davi N, D'Arrigo R, *et al.* 2018. Strip-Bark Morphology and Radial Growth Trends in Ancient *Pinus sibirica* Trees From Central Mongolia. *Journal of Geophysical Research: Biogeosciences* 123(3): 945–959.

Leuenberger M. 2007. To What Extent Can Ice Core Data Contribute to the Understanding of Plant Ecological Developments of the Past? In: Isotopes as Indicators of Ecological Change. Elsevier, 211–III.

Lévesque M, Siegwolf R, Saurer M, Eilmann B, Rigling A. 2014. Increased water-use efficiency does not lead to enhanced tree growth under xeric and mesic conditions. *New Phytologist* 203: 94–109.

Loader NJ, Robertson I, Barker AC, Switsur VR, Waterhouse JS. 1997. An improved technique for the batch processing of small wholewood samples to α-cellulose. *Chemical Geology* 136: 313–317.

Loader NJ, Robertson I, McCarroll D. 2003. Comparison of stable carbon isotope ratios in the whole wood, cellulose and lignin of oak tree-rings. *Palaeogeography, Palaeoclimatology, Palaeoecology* 196: 395–407.

Martin-Benito D, Anchukaitis K, Evans M, del Río M, Beeckman H, Cañellas I. 2017. Effects of Drought on Xylem Anatomy and Water-Use Efficiency of Two Co-Occurring Pine Species. *Forests* 8(9): 332.

Mastrotheodoros T, Pappas C, Molnar P, Burlando P, Keenan TF, Gentine P, Gough CM, Fatichi S. 2017. Linking plant functional trait plasticity and the large increase in forest water use efficiency: WUE Increase Revisited. *Journal of Geophysical Research: Biogeosciences* 122(9): 2393–2408.

Mathaux C, Mandin J-P, Oberlin C, Edouard J-L, Gauquelin T, Guibal F. 2016. Ancient juniper trees growing on cliffs: toward a long Mediterranean tree-ring chronology. *Dendrochronologia* 37: 79–88.

Matthes U, Kelly PE, Ryan CE, Larson DW. 2002. The Formation and Possible Ecological Function of Stem Strips in Thuja occidentalis. *International Journal of Plant Sciences* 163(6): 949–958.

Matthes U, Kelly PE, Larson DW. 2008. Predicting the age of ancient *Thuja occidentalis* on cliffs. *Canadian Journal of Forest Research* 38(12): 2923–2931.

Matthes U, Larson DW. 2009. Can Stem Strips Be Induced? An Experimental Investigation of Cliff-Face Thuja occidentalis. *International Journal of Plant Sciences* 170: 1109–1119.

Mayr S, Wolfschwenger M, Bauer H. 2002. Winter-drought induced embolism in Norway spruce (Picea abies) at the Alpine timberline. *Physiologia Plantarum* 115(1): 74–80.

Mayr S, Gruber A, Bauer H. 2003. Repeated freeze-thaw cycles induce embolism in drought stressed conifers (Norway spruce, stone pine). *Planta* 217(3): 436–441.

Mayr S, Schmid P, Laur J, Rosner S, Charra-Vaskou K, Damon B, Hacke UG. 2014. Uptake of Water via Branches Helps Timberline Conifers Refill Embolized Xylem in Late Winter. *Plant Physiology* 164(4): 1731–1740.

McCarroll D, Loader NJ. 2004. Stable isotopes in tree rings. *Quaternary Science Reviews* 23: 771–801.

McCarroll D, Gagen MH, Loader NJ, Robertson I, Anchukaitis KJ, Los S, Young GHF, Jalkanen R, Kirchhefer A, Waterhouse JS. 2009. Correction of tree ring stable carbon isotope chronologies for changes in the carbon dioxide content of the atmosphere. *Geochimica et Cosmochimica Acta* 73(6): 1539–1547.

McDowell N, Barnard H, Bond B, Hinckley T, Hubbard R, Ishii H, Köstner B, Magnani F, Marshall J, Meinzer F, *et al.* 2002. The relationship between tree height and leaf area: sapwood area ratio. *Oecologia* 132: 12–20.

McDowell N, Pockman WT, Allen CD, Breshears DD, Cobb N, Kolb T, Plaut J, Sperry J, West A, Williams DG, *et al.* 2008. Mechanisms of plant survival and mortality during drought: why do some plants survive while others succumb to drought? *New Phytologist* 178(4): 719–739.

Melvin TM, Briffa KR, Nicolussi K, Grabner M. 2007. Time-varying-response smoothing. *Dendrochronologia* 25(1): 65–69.

Melvin TM, Briffa KR. 2008. A "signal-free" approach to dendroclimatic standardisation. *Dendrochronologia* 26(2): 71–86.

Molod A, Takacs L, Suarez M, Bacmeister J. 2015. Development of the GEOS-5 atmospheric general circulation model: evolution from MERRA to MERRA2. *Geoscientific Model Development* 8: 1339–1356.

Morison JIL. 1985. Sensitivity of stomata and water use efficiency to high CO2. *Plant, Cell and Environment* 8(6): 467–474.

Norby RJ, Zak DR. 2011. Ecological Lessons from Free-Air CO_2 Enrichment (FACE) Experiments. *Annual Review of Ecology, Evolution, and Systematics* 42: 181–203.

Oribe Y, Kubo T. 1997. Effect of heat on cambial reactivation during winter dormancy in evergreen and deciduous conifers. *Tree Physiology* 17(2): 81–87.

Oribe Y, Funada R, Kubo T. 2003. Relationships between cambial activity, cell differentiation and the localization of starch in storage tissues around the cambium in locally heated stems of Abies sachalinensis (Schmidt) Masters. *Trees* 17(3): 185–192.

Pederson N. 2010. External characteristics of old trees in the Eastern Deciduous Forest. *Natural Areas Journal* 30(4): 396–407.

Pederson N, Hessl AE, Baatarbileg N, Anchukaitis KJ, Cosmo ND. 2014. Pluvials, droughts, the Mongol Empire, and modern Mongolia. *Proceedings of the National Academy of Sciences* 111(12): 4375–4379.

Peñuelas J, Canadell JG, Ogaya R. 2011. Increased water-use efficiency during the 20th century did not translate into enhanced tree growth: Tree growth in the 20th century. *Global Ecology and Biogeography* 20(4): 597–608.

Petris G, An R. 2010. An R package for dynamic linear models. *Journal of Statistical Software* 36(12): 1–16.

PRISM Climate Group, Oregon State University, http://prism.oregonstate.edu, created 4 Feb 2004.

R Core Team. 2016. *R: A Language and Environment for Statistical Computing*. Vienna, Austria: R Foundation for Statistical Computing.

Rienecker MM, Suarez MJ, Gelaro R, Todling R, Bacmeister J, Liu E, Bosilovich MG, Schubert SD, Takacs L, Kim G-K, *et al.* 2011. MERRA: NASA's Modern-Era Retrospective Analysis for Research and Applications. *Journal of Climate* 24(14): 3624–3648.

Robertson A, Overpeck J, Rind D, Mosley-Thompson E, Zielinski G, Lean J, Koch D, Penner J, Tegen I, Healy R. 2001. Hypothesized climate forcing time series for the last 500 years. *Journal of Geophysical Research: Atmospheres* 106: 14783–14803.

Roden JS, Lin G, Ehleringer JR. 2000. A mechanistic model for interpretation of hydrogen and oxygen isotope ratios in tree-ring cellulose. *Geochimica et Cosmochimica Acta* 64: 21–35.

Roden J, Siegwolf R. 2012. Is the dual-isotope conceptual model fully operational? *Tree Physiology* 32(10): 1179–1182.

Sakai A. 1966. Temperature fluctuation in wintering trees. *Physiologia Plantarum* 19: 105–114.

Sakai A, Larcher W. 1987. *Frost Survival of Plants: responses and adaptation to freezing stress. Ecological Studies 62*. Springer, Berlin Heidelberg New York.

Salzer MW, Hughes MK, Bunn AG, Kipfmueller KF. 2009. Recent unprecedented tree-ring growth in bristlecone pine at the highest elevations and possible causes. *Proceedings of the National Academy of Sciences* 106(48): 20348–20353.

Saurer M, Schweingruber F, Vaganov EA, Shiyatov SG, Siegwolf R. 2002. Spatial and temporal oxygen isotope trends at the northern tree-line in Eurasia. *Geophysical Research Letters* 29(9): 7–1.

Saurer M, Siegwolf RTW, Schweingruber FH. 2004. Carbon isotope discrimination indicates improving water-use efficiency of trees in northern Eurasia over the last 100 years. *Global Change Biology* 10(12): 2109–2120.

Saurer M, Spahni R, Frank DC, Joos F, Leuenberger M, Loader NJ, McCarroll D, Gagen M, Poulter B, Siegwolf RTW, *et al.* 2014. Spatial variability and temporal trends in water-use efficiency of European forests. *Global Change Biology* 20(12): 3700–3712.

Schaberg PG, D'Amore DV, Hennon PE, Halman JM, Hawley GJ. 2011. Do limited cold tolerance and shallow depth of roots contribute to yellow-cedar decline? *Forest Ecology and Management* 262(12): 2142–2150.

Schafer KVR, Oren R, Tenhunen JD. 2000. The effect of tree height on crown level stomatal conductance. *Plant, Cell and Environment* 23(4): 365–375.

Schauer AJ, Schoettle AW, Boyce RL. 2001. Partial cambial mortality in high-elevation Pinus aristata (Pinaceae). *American Journal of Botany* 88(4): 646–652.

Scheidegger Y, Saurer M, Bahn M, Siegwolf R. 2000. Linking stable oxygen and carbon isotopes with stomatal conductance and photosynthetic capacity: a conceptual model. *Oecologia* 125(3): 350–357.

van der Schrier G, Barichivich J, Briffa KR, Jones PD. 2013. A scPDSI-based global data set of dry and wet spells for 1901–2009. *Journal of Geophysical Research: Atmospheres* 118(10): 4025–4048.

Schulman E. 1954. Longevity under adversity in conifers. *Science* 119(3091): 396–399.

Schulman E, Ferguson C. 1956. Millenia-old pine trees sampled in 1954 and 1955. *Dendroclimatic Changes in Semiarid America, by E. Schulman*: 136–138.

Schulz M, Mudelsee M. 2002. REDFIT: estimating red-noise spectra directly from unevenly spaced paleoclimatic time series. *Computers & Geosciences* 28(3): 421–426.

Siegel AF. 1982. Robust Regression Using Repeated Medians. *Biometrika* 69(1): 242.

Speer JH. 2010. *Fundamentals of tree-ring research*. University of Arizona Press.

Sperry JS, Donnelly JR, Tyree MT. 1988. Seasonal Occurrence of Xylem Embolism in Sugar Maple (Acer saccharum). *American Journal of Botany* 75(8): 1212.

Sperry JS, Sullivan JE. 1992. Xylem embolism in response to freeze-thaw cycles and water stress in ring-porous, diffuse-porous, and conifer species. *Plant Physiology* 100(2): 605–613.

Sperry JS, Nichols KL, Sullivan JEM, Eastlack SE. 1994. Xylem Embolism in Ring-Porous, Diffuse-Porous, and Coniferous Trees of Northern Utah and Interior Alaska. *Ecology* 75: 1736–1752.

Sperry JS, Hacke UG, Pittermann J. 2006. Size and function in conifer tracheids and angiosperm vessels. *American Journal of Botany* 93(10): 1490–1500.

Stahle DW. 1996. Tree rings and ancient forest relics. *Arnoldia* 56(4): 2–10.

Stine AR, Huybers P. 2017. Implications of Liebig's law of the minimum for tree-ring reconstructions of climate. *Environmental Research Letters* 12(11): 114018.

Stoffel M, Bollschweiler M. 2008. Tree-ring analysis in natural hazards research? an overview. *Natural Hazards and Earth System Science* 8: 187–202.

Stokes MA, Smiley, TL. 1968. *An Introduction to Tree-Ring Dating*. Chicago, USA: The University of Chicago Press.

Swetnam TW, Brown PM. 1992. Oldest known conifers in the southwestern United States: temporal and spatial patterns of maximum age. *Old Growth Forests in the Southwest and*

Rocky Mountain Regions. USDA Forest Service General Technical Report RM-213: 24–38.

Tang K, Feng X, Funkhouser G. 1999. The δ13C of tree rings in full-bark and strip-bark bristlecone pine trees in the White Mountains of California. *Global Change Biology* 5: 33–40.

Tran TJ, Bruening JM, Bunn AG, Salzer MW, Weiss SB. 2017. Cluster analysis and topoclimate modeling to examine bristlecone pine tree-ring growth signals in the Great Basin, USA. *Environmental Research Letters* 12(1): 014007.

Tuovinen M, Jalkanen R, McCarroll D. 2005. The effect of severe ground frost on Scots pine (*Pinus sylvestris*) trees in northern Finland and implications for palaeoclimate reconstruction. *Fennia* 183(2): 109-117.

Vicente-Serrano SM, Beguería S, López-Moreno JI. 2010. A Multiscalar Drought Index Sensitive to Global Warming: The Standardized Precipitation Evapotranspiration Index. *Journal of Climate* 23(7): 1696–1718.

Visser H, Büntgen U, D'Arrigo R, Petersen AC. 2010. Detecting instabilities in tree-ring proxy calibration. *Climate of the Past* 6(3): 367–377.

Visser H, Molenaar J. 1988. Kalman filter analysis in dendroclimatology. *Biometrics*: 929–940.

Voltas J, Camarero JJ, Carulla D, Aguilera M, Ortiz A, Ferrio JP. 2013. A retrospective, dual-isotope approach reveals individual predispositions to winter-drought induced tree dieback in the southernmost distribution limit of Scots pine: Scots pine disposition to winter-drought dieback. *Plant, Cell & Environment* 36(8): 1435–1448.

Wang S, Zhang M, Che Y, Chen F, Qiang F. 2016. Contribution of recycled moisture to precipitation in oases of arid central Asia: A stable isotope approach. *Water Resources Research* 52(4): 3246–3257.

Wigley TML, Briffa KR, Jones PD. 1984. On the Average Value of Correlated Time Series, with Applications in Dendroclimatology and Hydrometeorology. *Journal of Climate and Applied Meteorology* 23(2): 201–213.

Williams AP, Allen CD, Macalady AK, Griffin D, Woodhouse CA, Meko DM, Swetnam TW, Rauscher SA, Seager R, Grissino-Mayer HD, *et al.* 2013. Temperature as a potent driver of regional forest drought stress and tree mortality. *Nature Climate Change* 3: 292–297.

Wilson R, Anchukaitis K, Briffa KR, Büntgen U, Cook E, D'Arrigo R, Davi N, Esper J, Frank D, Gunnarson B, *et al.* 2016. Last millennium northern hemisphere summer temperatures from tree rings: Part I: The long term context. *Quaternary Science Reviews* 134: 1–18.

Wright RD, Mooney HA. 1965. Substrate-oriented Distribution of Bristlecone Pine in the White Mountains of California. *American Midland Naturalist* 73: 257–284.

Yang B, Qin C, Wang J, He M, Melvin TM, Osborn TJ, Briffa KR. 2014. A 3,500-year tree-ring record of annual precipitation on the northeastern Tibetan Plateau. *Proceedings of the National Academy of Sciences* 111(8): 2903-2908.

Zang C, Biondi F. 2015. treeclim: an R package for the numerical calibration of proxy-climate relationships. *Ecography* 38(4): 431–436.

Zanne AE, Sweeney K, Sharma M, Orians CM. 2006. Patterns and consequences of differential vascular sectoriality in 18 temperate tree and shrub species. *Functional Ecology* 20(2): 200–206.

Appendices

Appendix A: Supplemental Figures and Tables for Chapter One

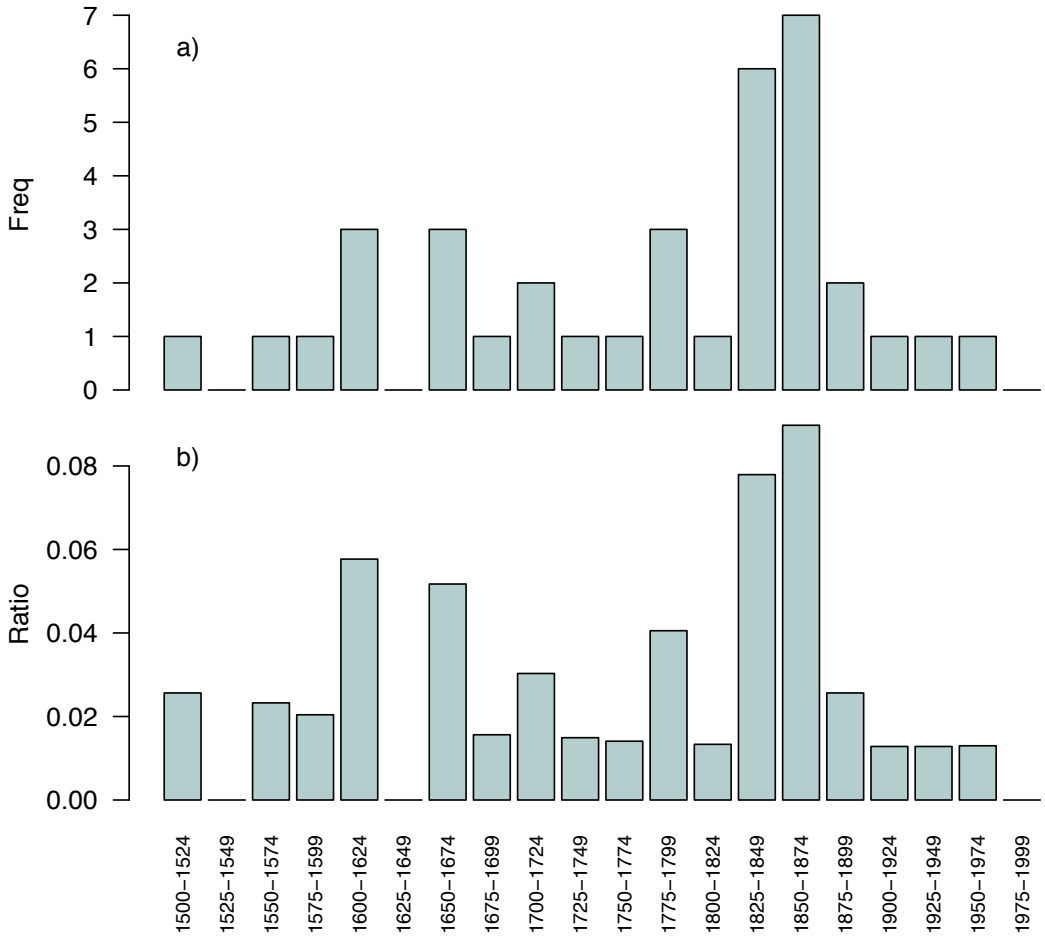

Fig. A.1. Cambial death dates through time; a) Frequency of estimated cambial death events for 25-year periods from 1500-1999; b) the ratio of the number of death events to the total number of series with a corresponding death date in each 25-year period.

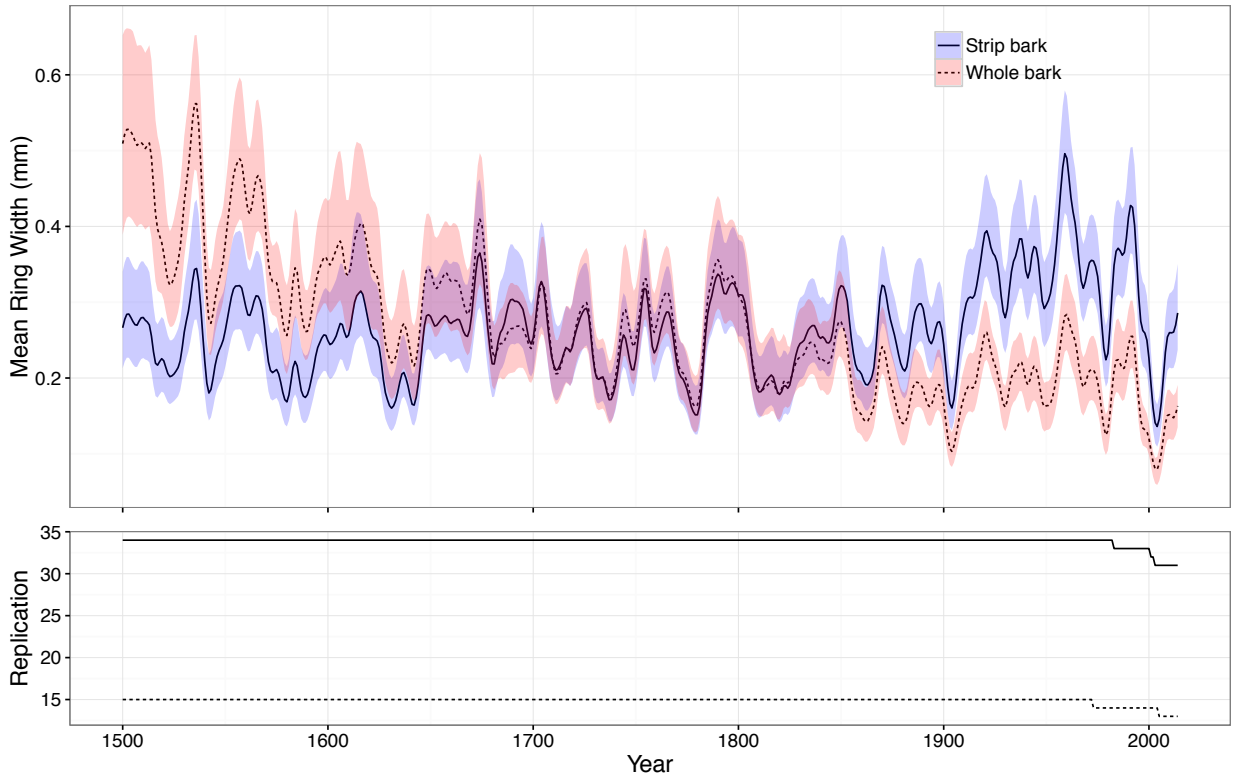

Fig. A.2. Mean ring-width comparisons of strip-bark and whole-bark trees using only cores with >515 rings. The top figure shows a 10-year spline of strip-bark (solid line) and whole-bark (dashed line) mean ring-width chronologies from 1500-2014. The 95% BCa bootstrap confidence intervals around the mean are shown in blue and pink for strip-bark and whole-bark trees, respectively. The bottom figure corresponds to the number of strip-bark (solid) and whole-bark (dashed) series over time.

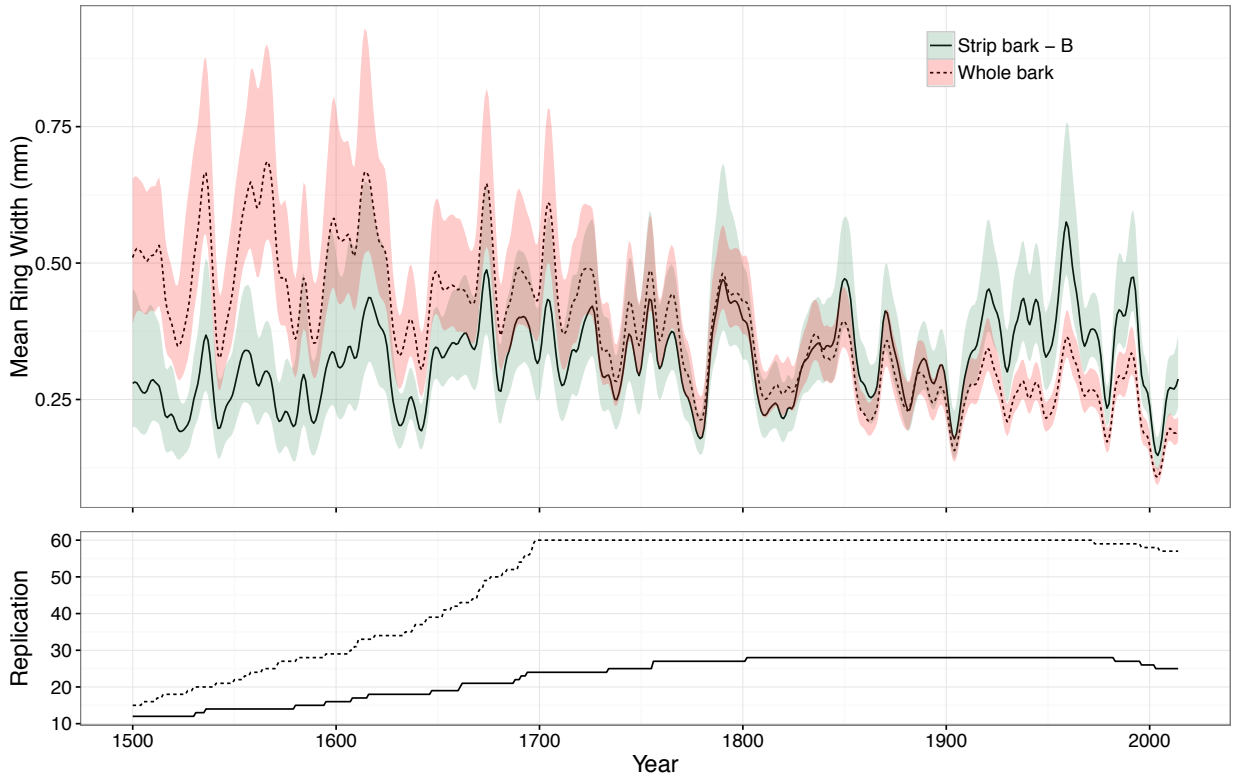

Fig. A.3. Mean ring-width chronology and 95% BCa bootstrap confidence intervals for "B" cores of strip-bark trees (green, solid), and all whole-bark trees (pink, dashed). The bottom panel shows the number of series for each population over time.

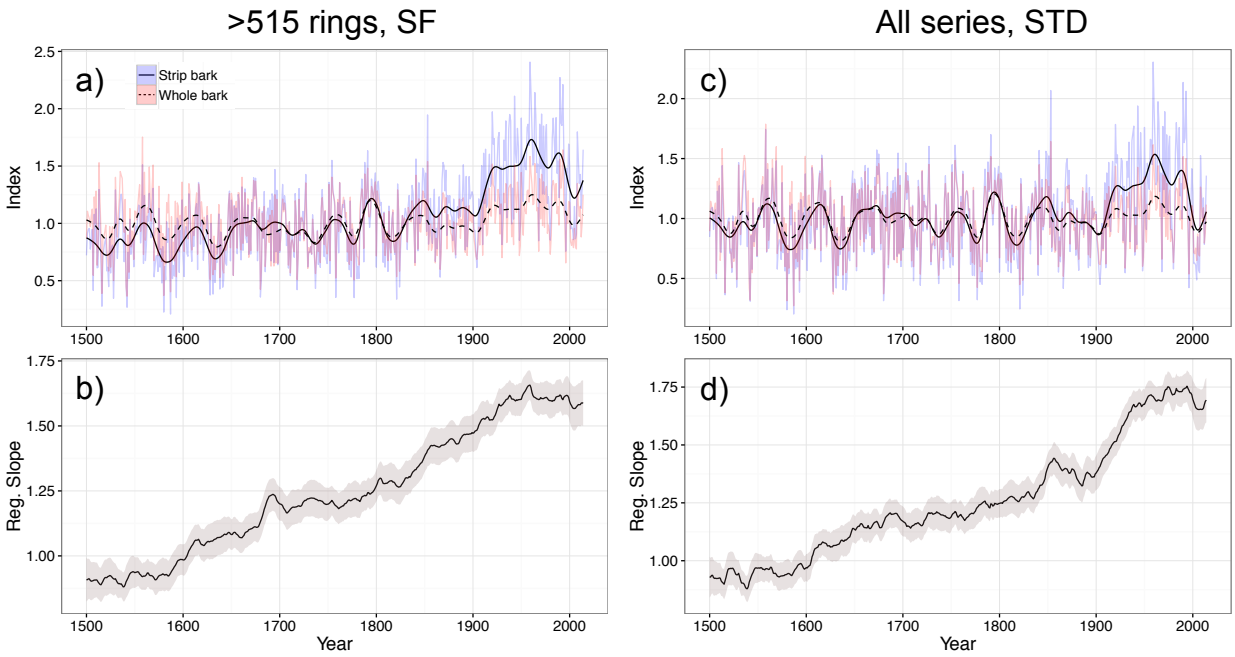

Fig. A.4. Strip-bark (blue with solid 30-year spline) and whole-bark (pink with dashed 30-year spline) standardized chronologies and corresponding dynamic regression coefficients based on only series with >515 rings using signal free methods (a,b), and all series using standard methods (c,d). Gray shading represents a 95% confidence interval.

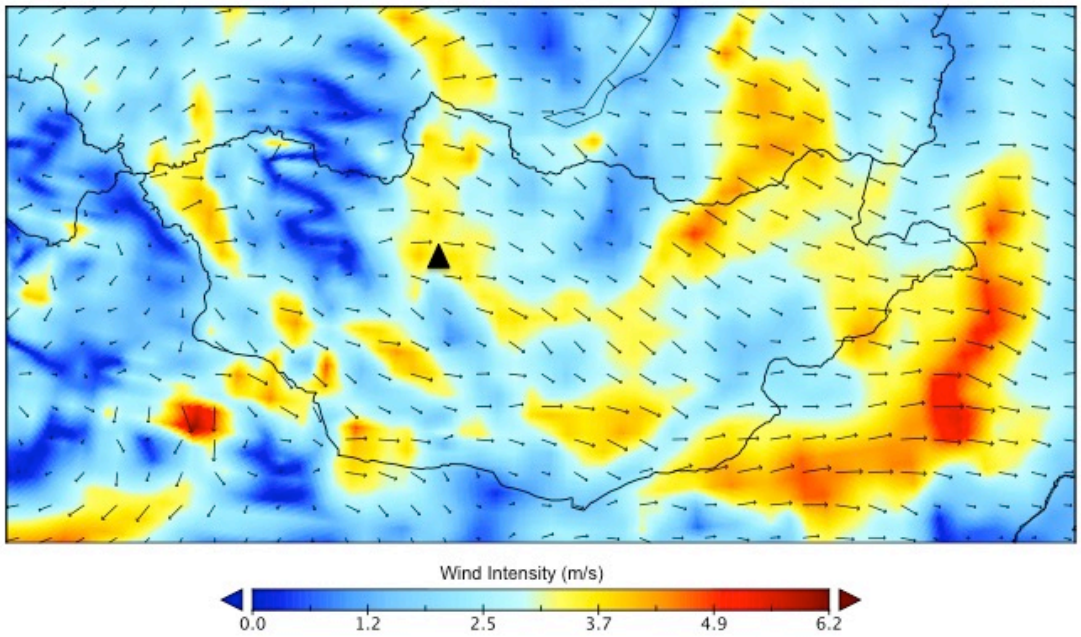

Fig. A.5. Vectors and velocity of surface wind across Mongolia averaged over 1980-2016. The reanalysis wind data was derived from NASA MERRA2 (second phase of the Modern Era Retrospective Analysis for Research and Application (Rienecker et al. 2011, Molod et al. 2015).

Table A.1. Mann-Whitney U test results for comparing the medians of strip-bark and whole-bark signal-free (SF) and standard (STD) chronologies in each century. Asterisks indicate significance at $p<0.05$.

	SF		***STD***	
Time Period	***W***	P_{wilcox}	***W***	P_{wilcox}
1500-1599	4027	0.018*	4379	0.1295
1600-1699	4512	0.2336	4941	0.8854
1700-1799	4352	0.1139	4800	0.6251
1800-1899	5142	0.7286	5154	0.7085
1900-1999	7047	<0.0001*	6713	<0.0001*

Appendix B: Supplemental Figures and Tables for Chapter Two

Table B.1. Test statistics and p-values from Wilcoxon Signed Rank tests comparing environmental variables from P3a (1940-1967; n=28) to P3b (1968-1995; n=28). Changes in June-July precipitation and temperature (CRU version 4.01; Harris et al. 2014), Standardized Precipitation-Evapotranspiration Index (SPEI; Vicente-Serrano et al. 2010), and atmospheric CO_2 concentration (Robertson et al. (2001) until 1993, updated with mean annual values from Mauna Loa until 2011) are assessed.

Environmental Variable	**Test statistic (p-value)**
Precip	226 (p=0.61)
Tavg	228 (p=0.18)
SPEI	234 (p=0.50)
Atm CO_2 conc	**0 (p<0.001)**

Table B.2. Comparisons of environmental periods using the Kolmogorov-Smirnov (K-S) test of distributions for RW_{dt}, $\delta^{13}C_{corr}$, and $\delta^{18}O$ of SB and WB trees. The number of samples (n) for the two respective periods that were compared is shown. Asterisks indicate D-statistics that are significant at $p \leq 0.05$.

	Period Comparison (n)	**Strip-Bark**	**Whole-Bark**
RW_{dt}	P1 – P2 (n = 55, 55)	D = 0.43*	D = 0.15
	P2 – P3 (n = 55, 56)	D = 0.21*	D = 0.08
	P3 – P4 (n = 56, 16)	D = 0.55*	D = 0.49*
$\delta^{13}C_{corr}$	P1 – P2 (n = 55, 55)	D = 0.31*	D = 0.07
	P2 – P3 (n = 55, 56)	D = 0.13	D = 0.04
	P3 – P4 (n = 56, 16)	D = 0.31*	D = 0.40*
$\delta^{18}O$	P1 – P2 (n = 55, 55)	D = 0.06	D = 0.25*
	P2 – P3 (n = 55, 56)	D = 0.13	D = 0.10
	P3 – P4 (n = 56, 16)	D = 0.13	D = 0.21

Table B.3. Root Mean Square Error (RMSE) calculated from residuals between the measured c_i/c_a and the simulated c_i/c_a from the three CO_2 response scenarios (Saurer et al. 2004). The lowest RMSE, in bold, is the scenario that best matches each tree.

Tree ID	**Scenario 1**	**Scenario 2**	**Scenario 3**
1830-2011			
All (mean)	**0.036**	0.040	0.090
1940-1995			
SB1	0.063	**0.043**	**0.043**
SB2	0.058	**0.043**	0.050
SB3	**0.032**	0.039	0.070
WB1	0.062	**0.047**	0.052
WB2	0.062	0.037	**0.035**
WB3	0.042	**0.038**	0.061

Table B.4. Rates of change per year of atmospheric CO_2 (c_a) and intrinsic water-use efficiency (WUE_i) over various periods of time. Percent increases in WUE_i were compared with results from other studies (last column).* indicates a significant slope ($p \leq 0.05$).

Period	Ca (ppm yr^{-1})	iWUE (µmol mol^{-1} yr^{-1})	Other/Comparison with Literature
P1 (1830-1884)	0.14*	0.19*	NA
P2 (1885-1939)	0.32*	0.13*	NA
P3 (1940-1995)	0.95*	0.31*	NA
P4 (1996-2011)	2.02*	1.02*	NA
P1-P4 (1830-2011)	0.48*	0.21*	NA
1850-2000	0.46*	0.18*	Percent increase from 1850:2000: **38.32%**. Compared to a 22.9% increase for conifers reported in Leonardi et al. (2012).
1861-1990	0.42*	0.16*	% iWUE increase from 1861-1890 mean to 1961-1990 mean = **16.92%**. Compared to 19.2 +/- 0.9% iWUE increase for trees across Eurasia (Saurer et al. 2004).
1901-2000	0.64*	0.23*	% iWUE increase from 1901-1910 mean to 1991-2000 mean = **18.85%**. Compared to 25.7 +/- 11.6% iWUE increase in conifers across Europe (Saurer et al. 2014). The % iWUE increase from the 1901-1910 reference period to 2002 in our study was **30.7%**. Compared to 22+/- 6% iWUE increase in European conifers, while controlling for climate impacts on iWUE, and ~30% iWUE increase without controlling for climate (Frank et al. 2015).
1901-1995 (excluding drought)	0.59*	0.19*	% iWUE increase from 1901-1910 mean to 1990-1995 mean = **12.43%** (i.e., excluding drought).
1992-2011	1.90*	1.42*	1992-2011 iWUE % change increase: **0.94% yr^{-1}**. Inherent water-use efficiency (IWUE) showed an increase of 2.3% yr^{-1} from 1992-2011 (Keenan et al. 2013), or 1.3% yr^{-1} when updated with additional years (1992-2014; Mastrotheodoros et al. 2017).

Table B.5. Test statistics and p-values from Wilcoxon Signed Rank tests comparing c_i/c_a of P3a (1940-1967) and P3b (1968-1995) for each tree individually.

Tree ID	**Test statistic (p-value)**
SB1	227 (p=0.60)
SB2	278 (p=0.09)
SB3	**346 (p<0.01)**
WB1	218 (p=0.75)
WB2	209 (p=0.90)
WB3	230 (p=0.55)

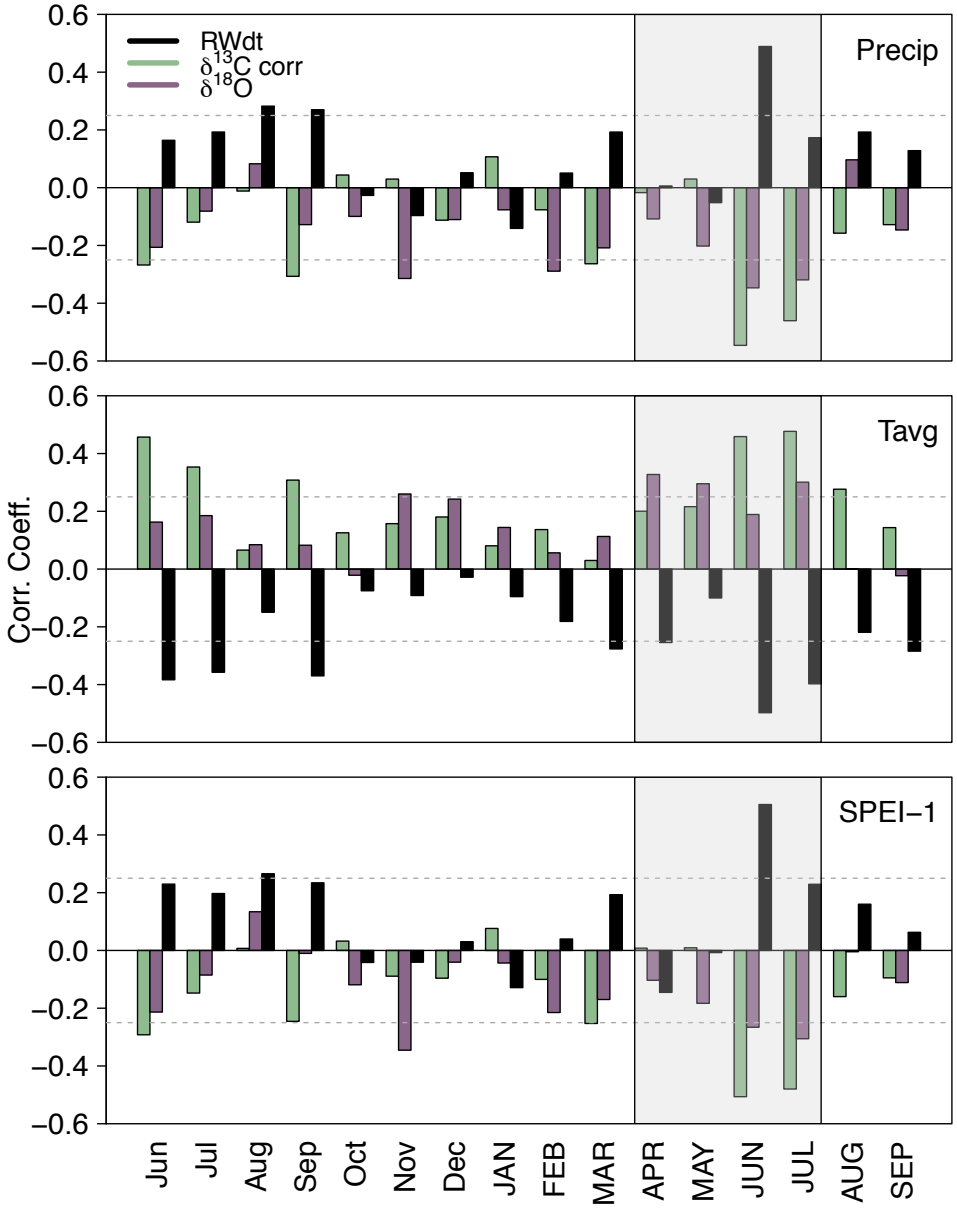

Fig. B.1. Pearson's correlation coefficients between monthly climate variables (CRU TS 4.01 precipitation and average temperature, and SPEI) and RW_{dt} (black), $\delta^{13}C_{corr}$ (green), and $\delta^{18}O$ (purple) chronologies derived from all trees. Correlation coefficients above/below the gray dashed line are statistically significant ($p<0.05$). The shaded area (April-July) represents months analyzed on an individual-tree basis in Figure 2.5.

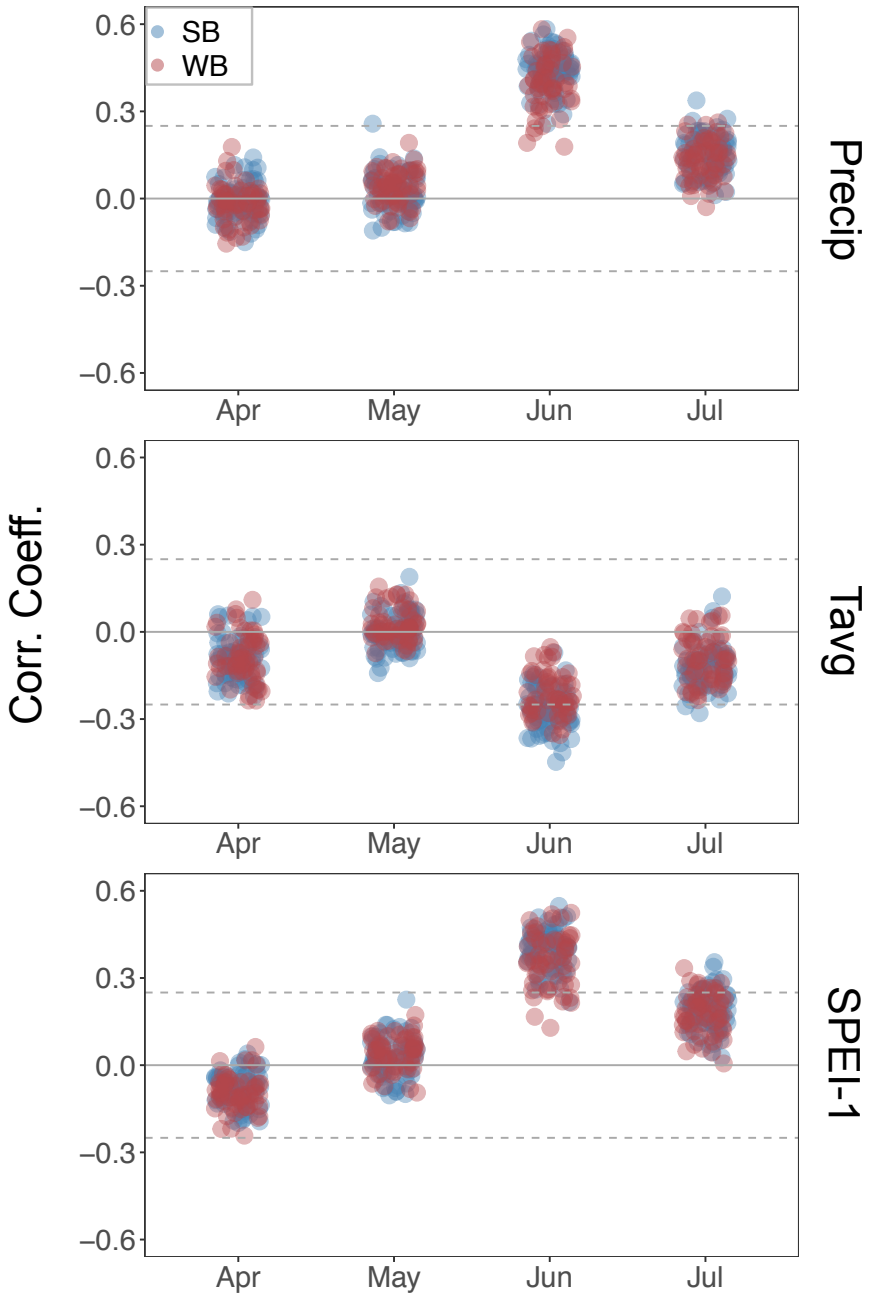

Fig. B.2. Pearson's correlation coefficients between April-July monthly climate variables (CRU TS 4.01 precipitation and average temperature, and SPEI-1) and all detrended ring-width series from Leland et al. (2018). Blue dots represent climate correlations for individual SB trees, and red dots represent WB trees. Correlation coefficients above/below the gray dashed line are statistically significant ($p<0.05$).

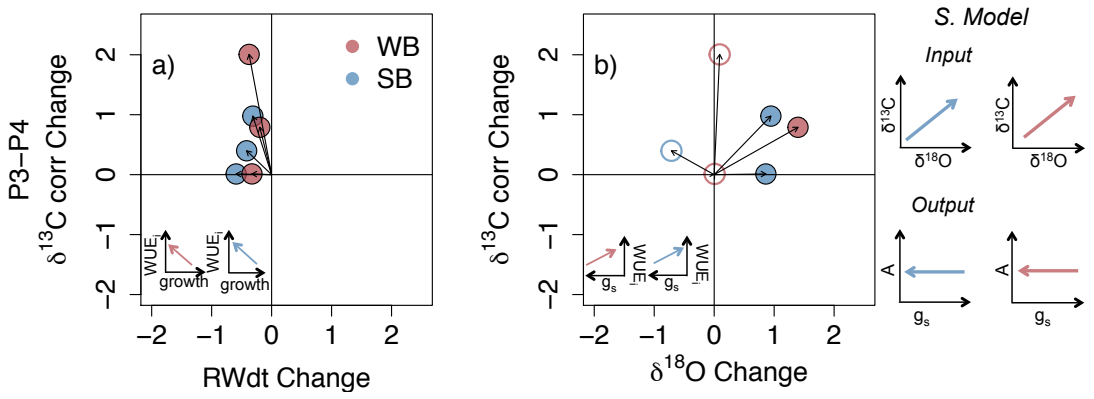

Fig. B.3. Changes in tree-ring parameters from P3 (pre-drought) set to the origin (0,0) to P4 (drought) for WB (red) and SB (blue) trees. The insets in a) and b) show how SB and WB trees changed intrinsic water-use efficiency (WUE_i), ring-width (growth), and stomatal conductance (g_s) from P3-P4. Interpretations in the right panel, assessing changes in g_s and assimilation (A) are based on the Scheidegger et al. (2000) dual-isotope method. The hollow circles in panel (b) represent trees with an insignificant correlation between $\delta^{18}O$ and June-July SPEI.

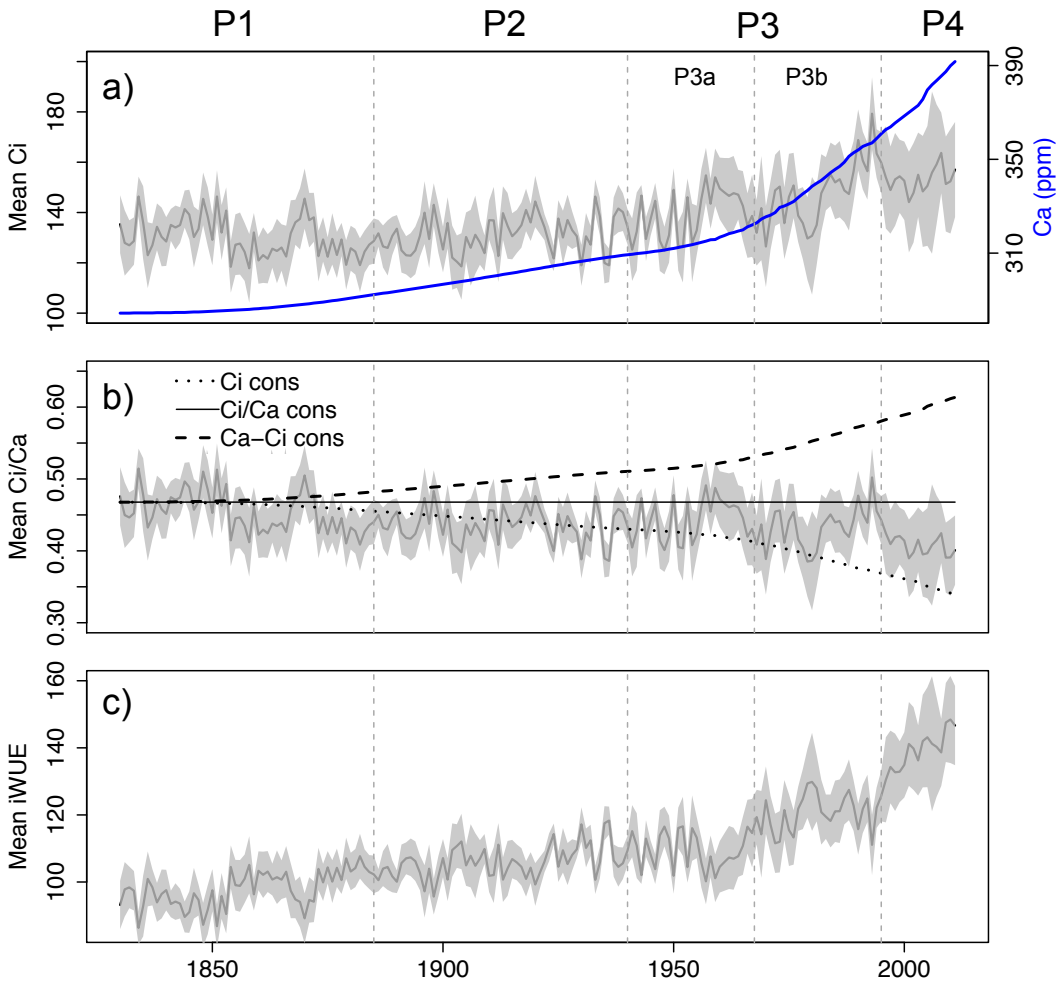

Fig. B.4. a) Mean intercellular CO_2 (c_i) across all analyzed trees, with 95% confidence interval in gray. The blue line indicates changes in atmospheric CO_2 (c_a, right axis). b) Mean c_i/c_a with 95% confidence interval in grey shading, compared with simulations following the three scenarios proposed by Saurer et al. (2004). c) Mean intrinsic water-use efficiency (WUE_i) across all analyzed trees.

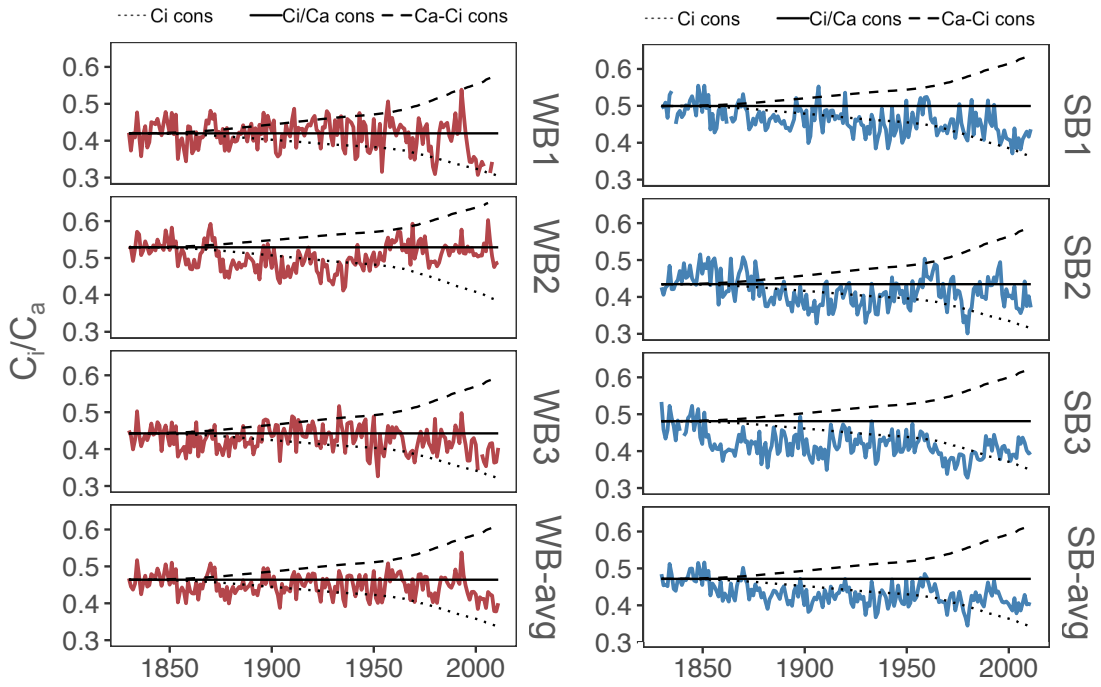

Fig. B.5. Comparisons of c_i/c_a for individual WB (red) and SB (blue) trees, and an average of each group (bottom row). Simulated scenarios for each series were calculated following Saurer et al. (2004).

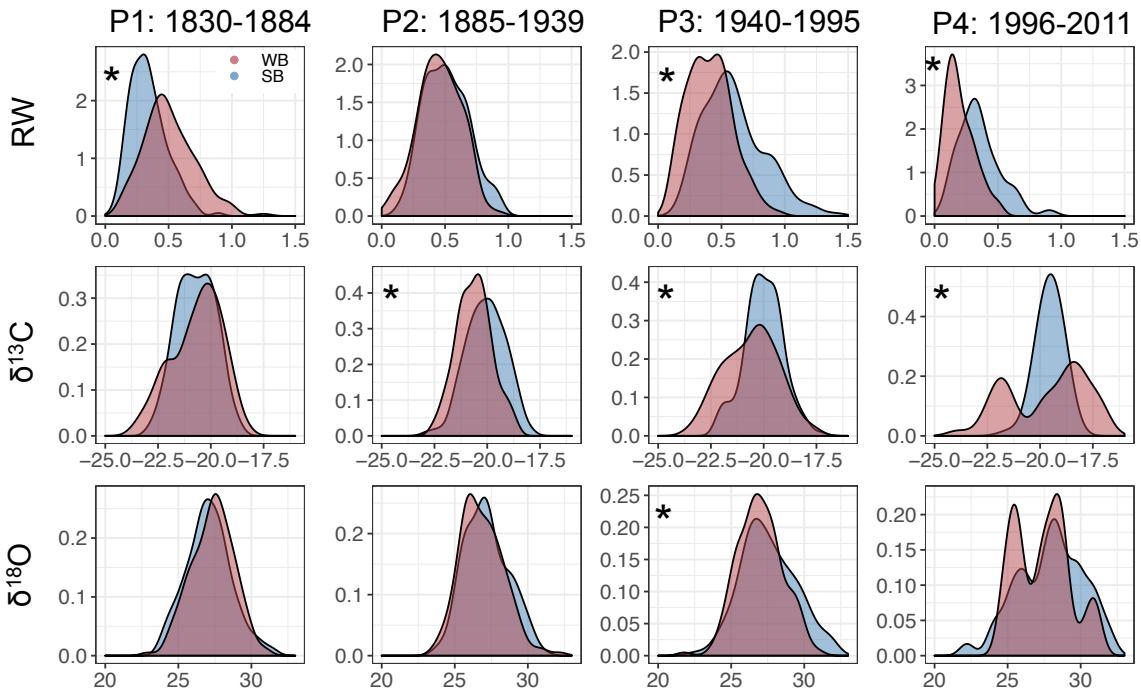

Fig. B.6. Comparisons of WB (red) and SB (blue) RW_{dt} (top), $\delta^{13}C_{corr}$ (middle) and $\delta^{18}O$ (bottom) distributions for each environmental period (P1-P4). Asterisks indicate significance ($p<0.05$). Note that here we compare RW (raw RW data without detrending).

Appendix C: Supplemental Figures and Tables for Chapter Three

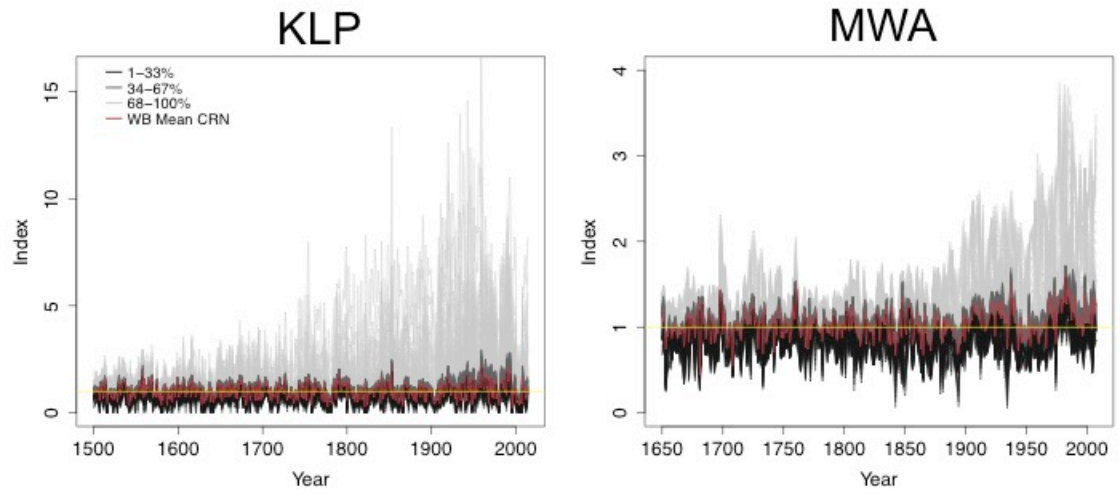

Fig. C.1. All percentile series calculated from indices of all trees (SB+WB) for KLP (left) and MWA (right). The color code indicates three ranges of percentiles (1-33%, black; 34-67% gray; 68-100% light gray). The WB mean chronology for each site is shown in red, and the mean of the WB chronology is shown in yellow.

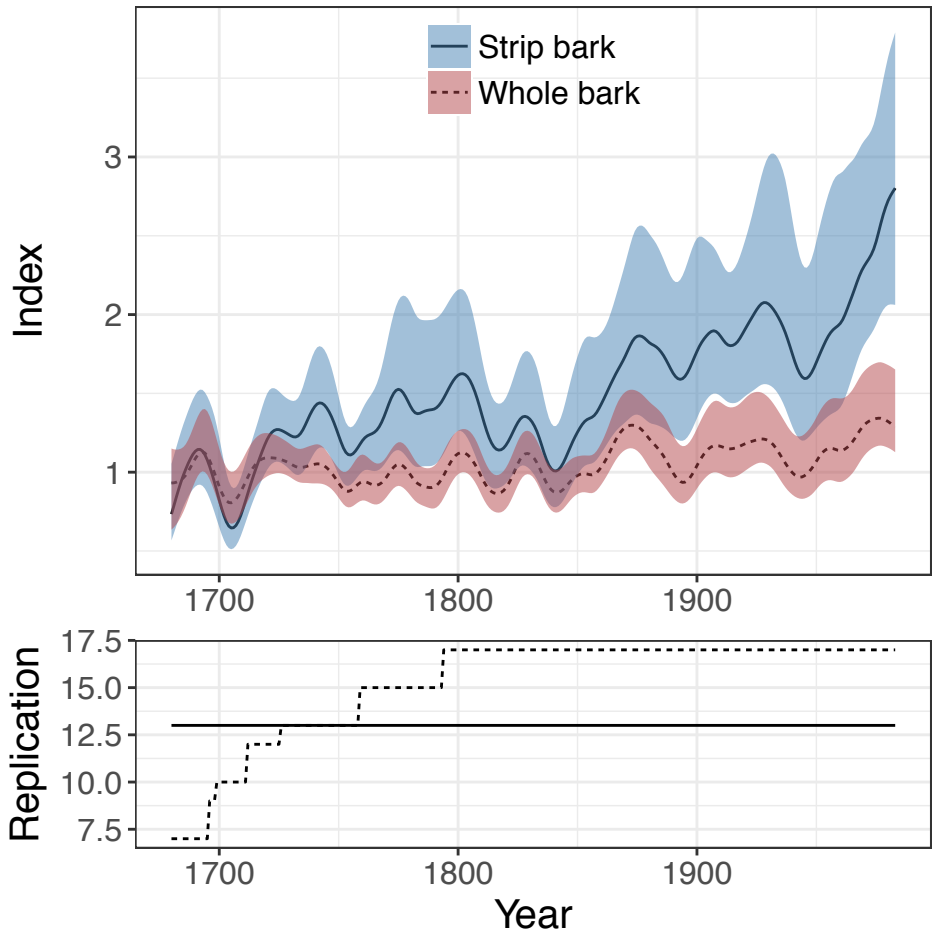

Fig. C.2. Standardized chronologies from the original Graybill and Idso (1993) Bristlecone pine collection from Sheep Mountain. The mean and 95% BCa bootstrap confidence intervals are shown for both SB (solid line, blue envelope) and WB (dashed line, pink envelope) trees. All chronologies were smoothed with a 20-year spline. Individual series were detrended following the same methods as other sites in this study, using an age dependent spline constrained to not increase. Mean raw ring-width strip-bark and whole-bark chronologies do not show a strong divergence during the 20th century, indicating that the recent divergence is exacerbated by the conservative standardization method chosen here (Salzer et al. 2009).

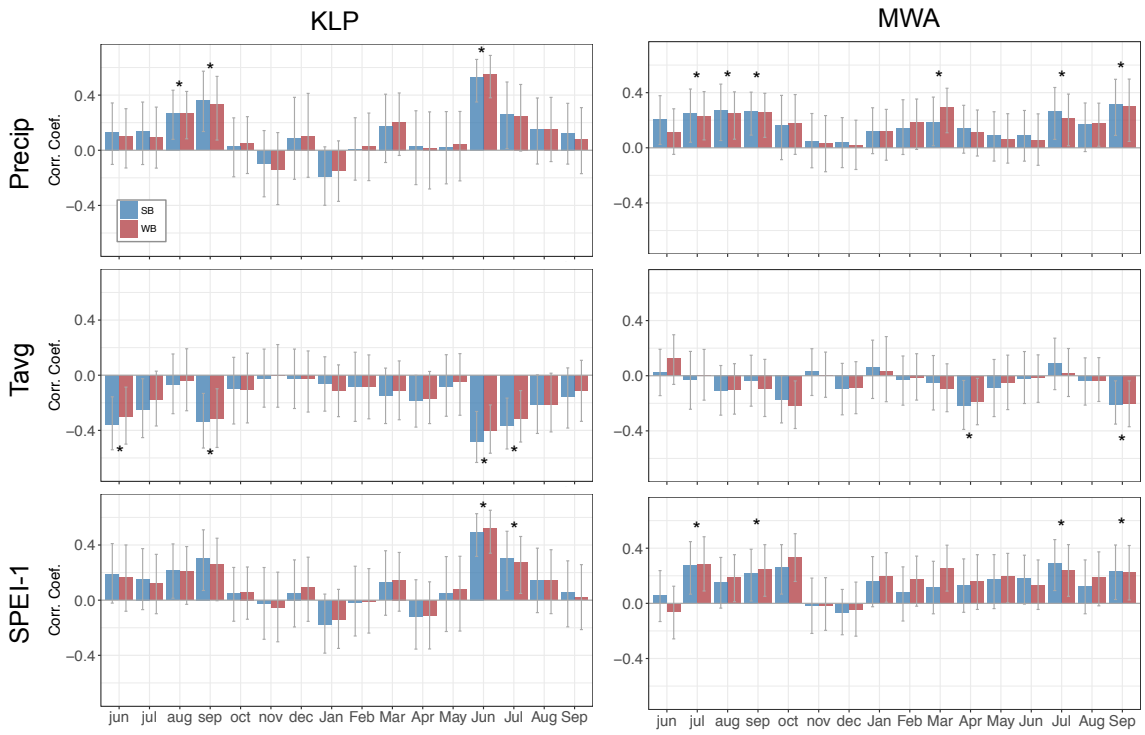

Fig. C.3. Climate response of KLP and MWA SB (blue) and WB (red) chronologies from the previous July to current September of the growing season over 1940 to 2014 (KLP) and 1901-2007 (MWA). The WB and SB chronologies were correlated with monthly precipitation and average temperature datasets from the Climatic Research Unit (CRU version 4.01) (Harris et al. 2014) and a 1-month Standardized Precipitation-Evapotranspiration Index (SPEI-1; Vicente-Serrano et al. 2010) based on the grid point nearest to the study site. MWA chronologies are compared with monthly precipitation and average temperature from the nearest PRISM grid point (PRISM Climate Group, 2004), and SPEI-1.